NOTICE

The quality of this microfiche is heavily dependent upon the quality of the original thesis submitted for microfilming. Every effort has been made to ensure the highest quality of reproduction possible.

If pages are missing, contact the university which granted the degree.

Some pages may have indistinct print especially if the original pages were typed with a poor typewriter ribbon or if the university sent us a poor photocopy.

Previously copyrighted materials (journal articles, published tests, etc.) are not filmed.

Reproduction in full or in part of this film is governed by the Canadian Copyright Act, R.S.C. 1970, c. C-30. Please read the authorization forms which accompany this thesis.

THIS DISSERTATION
HAS BEEN MICROFILMED
EXACTLY AS RECEIVED

AVIS

La qualité de cette microfiche dépend grandement de la qualité de la thèse soumise au microfilmage. Nous avons tout fait pour assurer une qualité supérieure de reproduction.

S'il manque des pages, veuillez communiquer avec l'université qui a conféré le grade.

La qualité d'impression de certaines pages peut laisser à désirer, surtout si les pages originales ont été dactylographiées à l'aide d'un ruban usé ou si l'université nous a fait parvenir une photocopie de mauvaise qualité.

Les documents qui font déjà l'objet d'un droit d'auteur (articles de revue, examens publiés, etc.) ne sont pas microfilmés.

La reproduction, même partielle, de ce microfilm est soumise à la Loi canadienne sur le droit d'auteur, SRC 1970, c. C-30. Veuillez prendre connaissance des formules d'autorisation qui accompagnent cette thèse.

LA THÈSE A ÉTÉ
MICROFILMÉE TELLE QUE
NOUS L'AVONS REÇUE.

BEARING CAPACITY AND SETTLEMENT OF CIRCULAR FOOTING ON SAND

by

M. G. Rahman

A Thesis Submitted to
the School of Graduate Studies
in Partial Fulfillment for the Degree of
Master of Applied Science
(Civil Engineering)

Department of Civil Engineering
University of Ottawa
Ottawa, Canada

November, 1980

to my parents

ABSTRACT

The introduction of rational criteria for foundation design is a relatively recent development in engineering practice, although the interest in analysis of ultimate loads of foundation can be traced back in literature more than 100 years. Modern research on this problem started with Prandtl and subsequently developed by others but Terzaghi's (1943) work has made a lasting impact on this subject.

As is well known, every foundation problem necessitates two quite different studies; one concerning the ultimate bearing capacity of the soil under the foundation, the other concerning the limit of deformation.

There exists quite a number of theories in the literature to determine the bearing capacity and settlement of foundation. In case of foundation on sand the settlement rather than bearing capacity criteria usually exert the design control. The magnitude of settlement in sand, as predicted by available method varies considerably. The individual methods are not consistent in being either above or below average for varying soil condition and foundation geometry.

The present research is undertaken to review the understanding of the problem of bearing capacity and settlement using the sand box which is one of the largest in-house testing

facilities known to date.

Tests were carried out with footings 30 cm in diameter on the surface of sand, deposited by free falling device in the sand box 2 by 2 by 15 metre long. One of the most important features of the tests was the filling of the box at any uniform density. This was accomplished by sand handling equipment consisting of a sand elevator and a spreader. By adjusting the horizontal speed of the spreader, rotation of the drum and height of fall of the sand, various densities could be achieved.

In all the tests, the parameters monitored are: total settlement at the surface, settlements at depths of 15, 30, 45 and 60 cm below the footing, radial deformation at a depth of 30 cm at three different diameters of 22, 56 and 90 cm, movement of the surface of sand around the footing, at various stress levels.

With all the known parameters and the soil properties, the bearing capacity and settlement are compared with the two well known bearing capacity equation, one proposed by Terzaghi (1943) and the other by Meyerhof (1951) and Brinch Hansen (1970) and a settlement calculation method proposed by Schmertmann (1970). Some differences between the measured and calculated values were noticed and modifications regarding the N_r-value in the bearing capacity equation and

I_z, the vertical strain influence factor in settlement calculation have been suggested. Moreover, a correction factor involving the stress level in relation to the ultimate bearing capacity is introduced in the equation proposed by Schmertmann.

ACKNOWLEDGEMENT

The writer is indebted to his adviser Professor T.I. Vladut of the Civil Engineering Department, for his guidance, valuable advice and suggestions throughout this investigation. He also has to be complimented for his interest and dedication to the project.

Thanks are due to Dr. B.H. Fellenius and Dr. W.J. Thompson, Professors of the Department of Civil Engineering for their valuable suggestion in preparation of the thesis and for the instructions during the course work.

Dr. Erik I. Hjeldnes, Professor, The University of Trondheim, Norway, is thanked for his valuable suggestion specially in the settlement analysis.

Grateful appreciation is extended towards Mr. R.J. Moore for his assistance in manufacturing the instruments and throughout the testing. Gratitude is also expressed to Mr. Guy Fellio and Mr. Luc Seguin and other machine shop staff for their skillful assistance in the testing program. Thanks are also due to Mrs. O. Biswas for her skillful typing of the manuscript.

The writer is thankful to the National Research Council for providing financial assistance (Grant A1011) in carrying out the research.

TABLE OF CONTENTS

LIST OF TABLES

LIST OF FIGURES

LIST OF SYMBOLS

B	Width/diameter of footing
C	Cohesion
C_1	Depth of embedment factor
C_2	Creep factor
C_t	Correction factor for depth of compressible layer
C_d	Correction factor for depth of footing
C_w	Correction factor for water table
D_w	Depth of water table
E_b	Young's modulus of plate
E_s	Modulus of soil media
H	Thickness layer
I	Influence factor
I_z	Vertical strain influence factor
K_r	Relative rigidity of plate
M	$= \frac{E}{1-\mu^2}$
N	S.P.T. blow count
N_c, N_q, N_r	Bearing capacity factors
P	Applied load
P'	Effective overburden pressure
P_p	Passive earth pressure
S	Factor of safety
S P T	Standard Penetration Test

a	Radius of plate
b_c, b_q, b_r	Base factor
c	Constant of compressibility
d_c, d_q, d_r	Depth factor
g_c, g_r, g_r	Ground factor
i_i, i_q, i_r	Inclination factor
q	Applied stress
q_a	Allowable bearing capacity
q_c	Static Cone penetration resistance
q_s	Load causing limit deformation
q_u	Ultimate bearing capacity
t	Thickness of plate
γ	Unit weight of soil
ΔP	Net load intensity at foundation depth (Schmertmann's equation)
Δ_z	Layer thickness
ΔP	Increment of pressure
δ	Settlement
μ	Poisson's ratio
ϕ	Angle of internal friction

INTRODUCTION

1.1 General

The design of a foundation for a structure is governed by two main conditions: a) that the soil must be safe against failure by shear which may cause plastic flow below the structure, b) that the structure must be safe against excessive settlement or movement due to consolidation of the soil under the foundation.

A safe design is one which satisfies both of the conditions stated above. If q_u represents the ultimate bearing capacity of the soil, q_a the allowable bearing capacity, q_s the load causing the limit deformation, and S the factor of safety, the allowable bearing capacity should be the lowest of the two limits:

$$q_a \leq \frac{q_u}{S}$$

$$\leq q_s$$

Another aspect of design is the cost of the foundation. To minimize cost, the design should be optimum with a reasonable amount of safety. To satisfy all these conditions, the geotechnical engineer must have first hand experience of the different types of soil and their behaviour under load.

For a foundation over sand, the settlement criteria, rather than the bearing capacity, usually governs the design

when the least width of the foundation exceeds about 1 m. So a reliable method of settlement prediction, which takes into account the soil properties and their deformation behaviour, is useful in predicting the allowable bearing capacity of a particular soil.

1.2 Problem Statement

The present practice in designing foundation on sand is to determine the allowable bearing capacity in relation to the depth and width of the foundation and then use the value in the appropriate formula for determining the settlement.

The magnitude of the settlement of a foundation in sand if calculated by the different available methods varies considerably. Furthermore none of these methods are consistent in being either above or below average for varying soil conditions and foundation geometry. Therefore, no method is wholly reliable in predicting settlements which in turn depend on the judgement of the engineer. The variability in prediction is due to the many factors affecting settlement and to the lack of understanding of their influence.

The present work was undertaken to review the understanding of the problem of bearing capacity and settlement in granular soils. It appears that most of the existing theories are either based on or verified by small scale laboratory tests

with footings as small as 2 cm in width. Of course, tests have been made with footings 20 to 25 cm in diameter on granular soils, but these took place in containers whose diameter or lateral dimensions and depths were small compared to the diameter of the footing. The effects of the lateral dimension or depth are not very well recorded. The following table lists some tests performed by various researchers since 1961.

TABLE

DIAMETER/WIDTH OF FOOTING TESTED IN THE PAST

RESEARCHER	YEAR	DIAMETER/WIDTH in cm
Jumikis, A.R.	1961	5, 7.5, 10, 12.5, 15
Hansen, B.	1961	3 to 15
Eggested, A	1963	20
Vesic, A.S.	1963	5 to 20
Feda, J.	1963	2.9, 4.8, 8.0
De Beer	1965	9, 15
Yamaguchi, H.	1976	2, 3, 4
Brinch Hansen, J	1977	10, 15, 20, 25 (on Pin model)
Pfeifle, Tom W.	1979	5

It is now possible to carry out tests on a reasonably large scale in the facilities of the Department of Civil Engineering at the University of Ottawa. The sand box, 2 by 2 by 15 meter long and equipped with a spreading device capable of depositing sand in layers at wide ranges of relative densities, was used to test footings of 30 cm in diameter.

Known soil properties, and various parameters monitored during the tests are used to check some of the more widely used theories and suggest some improvements in the method of evaluation of ultimate bearing capacity and settlement of circular footings on sand.

1.3 Objective and Scope of Study

The objective of the present study includes a survey of literature on the settlement characteristics of sand under vertical load, bearing capacity of sand, verification of the existing methods of evaluating settlement and bearing capacity with the known parameters available from the tests; improvement on the existing methods; make recommendation for future programs.

The extent of the testing program was limited to seven tests of a 30 cm diameter rigid footing located at the surface of sand at relative densities of 96, 80 and 63 percent. These densities were choosen for the test as it is extremely difficult to spread the sand at more than three different densities with

the current facilities available. In all the tests the following parameters were monitored:

a) Total load

b) Total settlement

c) Settlements at depths 15 cm, 30 cm, 40 cm and 60 cm

d) Radial displacements at three different radii at depth of 30 cm below the footing

e) Movement at the surface around the footing.

CHAPTER 2

REVIEW OF LITERATURE

2.1. Bearing Capacity

2.1.1 Definition

When a load is applied on the soil through a footing, the soil deforms both vertically and horizontally. For small loads, the magnitude of which depends on the type of soil, the soil behaves elastically, that is, the deformation is proportional to the load. Local yielding occurs with a further increase of the load and the size of the resulting plastic zone starts increasing as well. The deformation is no longer proportional and increases rapidly with a slight increase of load. The load at which general failure occurs may be called the ultimate bearing capacity of the footing.

It has been observed that bearing capacity failure occurs as a result of shear failure of the soil. Three principal modes of shear failure under a foundation have been described in the literature: general shear failure, local shear failure and punching shear failure.

General shear failure is characterized by a well defined failure load accompanied by a well defined failure pattern consisting of a continuous slip surface from one edge of the footing to the ground surface (Figure 2.1).

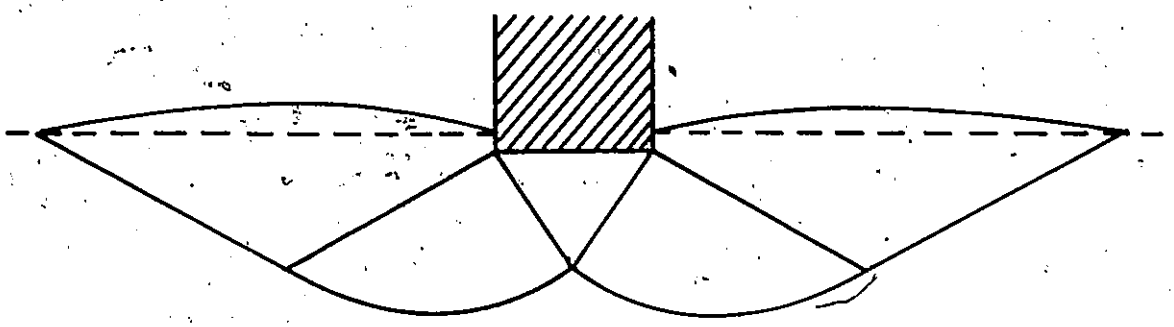

A) GENERAL SHEAR

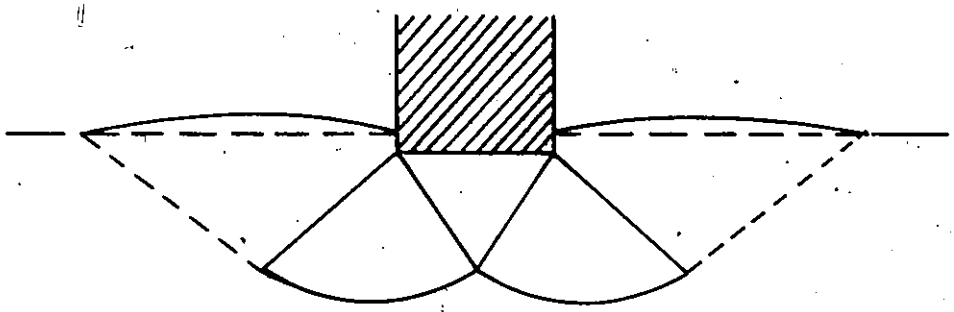

B) LOCAL SHEAR

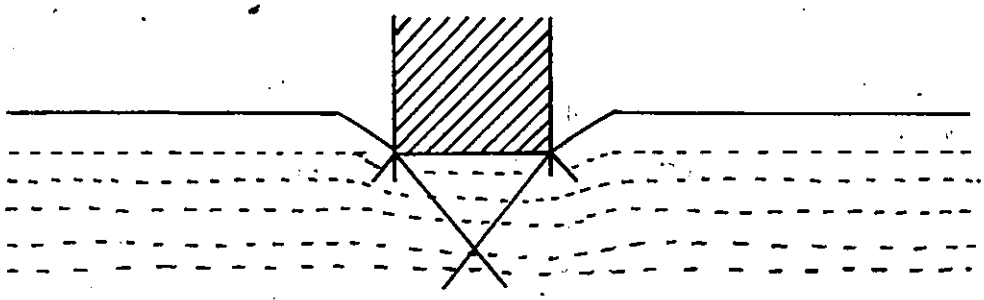

C) PUNCHING SHEAR

FIGURE 2.1 MODES OF FAILURE

At stress-controlled conditions, under which most foundations operate, failure is sudden and catastrophic. At strain-controlled conditions, a visible decrease of load is noticed. A tendency of the adjacent soil to bulge is another characteristic of this type of failure.

Punching shear failure normally occurs in loose soil and is generally characterized by the compression of the soil immediately beneath the footing. The footing penetrates continuously and is made possible by vertical shear around the perimeter of the footing. The soil outside the loaded area remains unaffected by the loading and deformation of the footing. The resistance to penetration increases continuously with the increase of footing penetration.

Local shear failure is characterized by a failure pattern which retains both general shear and punching shear failure characteristics. The failure pattern consists of wedge and slip surfaces, which start at the edges of the footing as in the case of general shear failure. There is a visible tendency of the soil to bulge around the footing. The slip surfaces end somewhere in the soil mass and only appear at the surface after considerable vertical displacement of the footing (up to 50% of footing diameter, Vesic 1973).

The failure mode depends primarily on the compressibility of the soil, relative depth of the footing and over-

burden pressure around the footing. Figure 2.1 shows the failure mode of footing in sand in relation to the relative density and relative depth. Generally, if the soil is practically incompressible and has a finite shear strength, it will fail in a general shear mode. On the other hand, if the soil is compressible, it will fail in a punching shear mode. It is important to understand that the failure mode is not only governed by the soil type. An incompressible soil may fail in a punching shear mode if the footing is located at great depth or the incompressible layer is underlain by soft compressible layer.

It is apparent from the preceding discussion that the failure of a loaded footing is well defined in the case of general shear failure, where the peak/ultimate load is reached simultaneously with the appearance of the slip line at the ground surface and is followed by the collapse of the foundation. The failure load is not very well defined for the other two modes of failure. In both cases, the load rises continuously with the penetration of the footing. Even in the case of general shear failure, a continuous rise of load is apparent, which may be attributed to the surcharge effect that develops once the footing has penetrated to considerable depth.

When the failure load is not defined it is very difficult to choose the ultimate load from the test results. The methods available in the literature are not very versatile

but can be applied with caution. Vesic (1963) defines the ultimate load as the point where the slope of the load settlement curve first reaches zero or a steady minimum value. Christiaens (see De Beer 1967) defines the ultimate load at the point of break of the load settlement curve in a log/log plot. Brinch Hansen (1963) proposed two methods to find the ultimate load. One - known as 90% criteria defines the ultimate bearing capacity as the load at which the settlement is twice the settlement at 90% of the ultimate capacity. The other known as the 80% criteria requires the plot of $\frac{\sqrt{\Delta}}{P}$ against Δ (Δ = movement, P = load) and defines the ultimate bearing capacity as the load that gives four times the movement of the footing as obtained for 80% of the load. However, all these criteria require, that the load test be carried to a very large displacement, preferably of the order of 50 percent of the foundation size (Vesic 1975).

From the practical point of view, it may be preferable to establish some other criteria to determine the ultimate bearing capacity of a foundation corresponding to a critical settlement. The magnitude of critical settlement may vary, depending on soil properties, overburden pressure or depth of foundation and the size of the footing. Skempton (1951) indicated that for saturated clay, these settlement values may be from 3 to 7 percent of the width of the foundation for surface footing and may go as high as 15% for deep

foundations. For footings on sand, somewhat higher critical settlement values are obtained. These values lie between 5 and 15 percent for surface footings and as high as 25 percent for deep foundations (De Beer and Vesic 1958; Vesic, 1963a; De Beer, 1967). De Beer (1967) noted that the critical settlement values increase with the size of the footing.

Vesic (1975) suggested that unless a clearly defined ultimate load can be observed earlier, it is advisable to carry load tests on footings on loose and compressible soils to settlements equal to at least 25 percent of the footing width. If the peak load cannot be determined with certainty, it is reasonable to adopt a limit value for critical settlement, such as 10 percent of the width of the footing as suggested by Vesic (1975). However, these values can be between 10 and 20 percent as suggested by various investigations depending on the factors mentioned earlier.

2.1.2 General

The problem of bearing capacity is an age-old problem. It has been recognized for centuries that the bearing capacity of different soils varies and a number of bearing capacity theories have been developed (Table 2.1). Some of these theories are based on theoretical considerations and some on empirical correlations. They agree well in some cases in the field, but disagree in may cases also. The review is made here

TABLE 2.1

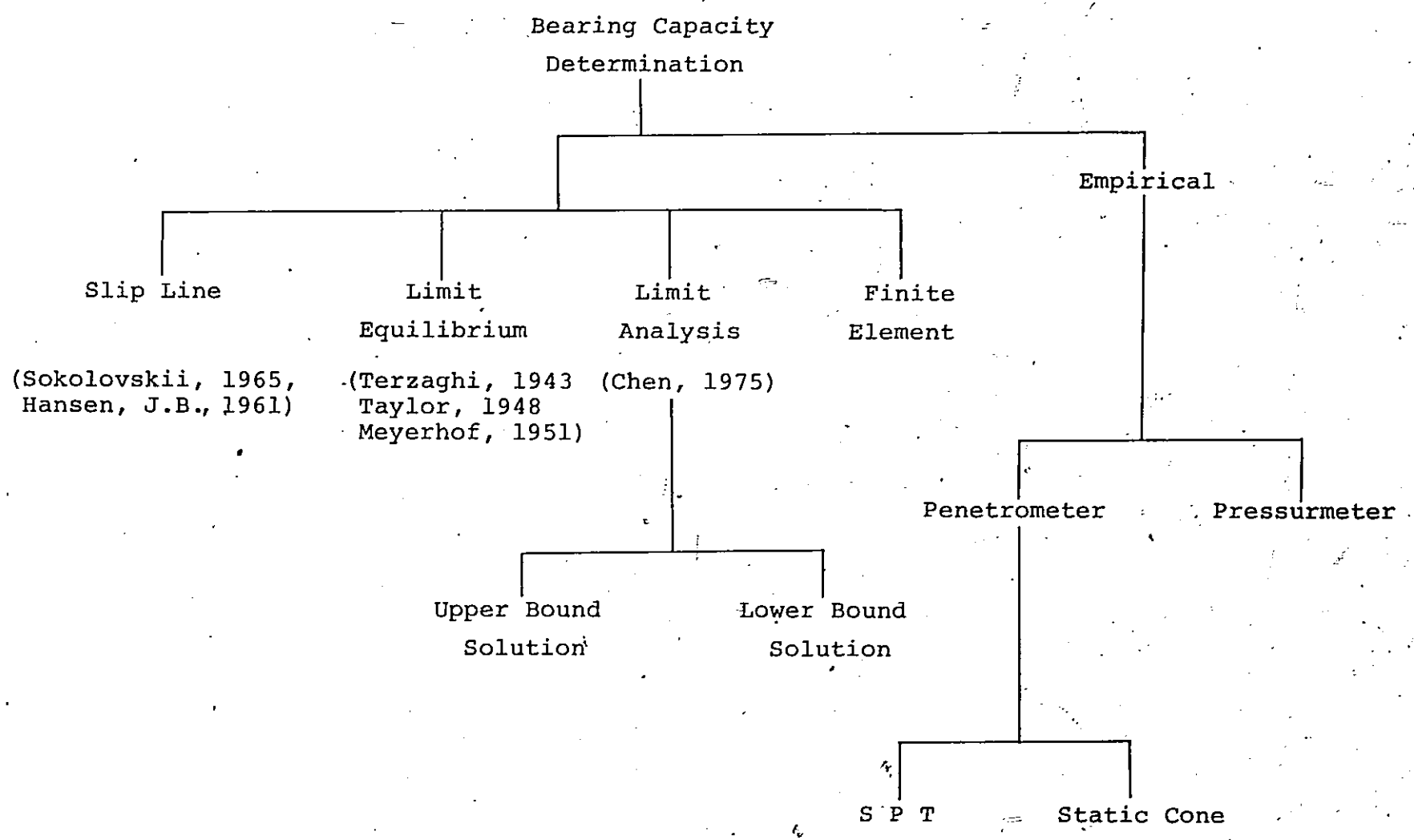
Bearing Capacity Determination
Slip Line
(Sokolovskii, 1965, Hansen, J.B., 1961)
Limit Equilibrium
(Terzaghi, 1943 Taylor, 1948 Meyerhof, 1951)
Limit Analysis
(Chen, 1975)
Upper Bound Solution
Lower Bound Solution
Finite Element
Empirical
Penetrometer
Pressurmeter
S P T
Static Cone

in relation to the shallow or surface footing on sand to enable a proper analysis of the test results from the footing test on sand in sand box. To simulate the tests in the sand box, only the circular footing with vertical loading with the surrounding ground horizontal has been considered.

In the middle of the 19th century attempts were made to obtain theoretically the bearing capacity of soil, based on Coloumb's earth pressure theory. These theories were only approximate.

Terzaghi (1943) presented a method of calculating ultimate bearing capacity which uses the principle of super-position where contributions to the bearing capacity from different soil and loading parameters are summed up. These contributions are represented by the expression

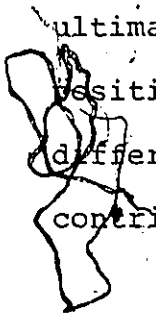

$$q_u = CN_c + qN_q + \gamma\frac{B}{2}N_r \qquad \text{----------2.1}$$

where q_u = Ultimate Bearing Capacity

C = Cohesion

B = Width of foundation

q = Overburden pressure

γ = Unit weight of the soil

N_c, N_q, N_r = Bearing capacity factors, which are functions of angle of internal friction (ϕ) of the soil.

Meyerhof (1951), using Terzaghi's concept, presents extensive numerical results for shallow and deep foundations by assuming failure mechanisms for the footing and by presenting results in the form of bearing capacity factors, (N).

The method presented by Terzaghi is still being used with modifications suggested by different authors at various occasions. The reason for using the simple method (super-position method) is largely due to the mathematical difficulties encountered when the conventional limit equilibrium method is used. The influence of the weight of a soil on the plastic equilibrium of a footing can be solved by formulating differential equations and integrating them either numerically or graphically for individual problems. The general bearing capacity problem can best be solved in two stages. The first stage assumes the soil to be weightless and gives the first part of the bearing capacity relation - $CN_c + qN_q$ in a closed form expression. This is basically the extension of analytical work by Prandtl (1920) and Reissner (1924). The second stage takes into account the weight of the material and gives the second part of the bearing capacity $r\frac{B}{2}N_r$ relation.

2.1.3 Computation of Bearing Capacity

The first comprehensive theoretical investigations of bearing capacity of a foundation were based on the Rankine's

earth pressure theory. Although this analysis is much too approximate for practical use, it illustrates in a simple way the factors that must be considered in a more accurate analysis. The main assumption in this theory is that the failure surfaces are plane (Fig. 2.2).

The bearing capacity can be obtained by computing active earth pressure for the Rankine active wedge - I and the passive earth pressure for the Rankine pressure wedge - II which can be represented by the following equation

$$q_u = CN_c + qN_q + r\frac{B}{2}N_r \quad \text{----------2.2}$$

where $N_c = 2\,(N_\phi^{3/2} + N_\phi^{1/2})$ ----------2.2a

$N_q = N_\phi^{2}$ ----------2.2b

$N_r = 1/2\,(N_\phi^{5/2} - N_\phi^{1/2})$ ----------2.2c

$N_\phi = \frac{1 + \text{Sin } \phi}{1 - \text{Sin } \phi}$ ----------2.2d

ϕ = angle of internal friction

For sand when C = 0 the equation reduces to

$$q_u = qN_q + r\frac{B}{2}N_r \quad \text{----------2.3}$$

The above solution grossly underestimates the actual bearing capacity mainly due to the simplified assumptions. The actual failure zone is bounded by curves, contrary to the assumed failure zone bounded by straight line. Another reason is that

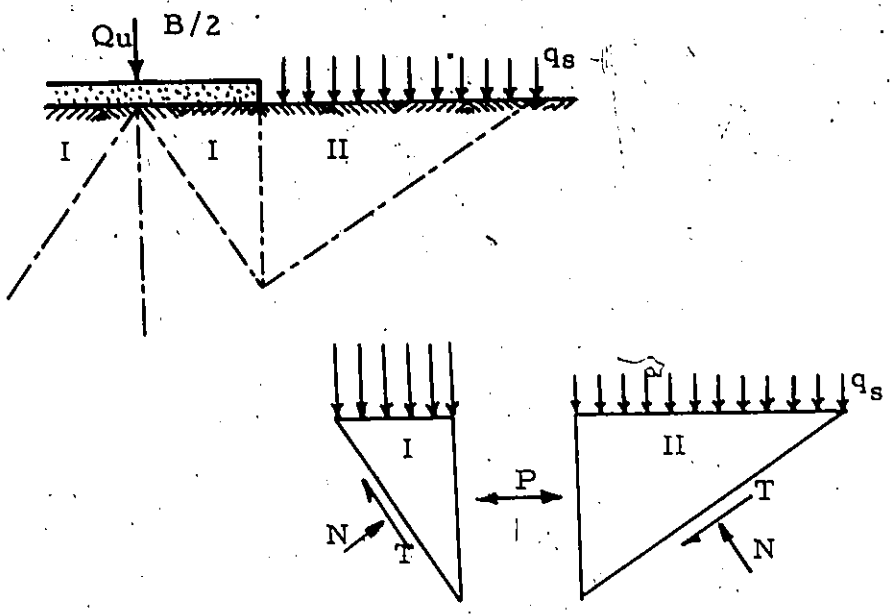

I - Active Rankine Zone

II- Passive Rankine Zone

FIGURE 2.2 RANKINE FAILURE PLANES

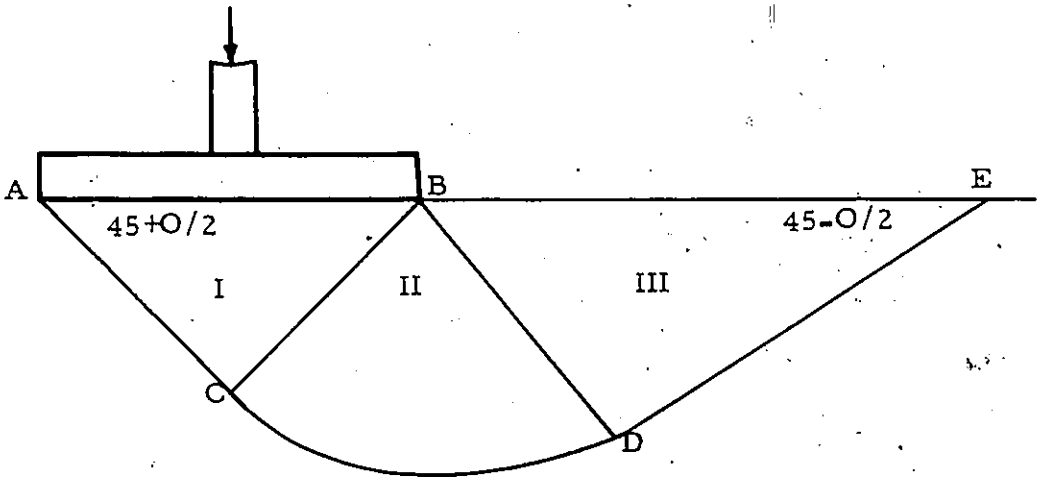

I - Active Rankine Zone

II - Prandtl Zone

III- Passive Rankine Zone

FIGURE 2.3 FAILURE ZONES, PRANDTL

the shear stress which must act upon the interface between the two Rankine zones is neglected.

Schwedler (see Schwab, 1976) was probably the first to assume a curved failure surface in the calculation of bearing capacity where a log-spiral with straight extension was used.

Prandtl (1920, 1921) analyzed the bearing capacity of a rigid-plastic, incompressible and weightless Coulombian material. His solution, based on failure patterns, consisted in considering of three zones (Fig. 2.3). The Zone I and Zone III are the Rankine's active and passive zones respectively. Zone II is Prandtl's zone. The shape of the curve CD depends on the angle of internal friction, overburden pressure and the weight of the material. For a material with $\phi = 0$, the curve becomes a part of a circle.

Among the other early solutions, a graphical solution using a cylindrical slip surface was proposed by Fellenius (1929).

For weightless soil ($r = 0$) Prandtl (1921) and Reissner (1924) have found that

$$q_u = CN_c + qN_q \qquad \text{----------2.4}$$

where N_c and N_q are dimensionless bearing capacity factors defined by

$$N_q = e^{\pi \tan\phi} \tan^2 \left(\frac{\pi}{4} + \frac{\phi}{2}\right) \text{ ----------2.4a}$$

$$N_c = (N_q - 1) \cot \phi \text{ ----------2.4b}$$

For cohesionless soil having no overburden ($C = 0, q = 0$) it can be shown that

$$q_u = 1/2 \; rB \; N_r \text{ ----------2.5}$$

where N_r is a dimensionless bearing capacity factor which can be evaluated by the analytical expression

$$N_r \simeq 2(N_q + 1) \tan \phi \text{ ----------2.5a}$$

For all intermediate soil conditions, where cohesion, angle of internal friction, and overburden are present, the equations 2.4 and 2.5 can be combined into

$$q_u = CN_c + qN_q + 1/2 \; rB \; N_r \text{ ----------2.6}$$

known as Buisman - Terzaghi equation (Buisman, 1940; Terzaghi, 1943).

In deriving the above expression Terzaghi assumed that i) the infinitely long footing having a rough base rests on a semi-infinite homogeneous ideal soil mass which possesses both cohesion and friction; ii) the wedge below the footing makes

an angle of ϕ with the horizontal, iii) the failure surface is a combination of logarithmic spiral and a plane section, iv) the overburden can be replaced by equivalent surcharge load without shearing strength.

The shear resistance of the overburden was first considered by Meyerhof (1951). The failure pattern consisted of three zones - an elastic central wedge directly below the foundation, a radial shear zone at the middle and a mixed shear zone at the end (Fig. 2.4). The size of the plastic zone varies with the depth of the foundation and the roughness of the foundation base.

Meyerhof used the same equation as Terzaghi's in calculating the ultimate bearing capacity. However, the general bearing capacity factors N_c, N_q and N_r used by Meyerhof depend on depth, shape and roughness of the foundation base as well as on the angle of internal friction of the soil and can be defined by the following expressions

$$N_c = \left[\text{Cot}\phi \frac{(1 + \text{Sin}\phi)\ e^{2\ \theta\tan\phi}}{1 - \text{Sin}\phi\ \text{Sin}\ (2\eta+\phi)} - 1\right] \text{---------2.7}$$

$$N_q = \frac{(1 + \text{Sin}\phi)\ e^{2\ \theta\tan\phi}}{1 - \text{Sin}\phi\ \text{Sin}\ (2\eta+\phi)} \text{----------2.8}$$

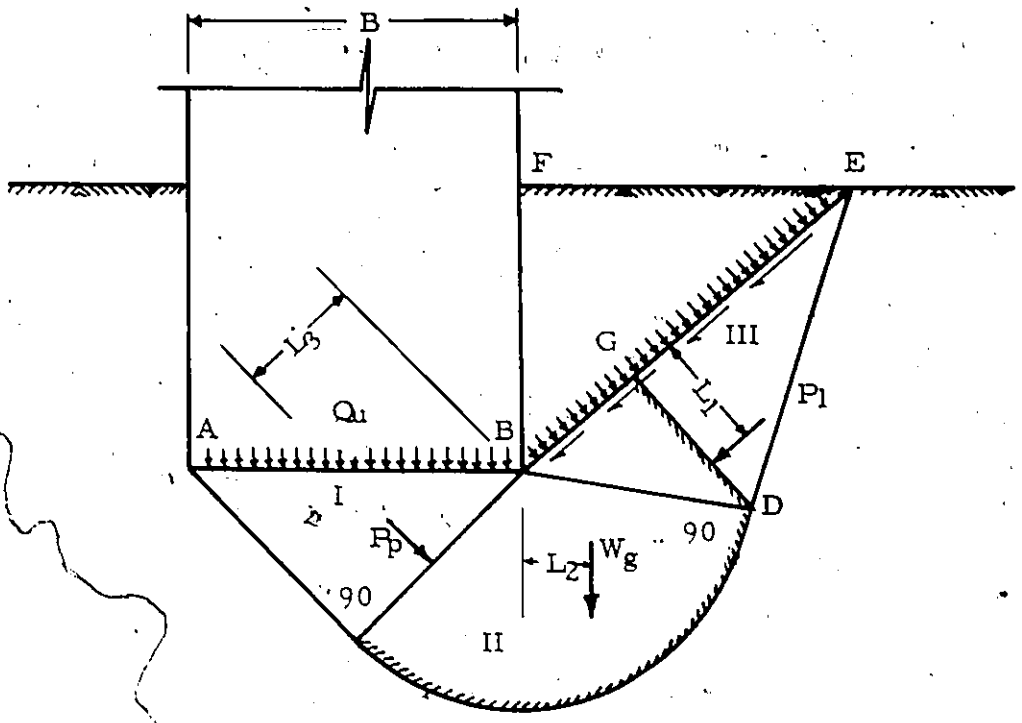

I - Elastic Zone

II - Radial Shear Zone

III- Mixed Shear Zone

FIGURE 2.4 FAILURE PATTERN FOR SHALLOW FOUNDATIONS, MEYERHOF

$$N_r = \frac{4P_p}{rB^2} \left(\text{Sin } \left(\frac{\pi}{4} + \frac{\phi}{2}\right)\right) - 0.5 \tan \left(\frac{\pi}{4} + \frac{\phi}{2}\right) \text{ -------2.9}$$

where θ is the angle subtended at the edge of the footing by the radial shear zone (Fig. 2.4) and η is the angle of the plane shear zone. P_p is the passive earth pressure on the surface BC which can be calculated from the equilibrium BCDG. Then

$$P_p = \frac{P_1 L_1 + W_g L_2}{L_3} \text{ ----------2.10}$$

P_1, L_1, W_g, L_2 and L_3 are explained in Figure 2.4.

Meyerhof (1963) proposed another equation to calculate the ultimate bearing capacity of a strip footing:

$$q_u = CN_c d_c + qN_q d_q + \frac{1}{2} rBN_r d_r \text{ ----------2.11}$$

where d_c, d_q and d_r are empirical depth factors which take into account the embedment of the foundation. These are given by the following expressions

$$d_c = 1 + 0.2 \sqrt{N_\phi}\, D/B \text{ ----------2.12}$$

$$d_q = d_r = 1 \qquad (\phi = 0) \text{ ----------2.13}$$

$$d_q = d_r = 1 + 0.1 \sqrt{N_\phi}\, D/B \quad (\phi > 10^o) \text{----------2.14}$$

The bearing capacity factors N_c and N_q are given by the equations 2.7 & 2.8 and N_r by the following equation

$$N_r = 1.5\,(N_q - 1) \tan \phi \text{----------2.15}$$

Brinch Hansen (1970) proposed and later extended a theory which takes into account the shape, depth, roughness of the base of foundation, surcharge, and inclination of the load. This theory gives better test Vs computed bearing capacities, than other available theories. According to the theory, the ultimate bearing capacity can be computed from the following expression

$$q_u = CN_c\, S_c d_c i_c g_c b_c + qN_q\, S_q d_q i_q g_q b_q + 1/2\, rBN_r\, S_r d_r i_r g_r b_r \text{------2.16}$$

where S = Shape factors to account for the shape of the foundation in developing a failure surface.

d = Depth factors to account for the embedment depth.

i = Inclination factors to allow for both horizontal and vertical foundation loads.

q = Effective surcharge pressure.

g = Ground factor.

b = Base factor.

The bearing capacity factors are computed as

$$N_q = \tan^2 (45 + \phi/2) \exp (\pi \tan\phi) \quad \text{---------- 2.17}$$

$$N_c = (N_q - 1) \cot\phi \quad \text{---------- 2.18}$$

$$N_r = 1.5 (N_q - 1) \tan\phi \quad \text{---------- 2.19}$$

The factors S, d, i, q, g, and b are combined from Brinch Hansen (1970), De Beer (1970) and Vesic (1973) and presented in appendix 1.

Other than the methods of computation of bearing capacity discussed in detail above, there have been numerous theories in recent years by various researchers. Prominent among them are Balla (1962), Hu (1964), Chen and Davidson (1973). All their theories make various assumptions regarding the formation of the wedge and in particular the angle between the base of the footing and the sides of the wedge and the shape of the failure surfaces.

2.2 Settlement

2.2.1 General

All structures ultimately transfer their load to the soil through the foundation which may settle for reasons such as the effect of additional loading of the soil by the structure, lowering of the ground water level, and diverse forms of ground surface sinking. In the following discussion, settlement produced by additional loading of the subsoil will be considered.

Feda (1978) has tabulated the available methods of calculating the settlement in four distinct groups (Figure 2.5) The first group includes mathematically exact solutions based on the theory of elasticity. As the constitutive equations do not usually correspond to real foundation soils, the results obtained are at considerable variance with reality. Moreover, as the selected mathematical model makes it impossible to predict time variations of the settlement, it is mainly employed in calculations of immediate settlement.

The second group of methods, widely used for settlement calculations for foundations on fine grained soil, makes use of the elastic theory for stress calculations; the stress-strain relations are derived from experiments. Solution obtained by this group of methods consists of several components such as immediate settlement, primary consolidation, secondary

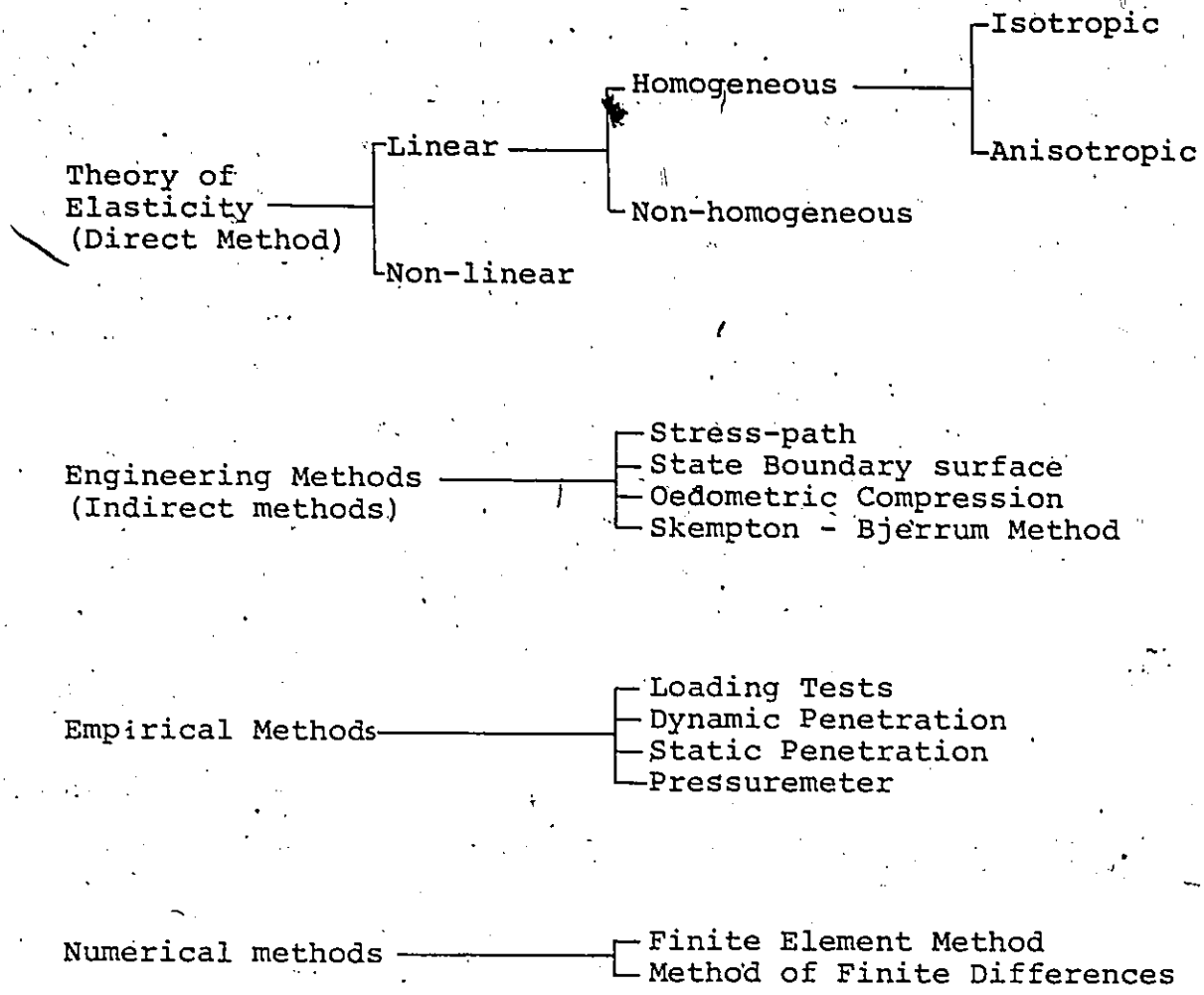

FIGURE 2.5 REVIEW OF METHODS FOR CALCULATING SETTLEMENT

consolidation and the settlement caused by the plastic pushing of the subsoil from beneath the foundation to the sides.

The third group contains empirical or semiempirical methods. These methods are used to extrapolate the results of load tests or other mechanical tests for the actual foundation specially on cohesionless soils.

The fourth group consists of numerical methods, which can handle the real non-linear stress-strain relation. The accuracy of the solution from the mathematical standpoint is limited only by the capacity of the computer. The numerical methods do not represent any independent group of methods, Rather, they are tools which can be used in the solution by means of many methods.

It is interesting to compare the methods of calculation of settlement for the foundation resting on cohesive and cohesionless soil. With cohesive soil, the approach is fairly standard based on laboratory tests requiring good representative soil samples. For that purpose with the help of improved site investigation techniques, it is possible to extract undisturbed samples from the cohesive soil deposit.

With the granular soils the situtation is different. There is a basic difficulty in obtaining an undisturbed sample apart from the question whether the sample is representative. Since the compressibility characteristics cannot be readily

obtained from the laboratory tests, methods of settlement calculation have been developed based on insitu tests from which the relative density and compressibility can be assessed. The two main types of field tests used are small scale plate loading tests and penetration tests. The penetration test could be dynamic or static depending upon the method of settlement calculation. The most common dynamic penetration test is the Standard Penetration Test (S P T), which is mostly used in North and South America and the United Kingdom. The static penetrometer test based on Dutch Cone Test has been used extensively in Europe and in recent years in the U.S.A. and Britain. The pressuremeter is also becoming increasingly popular to determine the insitu properties of the grannular soils.

2.2.2 Methods of Settlement Calculation

Terzaghi and Peck (1948) first proposed the following relationship based on the plate loading test

$$\frac{\delta_B}{\delta_A} = \left[\frac{2}{1 + A/B}\right]^2 \qquad \text{----------2.20}$$

where δ_B = Settlement of the footing

B = Width of the footing

δ_A = Observed settlement for 1 ft. square plate loaded to the same intensity

The validity of this relationship was investigated by Bjerrum and Eggested (1963). Their study of case records indicated that there can be appreciable scatter in the correlation between settlement and width of the loaded area.

Terzaghi and Peck (1948) were the first to propose a correlation between S P T blow count and the allowable bearing pressure by the Figure 2.6. The curves in Figure 2.6 can be approximated by the expression

$$\delta_B = \frac{3q_a}{N} \left[\frac{2B}{B + 1}\right]^2 \qquad \text{----------2.21}$$

where q_a = Allowable pressure obtained from the Figure 2.6

N = S.P.T. blow count

This correlation was subsequently corrected for the location of water table and the embedment of the foundation and was expressed as

$$\delta_B = C_w C_d \frac{3q_a}{N} \left[\frac{2B}{B + 1}\right]^2 \qquad \text{----------2.22}$$

where C_w = 1 for $D_w > 2B$

C_w = 2 for $D_w = 0$

C_d = 1 for $D/B = 0$

C_d = 0.75 for $D/B = 1$

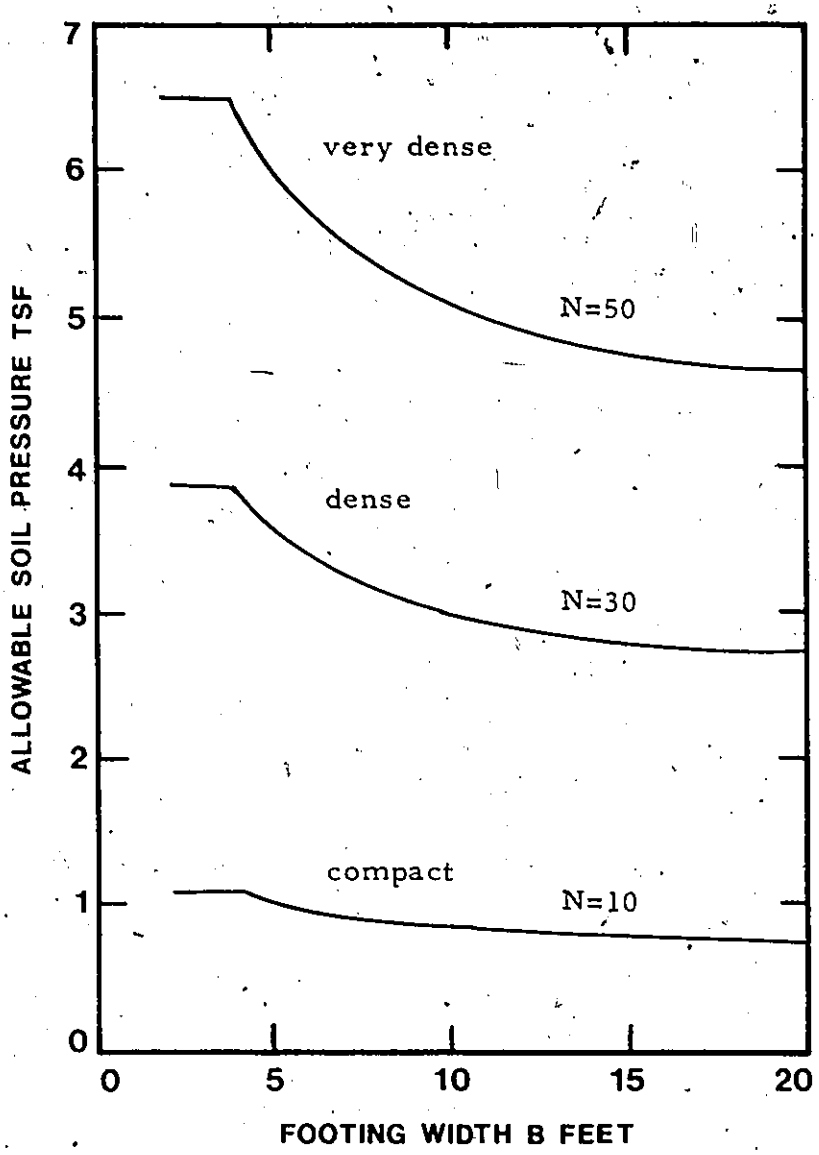

FIGURE 2.6 ALLOWABLE PRESSURE FOR NON-COHESIVE SOILS (after Terzaghi & Peck, 1948)

N = As measured for sand

N_c = 15 + 0.5 (N - 15) for very fine or silty sand below water table

Terzaghi and Peck stated that their correlation did not take into account the geologic origin and environment of the sand deposit and were therefore necessarily a conservative basis of design.

Subsequently modifications and improvements were suggested on the Terzaghi - Peck original correlation by Gibbs and Holtz (1957), Alpan (1964), Meyerhof (1965), Peck and Bazaraa (1969 and Peck (1974). Most of the modifications were on the Standard Penetration Test values and on the correction factor for ground water and embedment of footing.

Gibbs and Holtz (1957) were the first to put forward the major modification of the Terzaghi and Peck method. From laboratory investigations they demonstrated the influence of overburden pressure on the penetration resistance, which was subsequently confirmed by Mansur and Kaufman (1968), Philcox (1962), Zolkov and Wiseman (1965) from field work.

Other methods, as suggested by De Beer and Martens (1957), Meyerhof (1965), D'Appolonia (1970), Schmertmann (1970) and Parry (1971), reflected a different approach to the problem of calculating settlement. In those, the compressibility or equivalent elastic modulus is calculated for sand. The

approach by D'Appolonia et al (1970) and Parry (1971) are the obvious modifications of the classic elastic equation. These two methods are based on the direct correlation with Standard Penetration Test results. The remaining methods by De Beer and Martin, Meyerhof and Schmertmann used the Dutch cone test results as the basis of obtaining modulus of elasticity or compressibility values.

D'Appolonia (1970) proposed the following correlation to calculate the settlement

$$\delta = q\,B\,\frac{(1-\mu^2)}{E}\,I = \frac{qB}{M}\,I \qquad \text{----------2.23}$$

where q = Applied load

B = Width of footing

I = Influence factor

$M = \frac{E}{1-\mu^2}$

Poisson's ratio μ for sand is taken as 0.25 the correlations are

$E = 540 + 13.5N$ for a preloaded sand in Kg/cm^2

$E = 216 + 10.6N$ for a normally loaded sand in Kg/cm^2

The influence factor I takes into account the footing dimensions and the depth of the sand layer.

Parry (1971) put forward almost the same type of correlation as suggested by D'Appolonia with some modification in the influence factor and in the values of E based on the S P T value. This was expressed as follows

$$S = \frac{qB}{M} C_d C_w C_t \qquad \text{----------2.24}$$

$$M = \frac{E}{(1 - \mu^2)}$$

where $\mu = 0.25$

$E = 50N \quad Kg/cm^2$

N = Average value at depth $\frac{1}{4}$ B

C_d = Correction factor for depth footing

C_w = Correction factor for water table

C_t = Takes into account the depth of compressible layer

In general, D'Appolonia and Parry methods lead to lower estimates of settlements than those obtained from Terzaghi and Peck approach with modifications. In the recent years calculation of settlement of footing has moved away from the traditional Terzaghi - Peck approach with modifications.

De Beer and Marten (1957) proposed a method based on the Terzaghi - Buisman formula for the calculation of settlement of foundation on soils

$$\delta = \frac{2.3}{C} \log_{10}\left[\frac{P' + \Delta P}{P'}\right] H$$

where δ = Settlement

C = Constant of compressibility

P' = Effective overburden pressure at mid height of the layer considered

ΔP = Increment of pressure at the mid height due to the applied load on the foundation

H = Layer thickness

The value of C developed by Buisman can be represented as follows

$$C = 1.5 \frac{q_c}{P'}$$

$$CP' = 1.5\, q_c = \frac{1}{M_v} = E$$

where q_c is the static cone penetration resistance. The average ratio of the predicted settlement to the observed settlement of the cases considered by De Beer and Marten was 1.9. De Beer (1965) stated that the above method is applicable to normally loaded sand only.

Meyerhof (1965) suggested a modification on the De Beer - Buisman method on the basis of comparison of the observed settlement of 17 structures with those predicted by the method. He noted the ratio of predicted to observed settlement was about 2 and recommended an increase of allowable bearing capacity by 50% for the same calculated settlement.

Schmertmann (1970, 1978) proposed the following equation for calculating settlement

$$\delta = C_1 C_2 \Delta P \sum_{0}^{2B} \left(\frac{I_z}{E}\right) \Delta_z$$

where δ = Settlement

ΔP = Net load intensity at the foundation depth

I_z = Strain influence factor calculated from the Fig.

E = Young's modulus at the middle of the layer

Δ_z = Layer thickness

C_1 = Depth embedment factor which can be calculated from

$$C_1 = 1 - 0.5 \left(\frac{\sigma'_o}{\Delta P}\right) \geq 0.5$$

where σ'_o = Effective insitu overburden pressure at the foundation depth

C_2 = Creep factor dependent on time and can be expressed as

$$C_2 = 1 + 0.2 \log_{10} \left(\frac{t}{0.1}\right)$$

where t = Time expressed in years

In the above solution, Schmertmann adopts a simplified distribution of vertical strain under a foundation expressed as a strain influence factor I_z as shown in Figure 5.29. Using the theory of elasticity as a guide, the maximum value of strain influence factor is 0.6 which occurs at Z/B = 0.5. The influence factor reduced linearly to zero at a depth of 2B.

The value of Young's modulus E as suggested by Schmertmann (1978) is based on the Dutch cone test and given by

$$E = 2.5\ q_c$$

where q_c = Dutch cone bearing capacity in Kg/m^2 or ton/sq.ft.

Although not widely used, there exists some methods for settlement calculation as suggested by De Beer (1965), Martins (1963), D'Appolonia (1968) based on Oedometer test results and by Lambe (1967) based on stress path triaxial tests. All the authors realized the difficulty of simulating in the laboratory the real relationship between the horizontal and vertical stress in the field and also the stress history.

The magnitude of settlement in sand as predicted by available methods varies considerably. Simon (1974) made a comparison using eight methods to predict the settlements of 6 structures for which settlements have been observed.

The results are summarized in the Table 2.2.

TABLE 2.2

CALCULATED SETTLEMENTS BY EIGHT METHODS FOR SIX STRUCTURES WHERE SETTLEMENTS HAVE BEEN OBSERVED (after Simon et al 1975)

Methods	$\frac{S_{calc.}}{S_{obs}}$ Average	$\frac{S_{calc.}}{S_{obs}}$ Range
De Beer and Martens	3.22	1.0 - 4.8
Schmertmann	1.48	0.2 - 4.0
Terzaghi and Peck	1.89	0.5 - 3.2
Terzaghi and Peck (Modified by Meyerhof 1965)	0.70	0.2 - 1.1
Terzaghi and Peck (Modified by Tomlinson)	0.31	0.1 - 0.6
Peck and Bazaraa (1969)	0.63	0.3 - 1.4
Alpar	0.95	0.1 - 2.4
Parry (1971)	0.72	0.1 - 1.3

CHAPTER 3

INSTRUMENTATION AND TESTING

3.1 Instrumentation

The existing facilities available for the testing program are the sand box equipped with sand handling equipment. Other instruments used to monitor various parameters are designed and manufactured according to the need. The equipment used for all the tests in the program are:

3.1.1 Sand Box

3.1.2 Sand Handling Equipment

3.1.3 Loading Frame

3.1.4 Settlement Gauge

3.1.5 Extensometer

3.1.6 Dial Gauge

An instrumentation scheme showing the location of gauges is presented in Fig. 3.1.

3.1.1 Sand Box

The sand box 14.6 m long, 1.8 m wide and 2.2 m in depth is made of 12.7 mm thick steel plates held rigidly in place by 10WF sections 2.2 m long spaced at 0.90 m centres. The assembly of plates and WF columns are connected rigidly with horizontal I-beam (254 mm x 203 mm) which are again

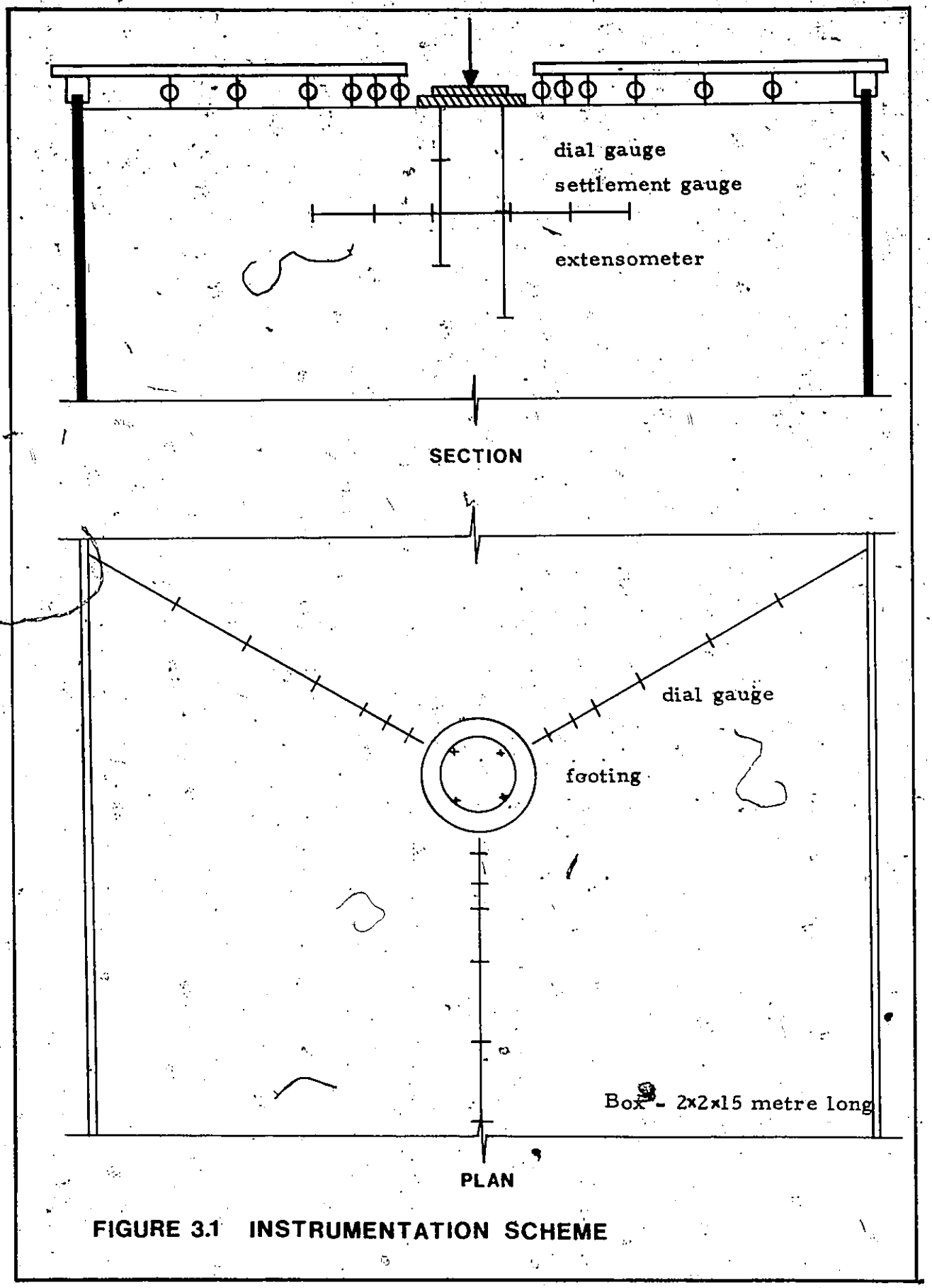

FIGURE 3.1 INSTRUMENTATION SCHEME

connected to the 0.90 m thick concrete reaction floor by 12 mm diameter steel anchors spaced at 0.9 m centre. The sand box was designed on the assumption that no appreciable deflection of the wall and the floor of the box would take place.

The box is divided into two compartments. While one is being used as a testing box, the other compartment serves as storage bin for the unused sand and the entire amount of sand in between tests.

3.1.2 Sand Handling Equipment

The sand handling equipment (Figure 3.2) consists of a spreader and an elevator. The spreader has a hopper, triangular in cross-section, 1.2 m high, 1.2 m wide at the top and 1.9 m long. The hopper with accessories is mounted on a frame which can move back and forth along the length of the box. The hopper can move vertically along the frame to facilitate the adjustment of the height of fall.

At the bottom of the hopper there is a rotating drum. The sand in the hopper first falls onto the rotating drum and then falls freely into the box. The drum speed controls the intensity of fall. There is also a deflector plate at the exit of sand which can be adjusted to give different angles of deflection. All the controls concerning the hopper, the drum and the frame are hydraulic. The height of fall, speed of drum rotation and the horizontal travelling speed of

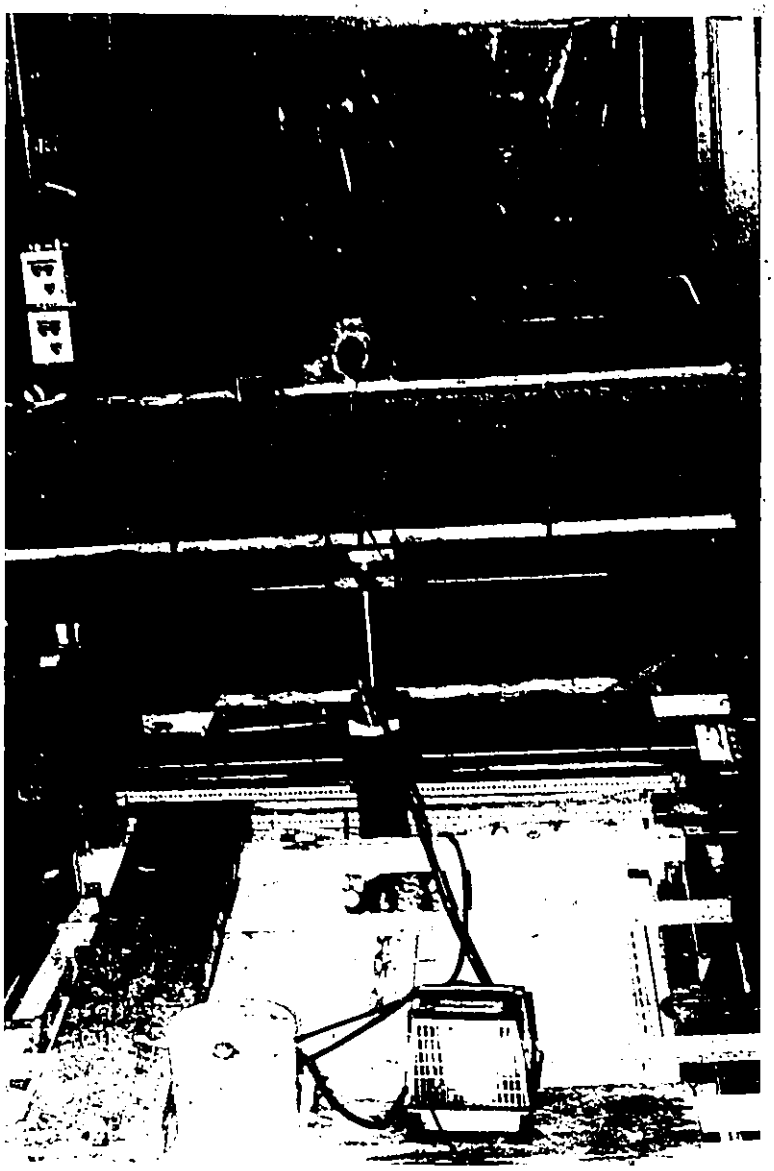

FIGURE 3.2 SAND BOX SHOWING SAND HANDLING EQUIPMENT AND LOADING FRAME

the spreader control the density of sand in the box.

The sand elevator consisting of a series of small buckets assembled on a chain is designed to feed the spreader. When the chain advances, the buckets dig into and pick up the sand and discharge into a funnel by centrifugal action. The sand is then directed into the hopper by a chute attached to the funnel. The whole assembly is held in place by a rigid frame which can move horizontally on rails along the length of the box.

3.1.3 Loading Frame

The loading frame (Figure 3.2) consists of a 514 mm x 159 mm I-Beam welded to two sets of channels 2.41 m long at both ends. The I-beam acts as horizontal member and the channels as the vertical member of the frame. The I-beam is stiffened by 13 mm thick plates at the point where the hydraulic jack is installed.

The whole frame is held at the desired locations by means of twelve 25 mm diamter bolts on either side with the vertical I-beam holding the box. A hydraulic jack was welded to 152 mm by 152 mm by 16 mm plate which was subsequently bolted to the reaction beam. The pressure exerted by the jack was monitored by a callibrated load cell between the jack and the reaction beam and linked to an electronic read-out unit.

The whole assembly of loading frame and jack is designed in such a way that the mechanism of applying loads to the model foundations can be set up over the sand without disturbing it; thus avoiding any risk of altering the initial state of compaction of the sand.

3.1.4 Settlement Gauge

A settlement gauge as shown in the Figure 3.3 was designed to monitor the settlement at various depths directly below the footing. The gauge does not give the total settlement, rather it was designed to measure the compression of the layer between the base plate of the gauge and the bottom of the footing.

The gauge was manufactured out of a tough plastic tube with an internal diameter of 4.5 mm attached to a 50 mm by 50 mm by 4.5 mm thick plexiglass plate at the base and a 3 mm diameter brass piston rod attached to a rubber piston which fits airtight in the 4.5 mm diameter cylinder. The length of the cylinder and the piston rod vary according to the depth at which they are placed. The end of the cylinder is sealed and a flexible nylon tube with an internal diameter of 1.5 mm and 3 mm external diameter is glued into a drilled hole at the side. The nylon tube is then connected to a thick walled tube having small internal diameter. Dyed water was used in the system. All the gauges were calibrated and consistent results

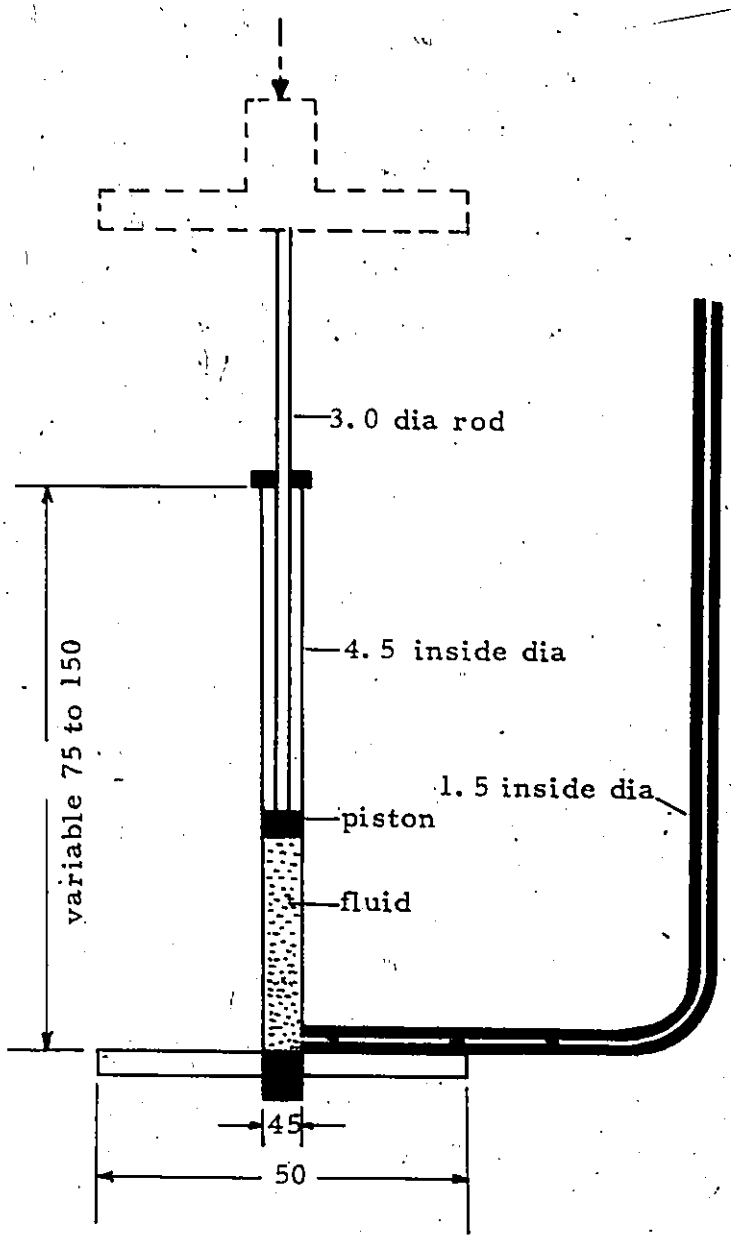

FIGURE 3.3 SETTLEMENT GAUGE
(all dimensions in mm)

were obtained. The ratio of the movement of the piston to that of the fluid in the thick walled tube was 1: 22.8.

3.1.5 Extensometer

The extensometer shown in Figure 3.4 is designed to measure the radial deformation of the media below the footing at different stages of loading. It consists of a cylinder with an internal diameter of 4.5 mm, a length of 100 mm and a rubber airtight piston attached to a brass rod of 3 mm diameter. At the end of the cylinder a 50 mm by 50 mm by 3 mm thick plexiglass plate is attached and the same end of the cylinder is connected to a thick walled stand pipe by a high pressure resistant nylon tubing. The nylon tube is coiled to accommodate the deformation and thus to avoid excessive stressing of the tubes. A 50 mm by 50 mm by 2 mm brass plate is welded at the other end of the brass rod.

When the instrument is put in place, the piston is pushed through almost the whole length of the cylinder leaving only a small space between the piston and the cylinder head to accommodate any movement of the media towards the centre of the footing. The space between the two plates attached at the ends of the cylinder and the piston rod is the monitoring zone for the radial displacement. When the plates move away, the piston draws the fluid into the cylinder. The ratio of the movement of the piston to the movement of the fluid in the

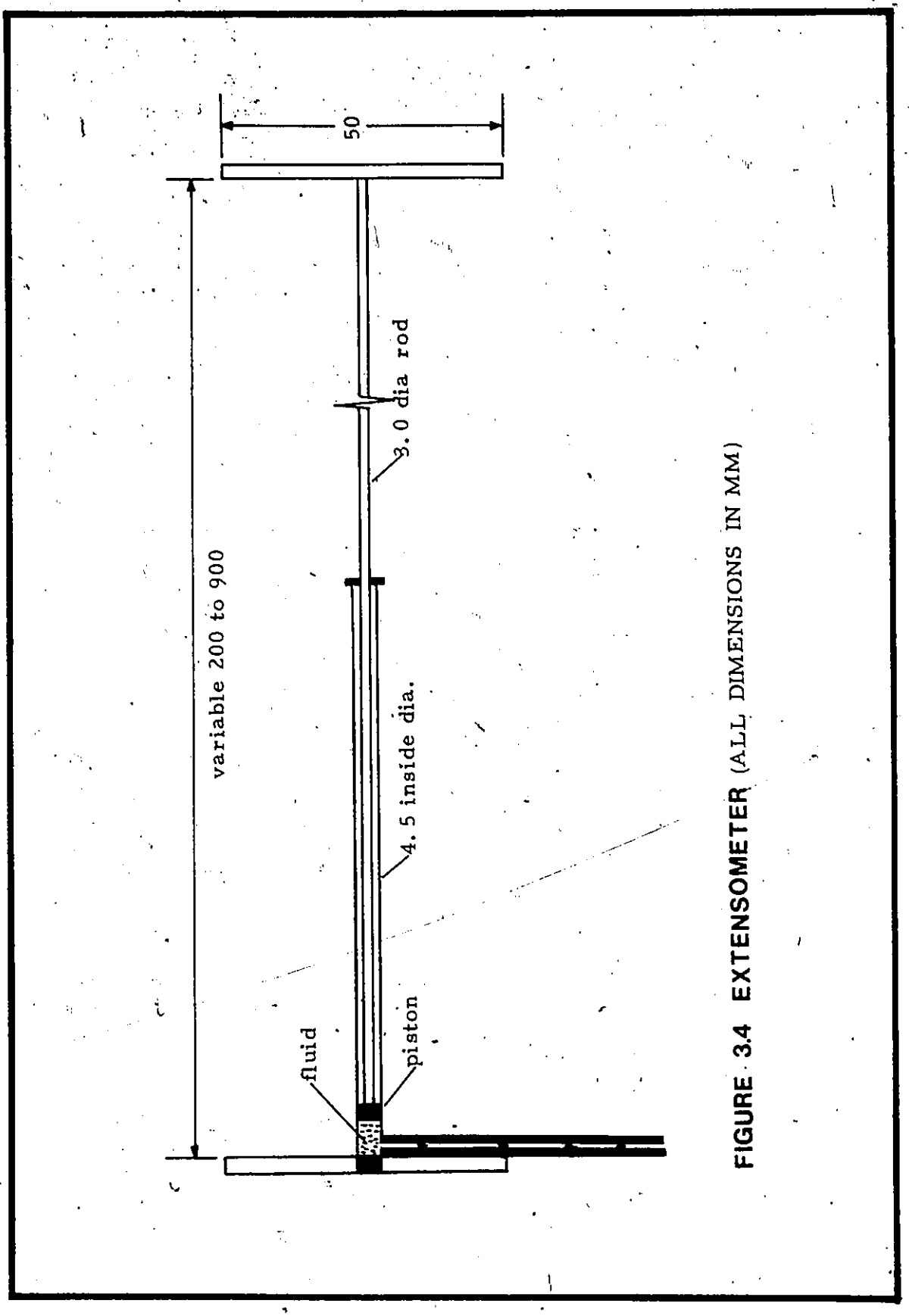

FIGURE 3.4 EXTENSOMETER (ALL DIMENSIONS IN MM)

stand pipe is 1:22.

3.1.6 Dial Gauges

Dial gauges were used to monitor the movement of the surfaces of sand around the footing. Glass plates 4 mm by 4 mm were placed at every monitoring point on the sand surface so that the stems of the dial gauges did not penetrate into the sand. A frame was made of angles, with three arms at 120° apart. Six dial gauges were fixed on each arm (Figure 3.5). The whole frame is supported by the sides of the box. The accuracy of the dial gauges used is 0.01 mm.

3.2 Testing Process

The testing process is divided into several steps: spreading of sand, measurement of densities, instrument placing, positioning the footing and loading frame, and load application. Altogether seven tests were run, two at each of the three relative densities (63, 80 and 96 percent) preceded by a pilot test using various types of instruments. The performances of the instruments used in the subsequent tests were verified and tested with pilot test.

3.2.1 Sand Used in the Test Program

The sand used in the experiments is a factory crushed quartz white sand. The manufacturer designated the sand as

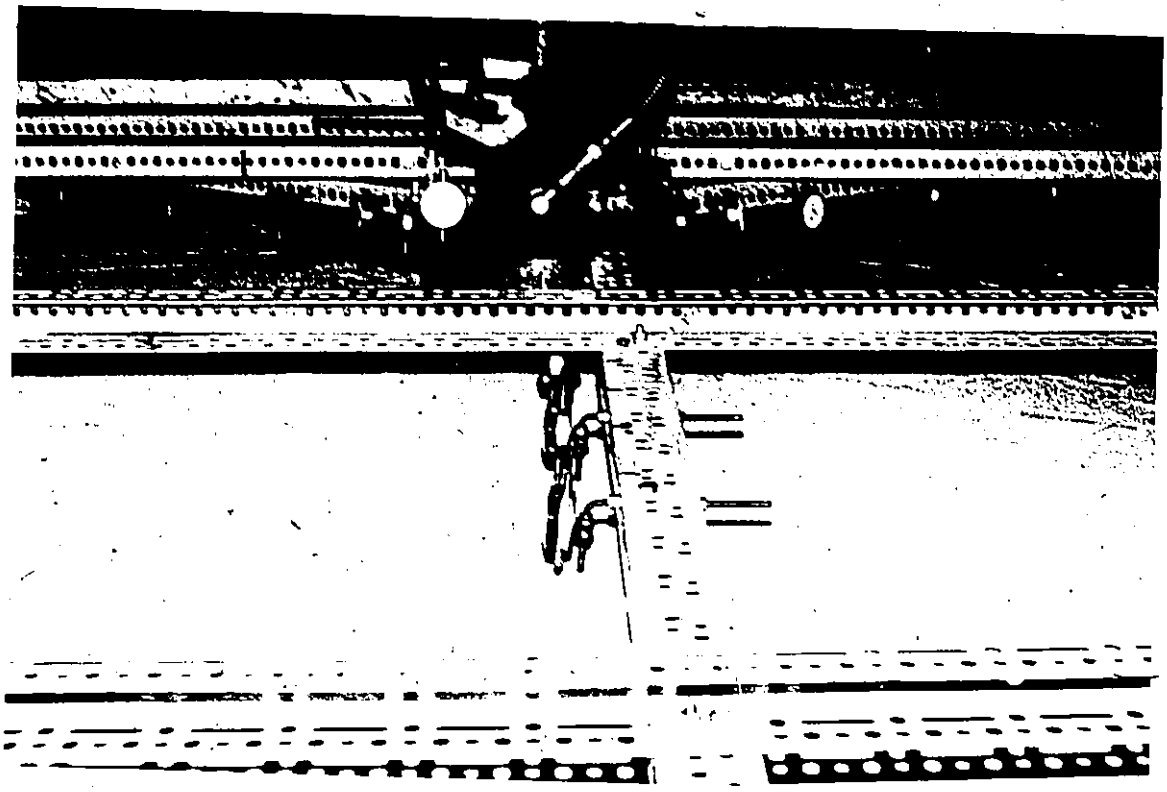

FIGURE 3.5 DIAL GAUGE WITH THE FRAME

silica-24. The strength properties of the sand were determined by Hasnain (1974) who performed a number of triaxial and direct shear box tests. The preparation of the samples for the tests was simulated with the spreading operation followed in the sand box. The sand was spread in layers using a miniature spreader.

Figure 3.6 shows the grain size distribution curve which confirms the sand to be in fine to medium range. With a uniformity coefficient of about 2.1, it can be classified as a uniform sand. The maximum and minimum densities using ASTM procedures are 1660 kg/m^3 and 1250 kg/m^3 respectively. The specific gravity of the particle is found to be 2.66. The minimum and maximum void ratios are 0.61 and 1.13 and corresponding porosities are 0.38 and 0.53 respectively. Figure 3.7 shows the relationship between the unit weight and the relative density of the sand. And Figure 3.8 shows the variation of angle of internal friction with the relative density of sand. Some other properties are presented in the Appendix 2.

3.2.2 Spreading of Sand

The spreading operation was accomplished with the help of sand handling equipment described earlier. The sand is loaded in the hopper with the elevator. The height of fall, drum speed and the horizontal travelling speed of the assembly are adjusted according to the calibration for each

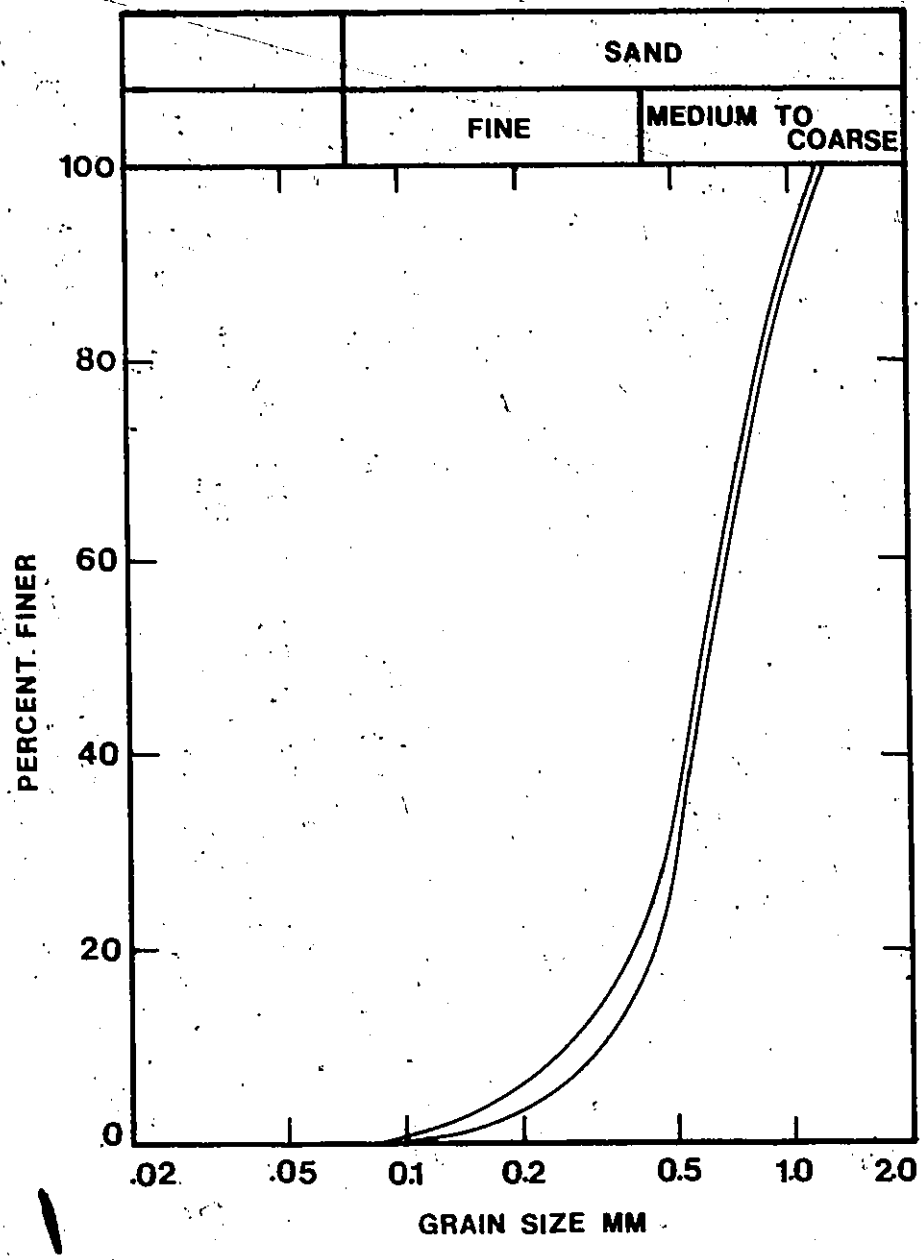

FIGURE 3.6 GRAIN SIZE DISTRIBUTION OF SAND

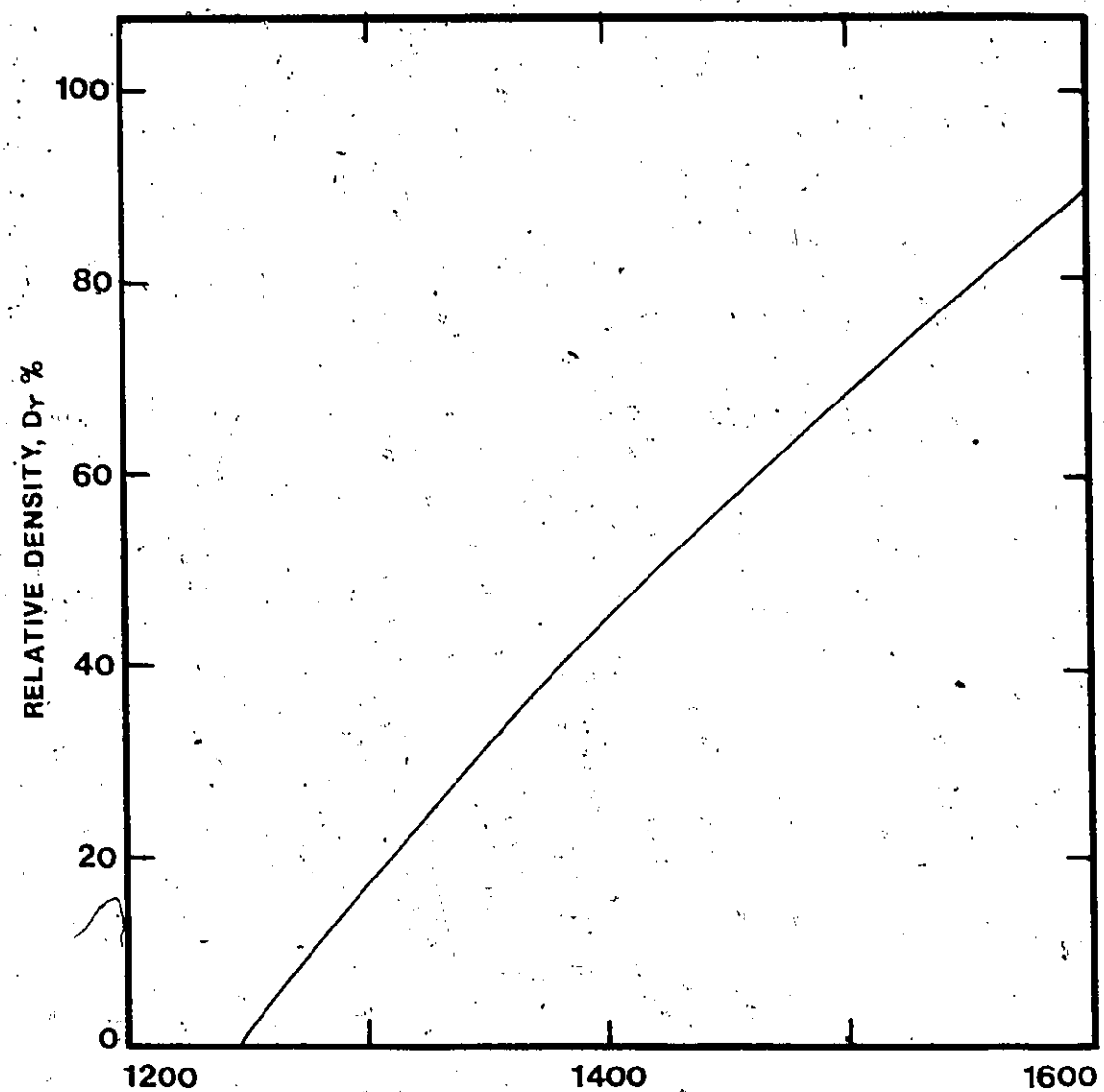

FIGURE 3.7 ϒ - D_r RELATIONSHIP

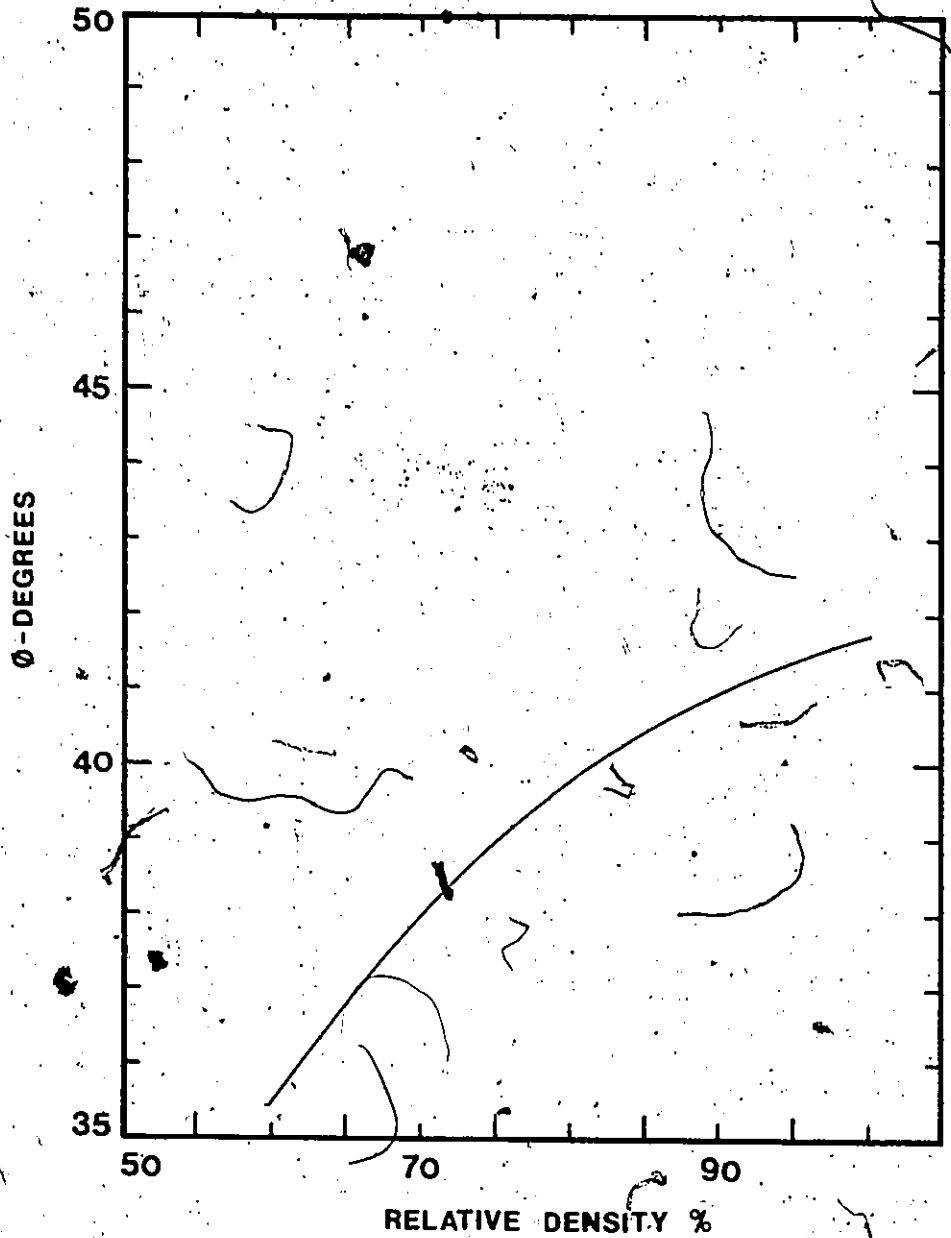

FIGURE 3.8 Ø - RELATIVE DENSITY RELATIONS

particular density. As the box is being filled up, all the parameters are adjusted to maintain a constant density. Between 7 and 10 days are required to fill the box to achieve the highest density (D_r = 96%). As the dust from the spreading operation is very fine and takes long time to settle, some precautionary measures are taken to prevent the dust from spreading. The box is housed in a plastic tent equipped with a high capacity exhaust system. Moreover, masks and eye protection are necessary during the spreading.

3.2.3 Measurement of Densities

Although the spreader is calibrated to give the desired density of the sand, measurements are carried out at various depths using containers of known volume. The edges of the containers are very sharp in order to minimize dropping of the sand grains after hitting the container. Three containers are placed along the length of the box at a particular depth. To obtain the relative density/density for each setup, the average of all the measurements is chosen. The Table 3.1 shows the density measurements during spreading for various tests.

3.2.4 Instrument Placing

Several types of instruments are used during pilot test to assess their performance so that they can be used

TABLE 3.1

DENSITY MEASUREMENTS

	Depth (in m.)	Unit Weight (gm/cc)	Relative Density (%)	Average Relative Density (%)
	(1)	(2)	(3)	(4)
TEST SET I	1.07	1.610	94.50	
		1.636	102.00	
		1.614	96.60	
	0.64	1.592	90.96	
		1.636	102.34	96.63
		1.612	95.98	
	0.31	1.593	91.26	
		1.632	100.91	
		1.608	95.06	
SET II	0.76	1.574	86.29	
		1.535	75.83	
		1.562	83.11	
	0.46	1.569	85.09	
		1.530	74.53	79.95
		1.537	76.36	≈80.00
SET III	0.23	1.569	85.09	
		1.539	77.14	
		1.536	76.02	
	0.76	1.489	62.71	
		1.494	64.30	
		1.482	60.70	
	0.23	1.402	60.85	
		1.495	64.66	63.47
		1.506	67.60	

for subsequent tests. The instruments used for subsequent tests were:

1. Settlement Gauges
2. Extensometers
3. Dial Gauges

The settlement gauges were placed at four different depths - 60, 45, 30 and 15 cm directly below the footing and at a distance of 10 cm from the centre of the footing (Figure 3.1). These are used to monitor the settlements at the depths mentioned above. The settlement gauges were placed during the spreading operation (Figure 3.9) when a desired depth was reached. The nylon tubings leading from the instrument to the stand pipe outside the box are passed through the predetermined holes on the wall of the box.

The extensometers were placed (Figure 3.10) at a depth of 30 cm below the base of the footing to monitor the movement of sand in the horizontal plane. The monitoring zones were 0.22, 0.56 and 0.9 metre and the instruments were centered with the centre of the footing. The tubings connecting the instruments to the outside stand pipe were passed through the holes made earlier in the sand box wall.

A total of eighteen dial gauges - six in each direction 120° apart around the footing (Figure 3.4) were used to monitor the movement of sand surface at various stress levels.

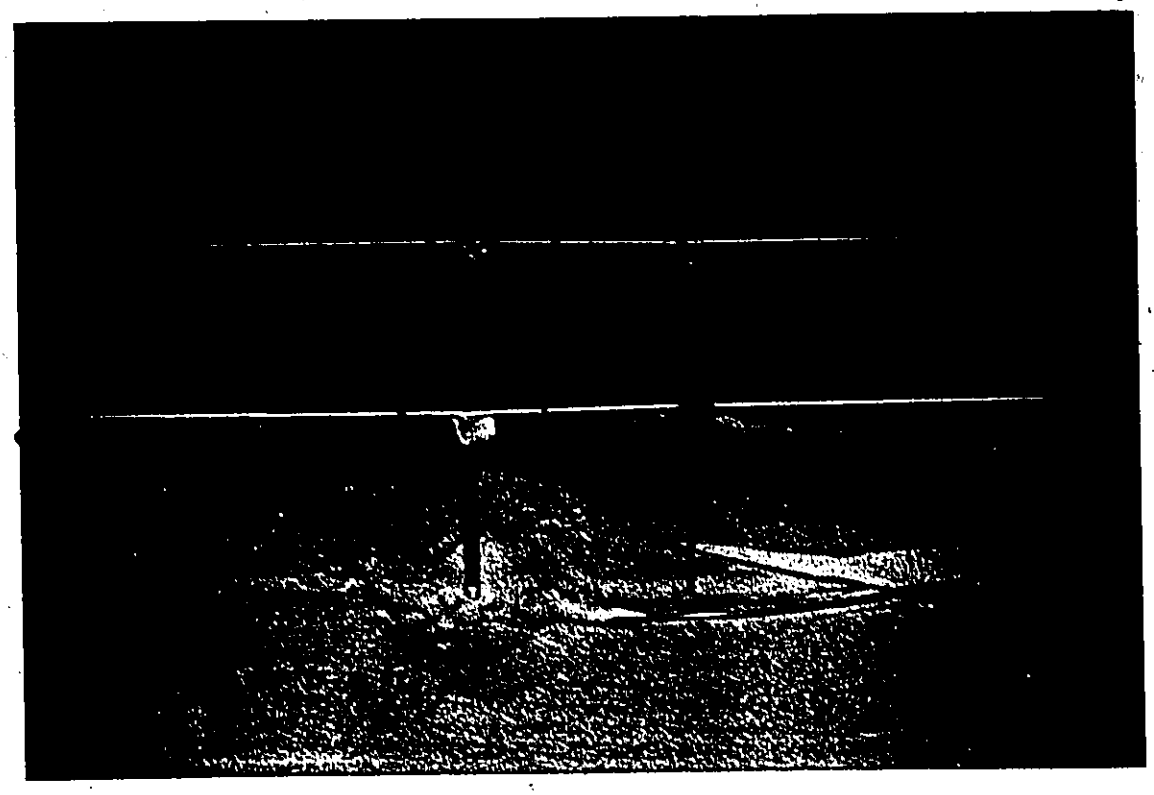

FIGURE 3.9 SETTLEMENT GAUGE IN POSITION

FIGURE 3.10 EXTENSOMETER IN POSITION

Another three dial gauges at 120° apart were placed right on the footing to monitor the footing movement at different stages of loading.

3.2.5 Positioning the Footing and Loading Frame

After the sand is spread and brought to the desired level of testing, the footing is positioned by the overhead crane on the sand surface so that the centre of the footing lies directly on a predetermined point through which the vertical axis of the loading jack passes.

With the footing in position, the loading frame is transported by the overhead crane and bolted to the vertical I-beam fixed to the walls of the box. Necessary care was taken so that the centre of the footing and the vertical axis of the loading jack attached to the frame lie in the same plane. The jack was then lowered into position as that it just touched the footing. A measuring tape is attached to monitor the movement of the jack.

3.2.6 Testing

The footings are then progressively loaded to failure. To facilitate the reading of various instruments used to monitor the different parameters, the load is applied by increments. When the sand is at relative density of 96 percent, the increment is 60 kPa but for the relative densities

of 80 and 63 percent the load increments are 30 kPa. In at least one test for every setting, the footing was pushed into the sand to determine the location of the failure surface and the extent of the heaving area.

3.3 Experiment Results

The results of experiments are presented in the following pages. Figures 3.11, 3.12 and 3.13 represent the load settlement curves for the tests at various relative densities. The two curves on the same figure represent the two tests performed on the sand at same relative density. Although the two tests were performed at the same relative density, there is a deviation of one from the other in all the tests. This may be attributed to factors such as particle rearrangement, inter-particle contacts, angularity of the particles, and moreover the variation of relative densities at different points in the box.

From the curves it can be observed that there is no distinct failure point in any of the test at the three different densities. Load increases continuously with the increase of penetration of the footing even without any yield point on the curves. This continuous load increase may be due to the surcharge effect that develops as the footing starts penetrating into the soil and partly to the increase in density due to consolidation specially at loose state

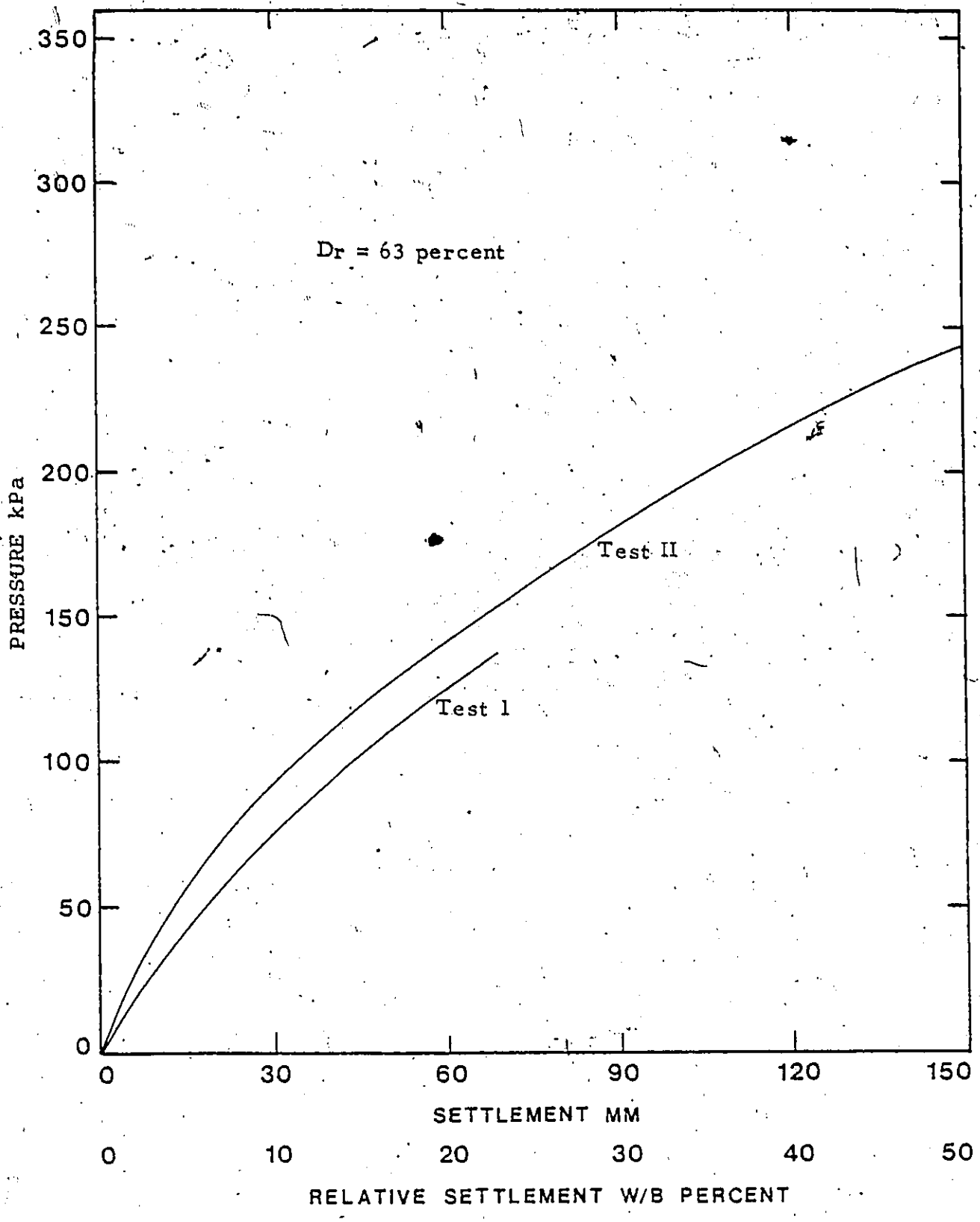

FIGURE 3.11 LOAD-SETTLEMENT CURVE

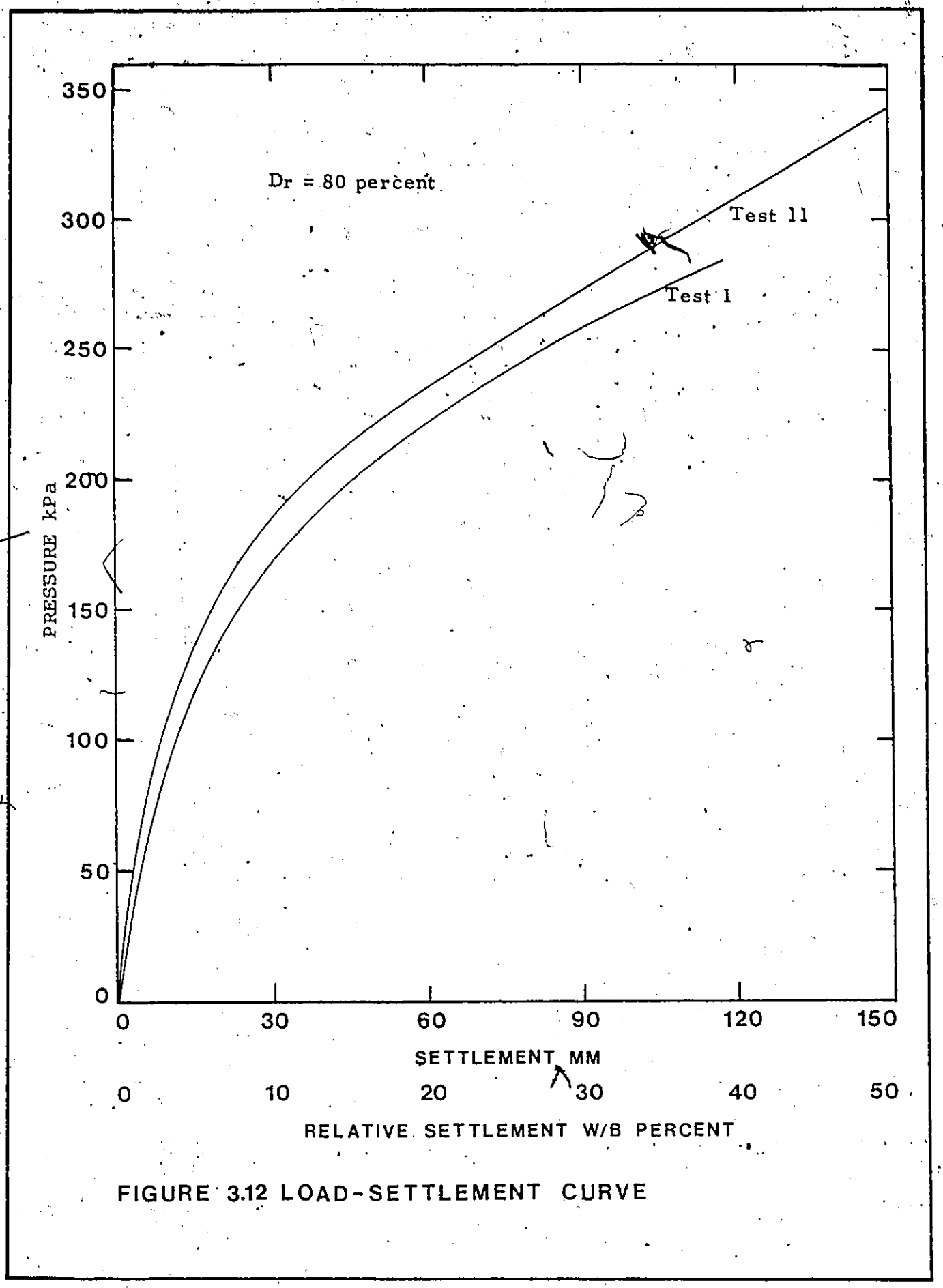

FIGURE 3.12 LOAD-SETTLEMENT CURVE

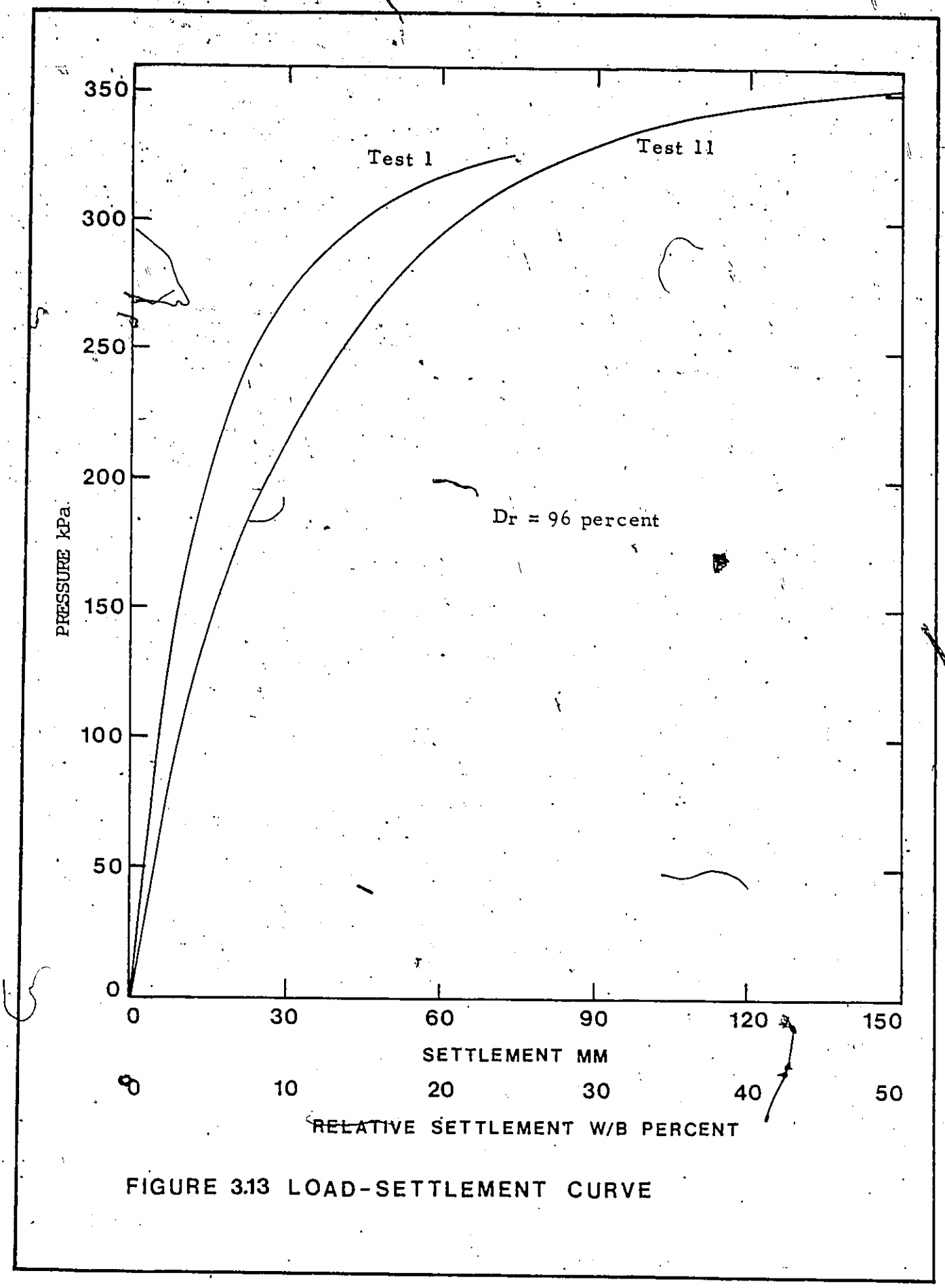

FIGURE 3.13 LOAD-SETTLEMENT CURVE

of sand.

At least one test at each density was carried out up to a settlement value equal to 50 percent of the footing diameter.

Figures 3.14 (a), 3.14 (b) and 3.14 (c) represent the variations of settlment with depth at different stress levels for the three densities. It is evident from all the curves that an appreciable amount of settlement occurs at a depth twice the diameter of the footing. The surface settlements are much higher at lower density than that at higher density. For example, the surface settlements at a load of 61 kN/m^2 are 16 mm, 7 mm and 6 mm for the relative densities 63, 80 and 96 percent respectively. Again, the variation of surface settlement with densities will depend on the stress level as the failure occurs at low stresses for sand at a lower density.

Figure 3.15 represents the variation of radial deformation in percentage of the distance between the two monitoring plates with the radial distance from the centre. The radial deformation was monitored at a depth of 30 cm from the bottom of the footing and the monitored zones were 22, 56 and 90 cm in diameter.

It was observed that the deformation varies almost linearly at low stress levels for higher densities but for

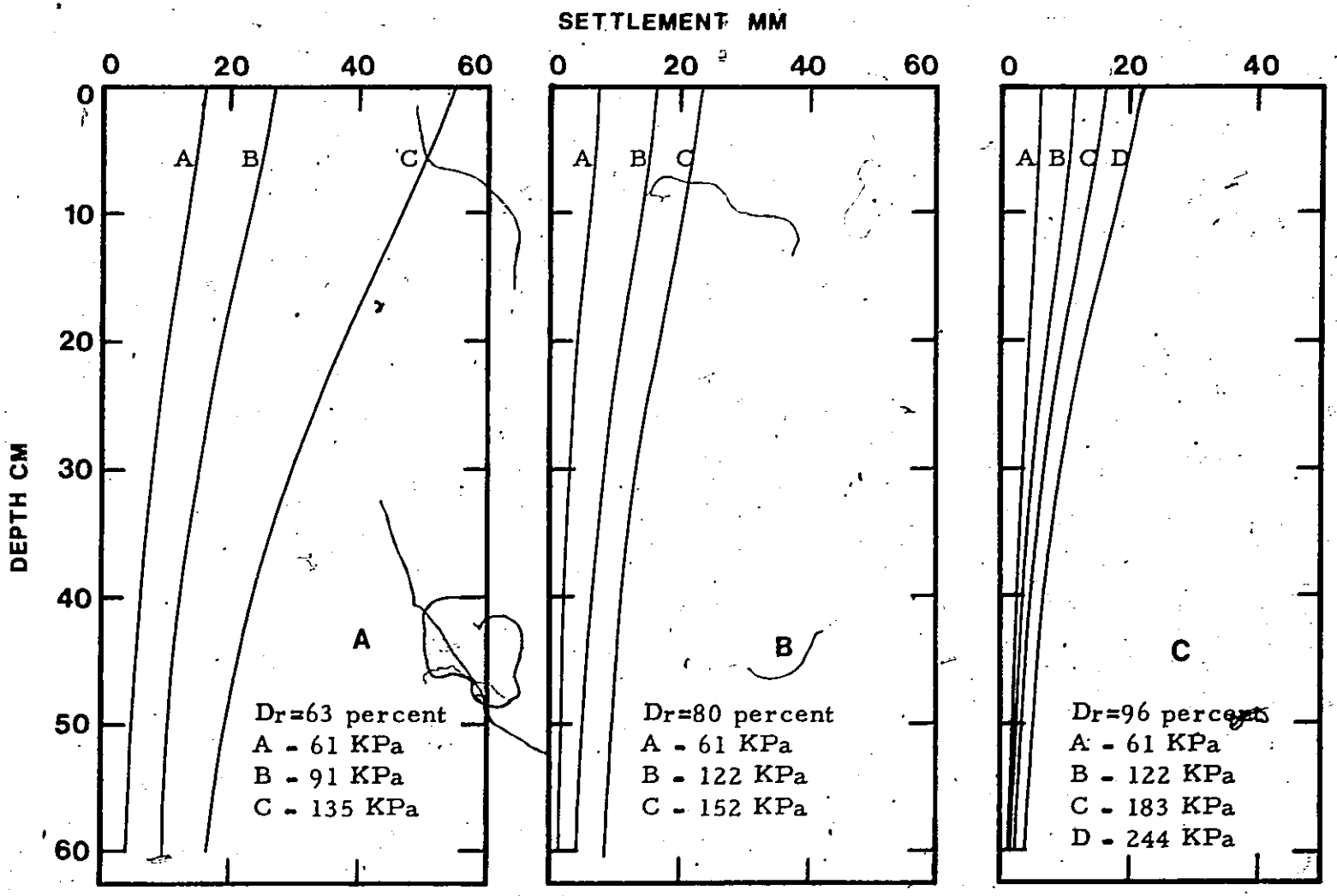

FIGURE 3.14 SETTLEMENTS AT VARIOUS DEPTHS BELOW THE FOOTING

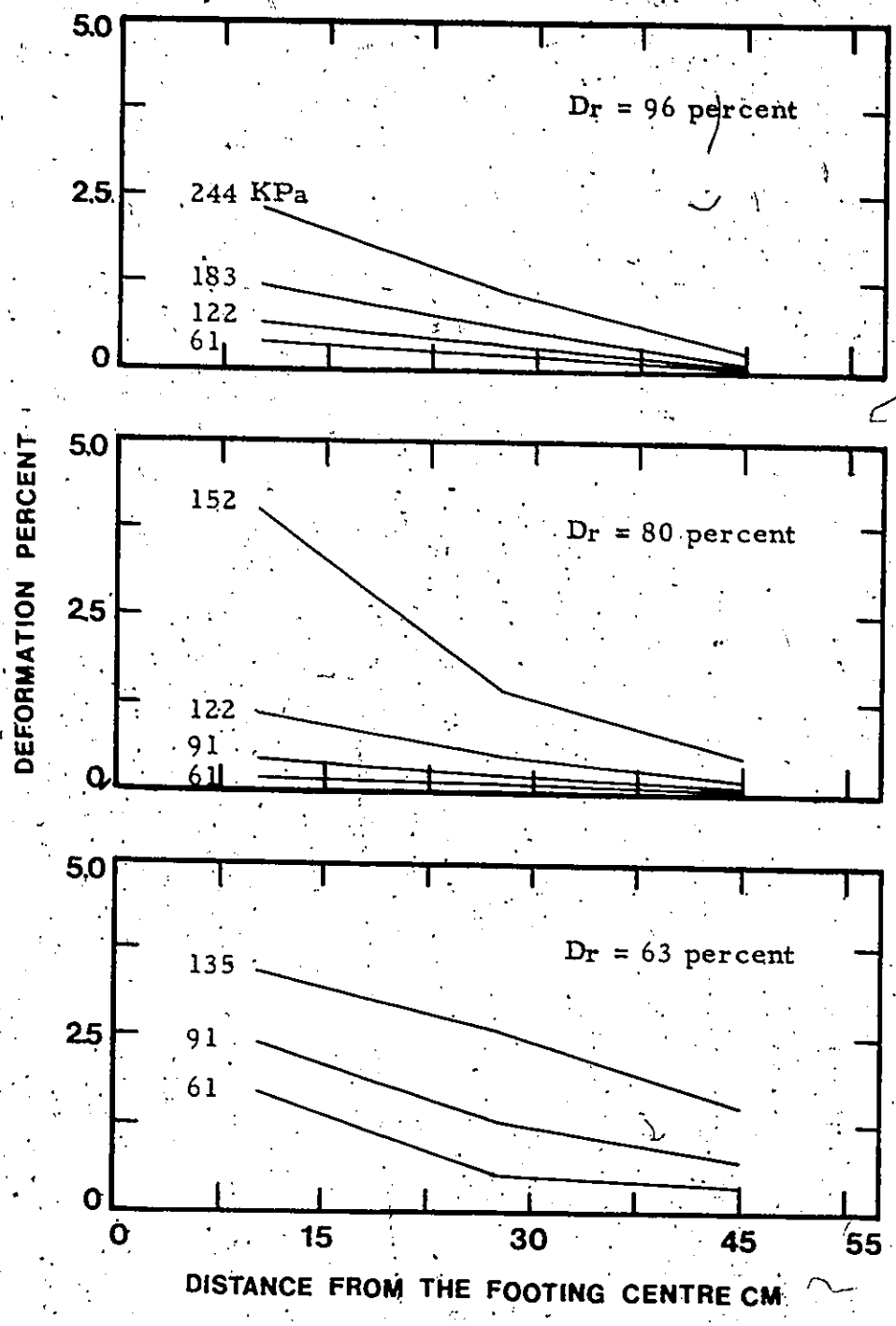

FIGURE 3.15 RADIAL DEFORMATION AROUND THE FOOTING

low densities, the deformation is more in the vicinity of the footing and decreases rapidly as the distance from the footing increases. The deformation is negligible at, and beyond 45 cm from the centre of the footing.

Figures 3.16, 3.17 and 3.18 represent the movement of the sand surface around the footing at various stress levels and increasing distance from the edge of footing. At a higher relative density, considerable heaving takes place at all stress levels. But at a relative density of 63 percent, there is very little heaving that the sand is being consolidated under the loading.

Figure 3.19 represent the failure surfaces at 96 per cent reactive density. At this density, the failure surface was distinct and easy to locate with a probing rod. At other densities there is no distinct failure surface and it was difficult to locate the failure plane.

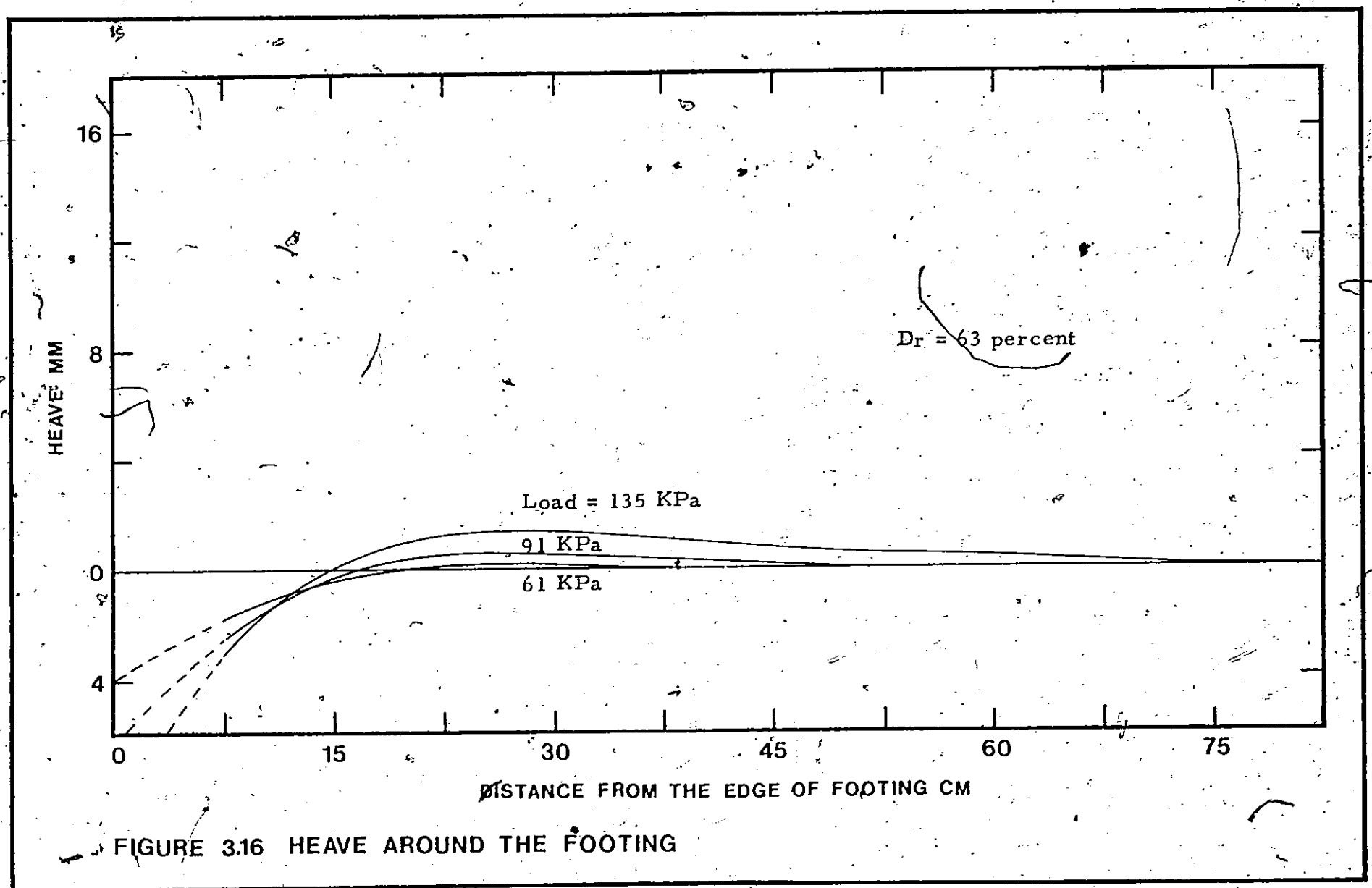

FIGURE 3.16 HEAVE AROUND THE FOOTING

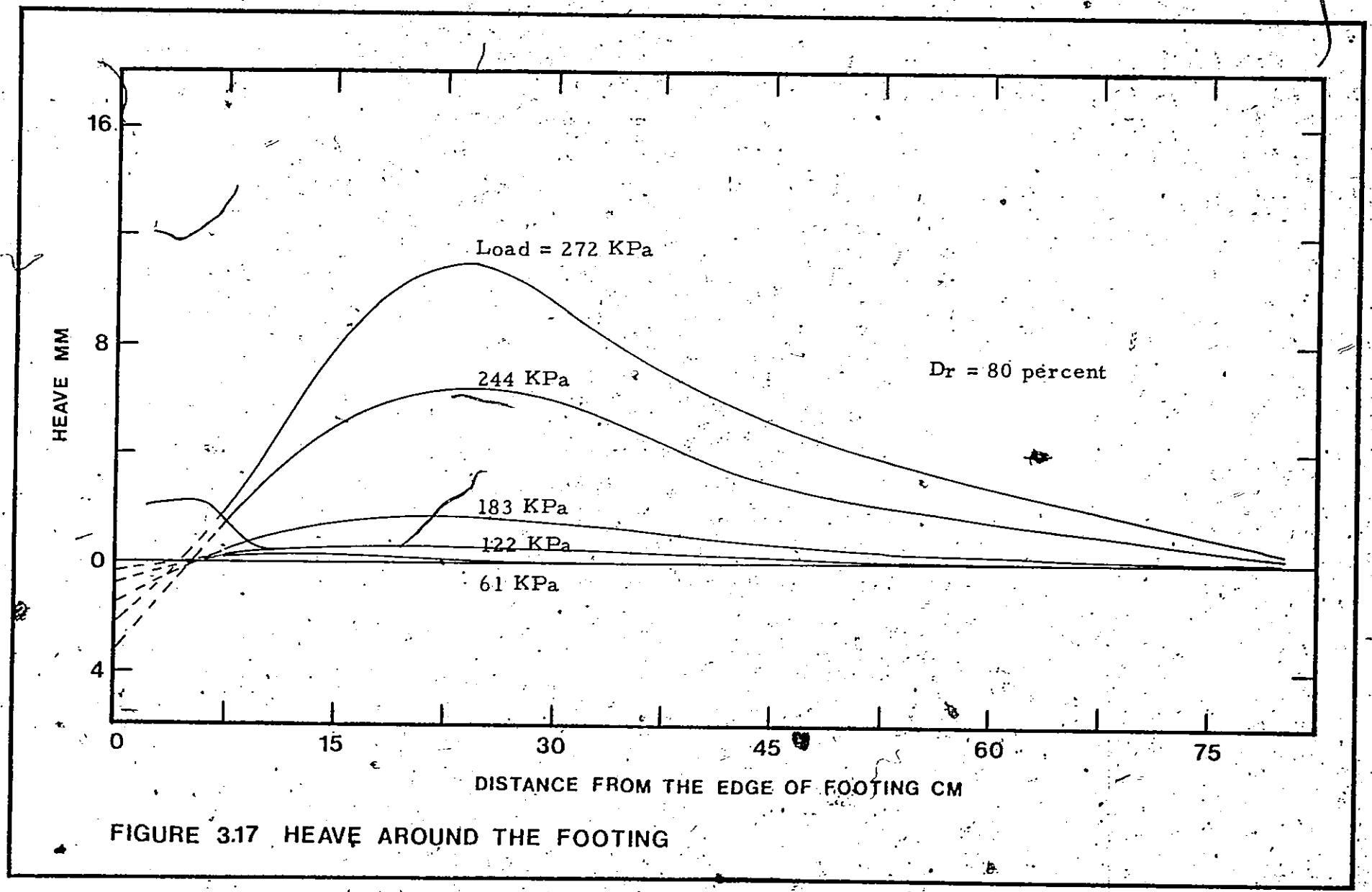

FIGURE 3.17 HEAVE AROUND THE FOOTING

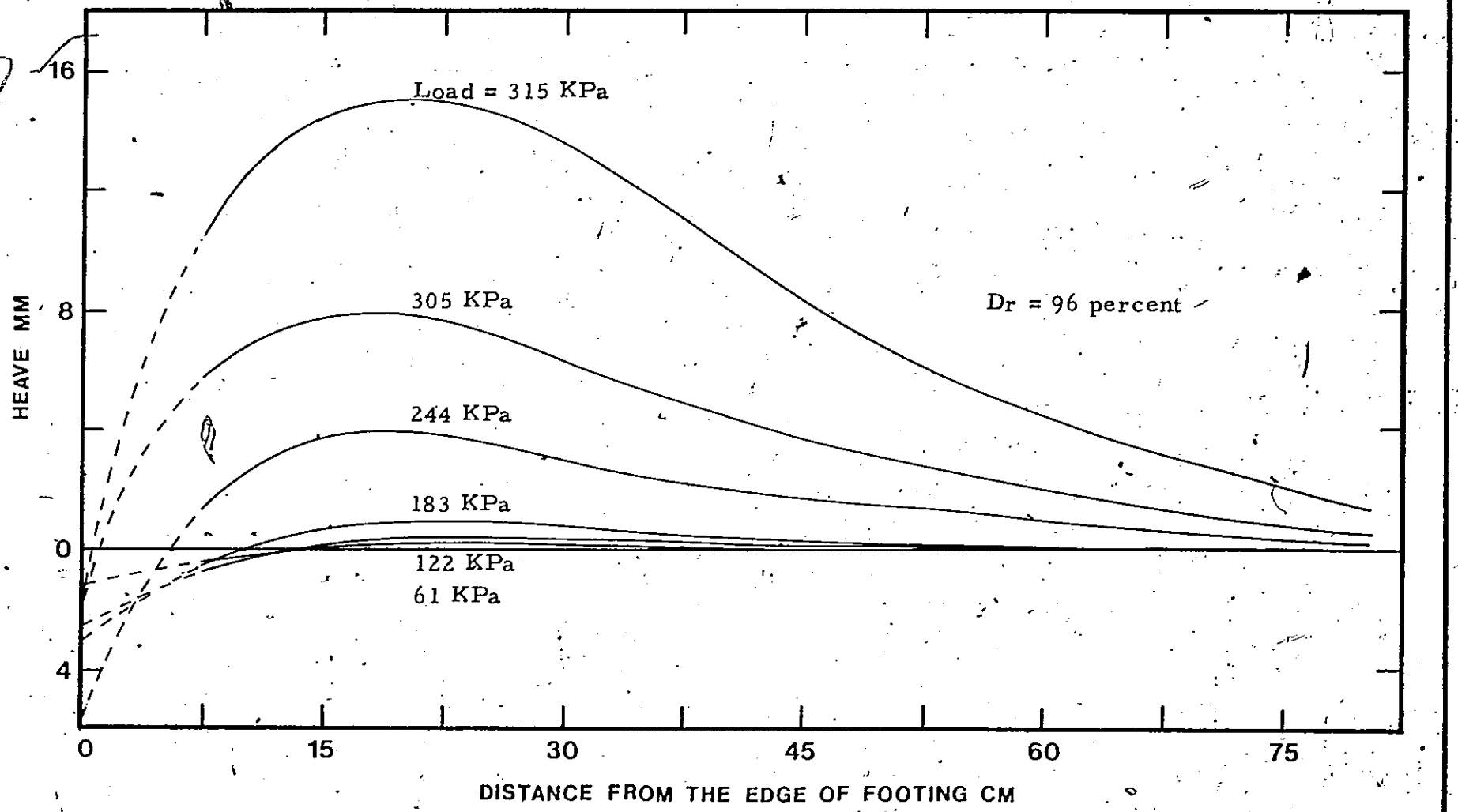

FIGURE 3.18 HEAVE AROUND THE FOOTING

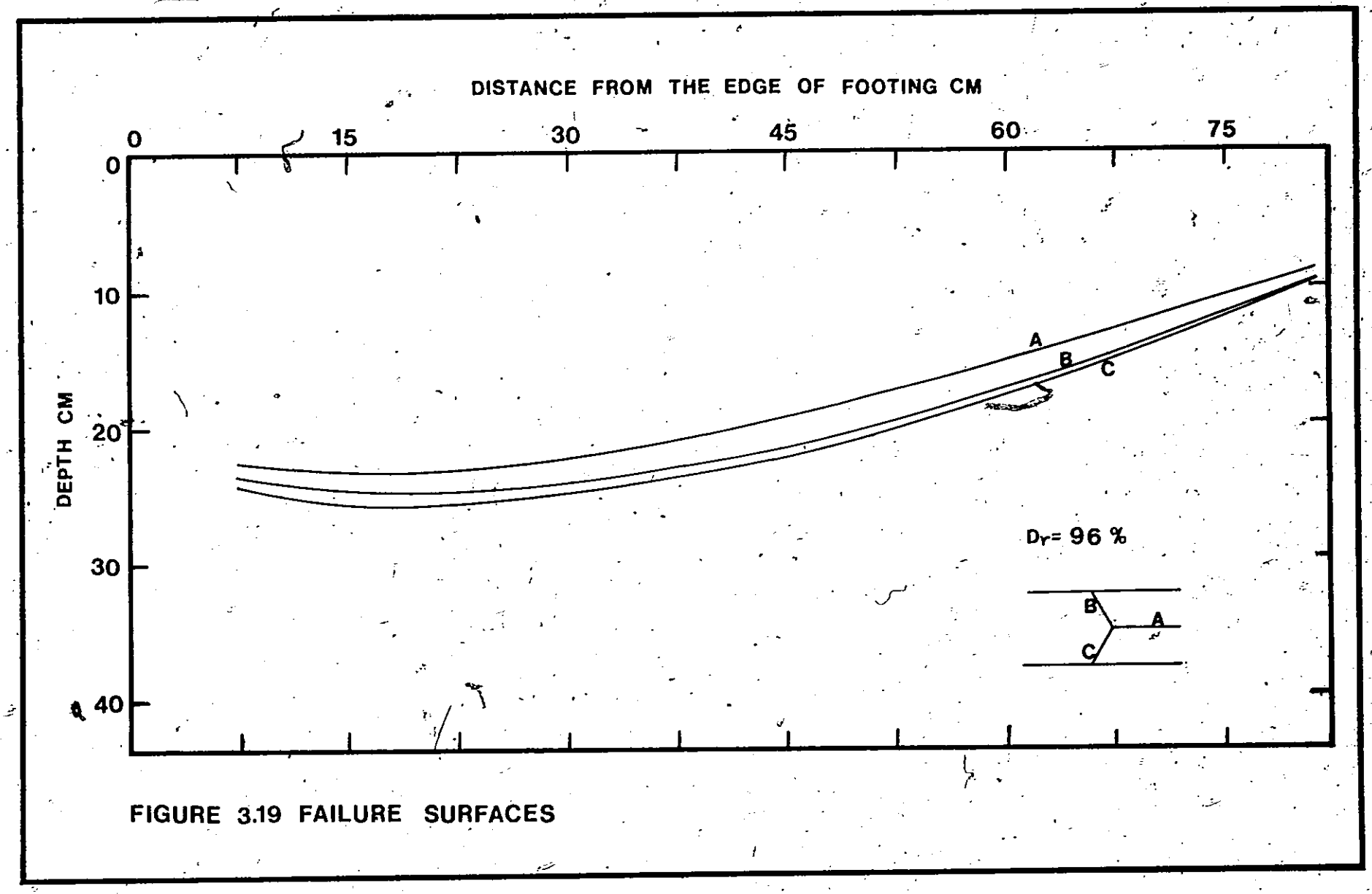

FIGURE 3.19 FAILURE SURFACES

CHAPTER 4

FINITE ELEMENT ANALYSIS

4.1 General

A simulation of the footing test is done with a mathematical model and finite element analysis is considered as the basis for the elaboration of the model. In the analysis the footing is considered as a rigid plate with some finite rigidity defined by the following equation:

$$K_r = \frac{E_b}{E_s} (1 - \nu^2) \left(\frac{t}{a}\right)^3$$

where K_r = Relative rigidity of the plate

E_b = Young's modulus of the plate

t = Thickness of the plate

a = Radius of the plate

E_s = Modulus of soil media

ν_s = Poisson's ratio of the soil mass

$K_r = 0$ represents a completely flexible plate i.e. the load is directly applied on the soil media whereas a very stiff plate is represented by $K_r \geq 100$.

As the plate used during the test is rigid, the load applied through the jack is considered uniformly distributed over the area of the plate. The soil media, i.e. the sand,

is considered isotropic elastic solid media, which may behave as homogeneous or nonhomogeneous, where the properties change with depth. For simplicity, the contact between the plate and the supporting elastic media is assumed to be smooth.

It should be noted that the problem described above is essentially a three dimensional problem. However, since the problem is limited to only axisymmetric loads and plates, it can be reduced to a two dimensional one. Furthermore, the analysis is restricted to only elastic range.

4.2 The Finite Element Method in General

The finite element method has recently become a useful tool for the analysis of practical problems encountered in Geotechnical Engineering. The extensive use of this method is made possible through the availability of fast computers with vast storage capacity and the refinement of the method itself. One of the main advantages of finite element method is that the problem is formulated in such a way that it requires only the solution of simultaneous linear equations. Although these equations may contain a large number of unknowns, they can be efficiently arranged to produce banded matrices.

The solution, with this method, follows an orderly procedure which can be summarized as follows (Desi and Abel, 1972):

1. Discretization of the continuum

Discretization may be described as the process in which the continuum is subdivided into an equivalent system of finite elements. In the present analysis, axisymmetric solid elements of triangular cross section are used to subdivide the solid media.

2. Selection of displacement model

Displacement functions are chosen in the form of polynomials to represent approximately the actual distribution of displacements. The number of terms to be retained in the polynomials depends on the degree of freedom chosen for each node.

3. Derivation of the element stiffness matrix

The stiffness matrix consists of the coefficients of the equilibrium equations derived from the material and geometric properties of an element.

4. Assembly of the algebraic equations for the continuum

This is the process during which the overall stiffness matrix of the entire structure from the individual element stiffness matrices and the overall force from the element nodal force vectors are assembled.

5. Solution for the unknown displacements

The algebraic equations assembled in step 4 are solved for the unknown displacements.

6. Computation of stress

In general, the stresses, strains and flexural moments are in the derivatives of the nodal displacement. Since the displacement at any point within the element can be determined from the nodal displacement, so can the stresses, strains and moments.

4.3 Assumptions in the Analysis

1. The flexural behaviour of the structural foundations is represented by the classical Poisson-Kirchoff thin plate theory which assumes that

   a) the thickness of the plate is small in comparison to its lateral dimensions

   b) the deflection of the plate is small compared to its thickness

   c) the strain energy is composed of only the flexural energy.

2. The plate (footing) is supported by the solid media (soil) assumed to behave as an isotropic and elastic continuum.

3. The contact between the circular plate and the soil is assumed to be smooth and capable of sustaining tensile fractions.

The assumption 3 is not realistic, because it neglects the frictional forces developed at the interface. It has been observed that for a completely rigid plate resting on a very compressible elastic half-space, the central deflection for smooth contact is about 9.0 percent higher than those for rough contact. However, as the Poisson's ratio of the elastic media approaches to 0.5, the effects of types of contact become insignificant.

4.4 Method of Analysis

The solution of the problem using finite element method of analysis follows an orderly step-by-step procedure which has been described earlier. A brief description of the development of the finite element model for the particular problem is given below:

The circular plate is modelled as an assemblage of annular plate elements with three degrees of freedom. The isotropic elastic solid media is modelled using axisymmetric solid elements of triangular cross-section as shown in Figure 4.1.

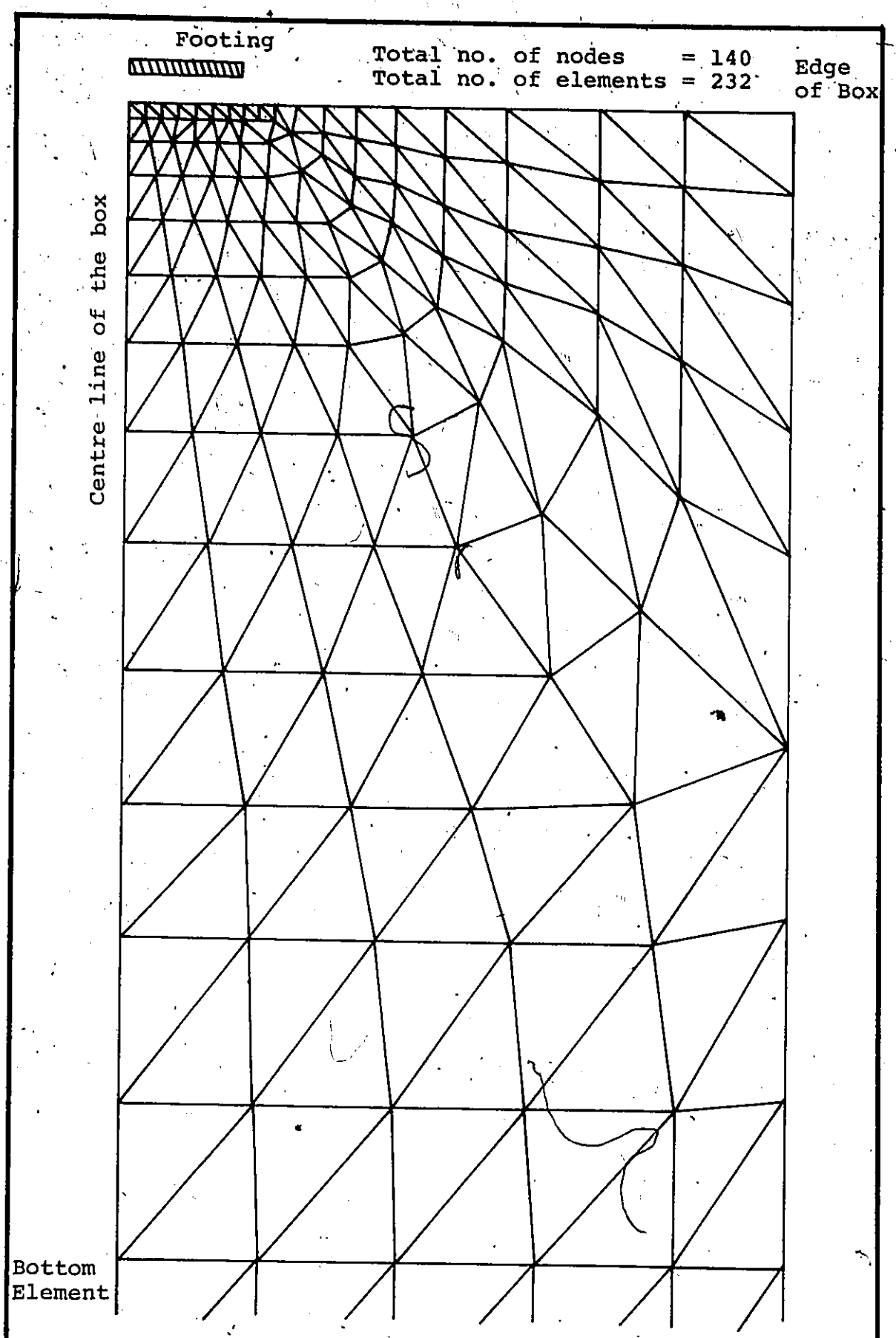

FIGURE 4.1 FINITE ELEMENT GRID

Using these models, element stiffness matrices for the plate and the solid elements are evaluated separately and then added together to form the global stiffness matrix [K] for the total structure. The global force vector [F] is then set up for the given loads. These matrices are related to the global displacement vector [U] as follows:

$$[K]\ [U] = [F]$$

The above equation represents a set of simultaneous linear equations, which, when solved, yield the nodal displacement and thereby the other qualities of interest such as stresses, moments etc.

4.5 Limitations

1. This method cannot deal with an incompressible solid media ($\nu_s = 0.5$) not even when the Poisson's ratio only approaches 0.5. The corresponding stiffness matrix becomes very large. However, this model was tested for a value of Poisson's ratio, $\nu_s = 0.49$. approximating a nearly incompressible solid without a significant loss of accuracy.

2. For a rigid circular foundation on a homogeneous elastic half-space, the normal contact stress becomes singular at the edge of the raft (Boussinesq, 1885). The finite element analysis, on the other hand, yields a finite value at the edge.

In a real situation, some local yielding takes place in regions of high stress and this results in a redistribution of the contact stresses. The finite element model cannot take into account the effects of such plastic deformations. For practical purposes, local yielding has a negligible effect on the displacement, but the flexural moments are erroneous (Brown, 1968).

4.6 Results of Analysis

As assumed previously, the elastic plate rests on the surface of the isotropic elastic solid media. The elastic constants, the Young's modulus and Poisson's ratio of the material of the plate are assumed to be 207×10^6 kPa and 0.3 respectively. The value of the Poisson's ratio for the solid media varies between 0.28 and 0.35, whereas the modulus is assumed to increase linearly at a rate of 7.534 kN/m^2 per millimetre of depth with a value of 1722.5 kN/m^2 at the surface. The basis for this assumption is the values obtained in the triaxial tests and the in situ measurements in the sand box. Although the value of the Poisson's ratio varied from 0.25 to 0.35, the real value, obtained in the triaxial test, for the material lies between 0.27 and 0.30 depending on the relative density. The applied load is assumed to be 183 kN/m^2 distributed uniformly over the plate.

Figure 4.2 through 4.4 represents the variation

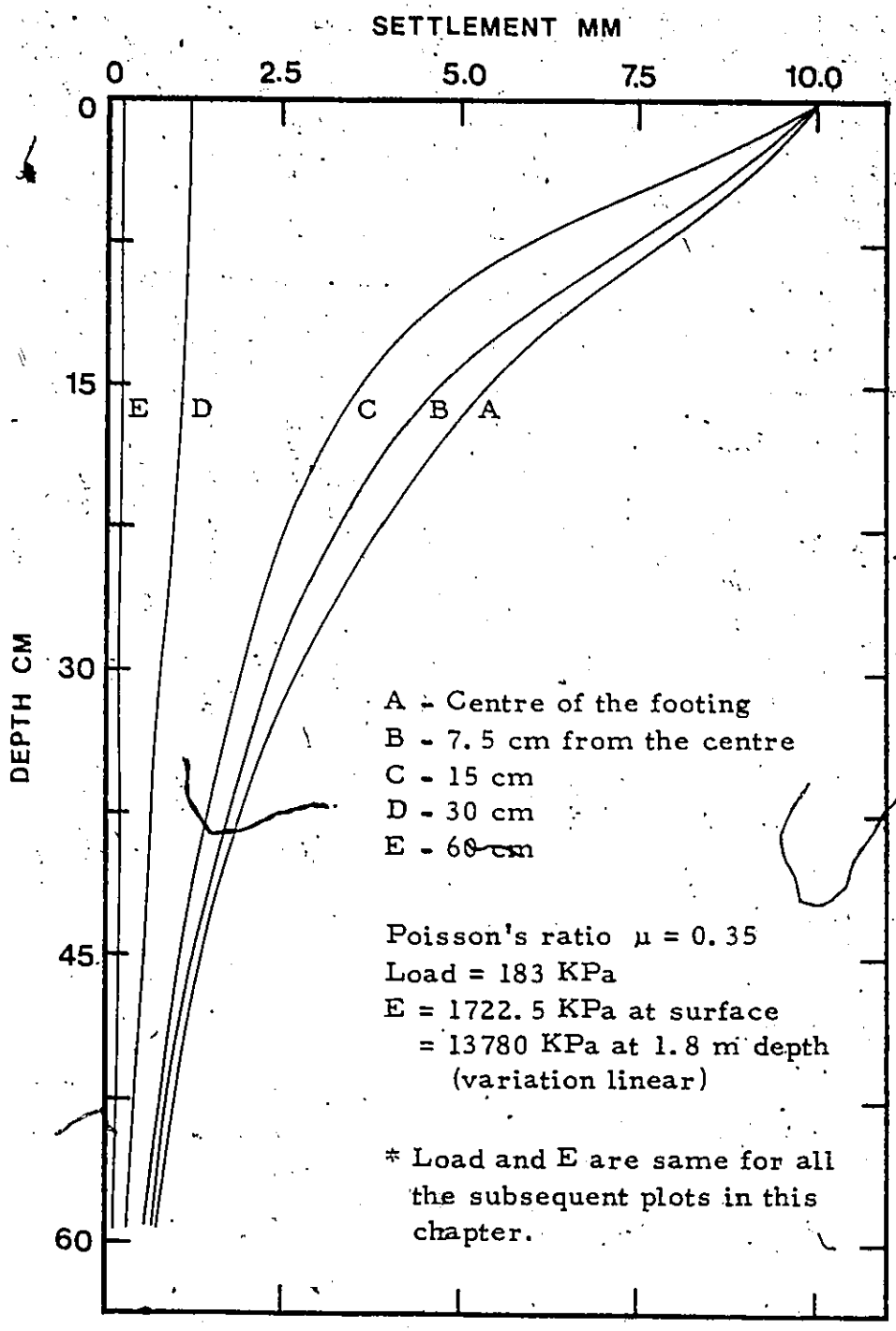

FIGURE 4.2 VARIATION OF SETTLEMENTS WITH DEPTH

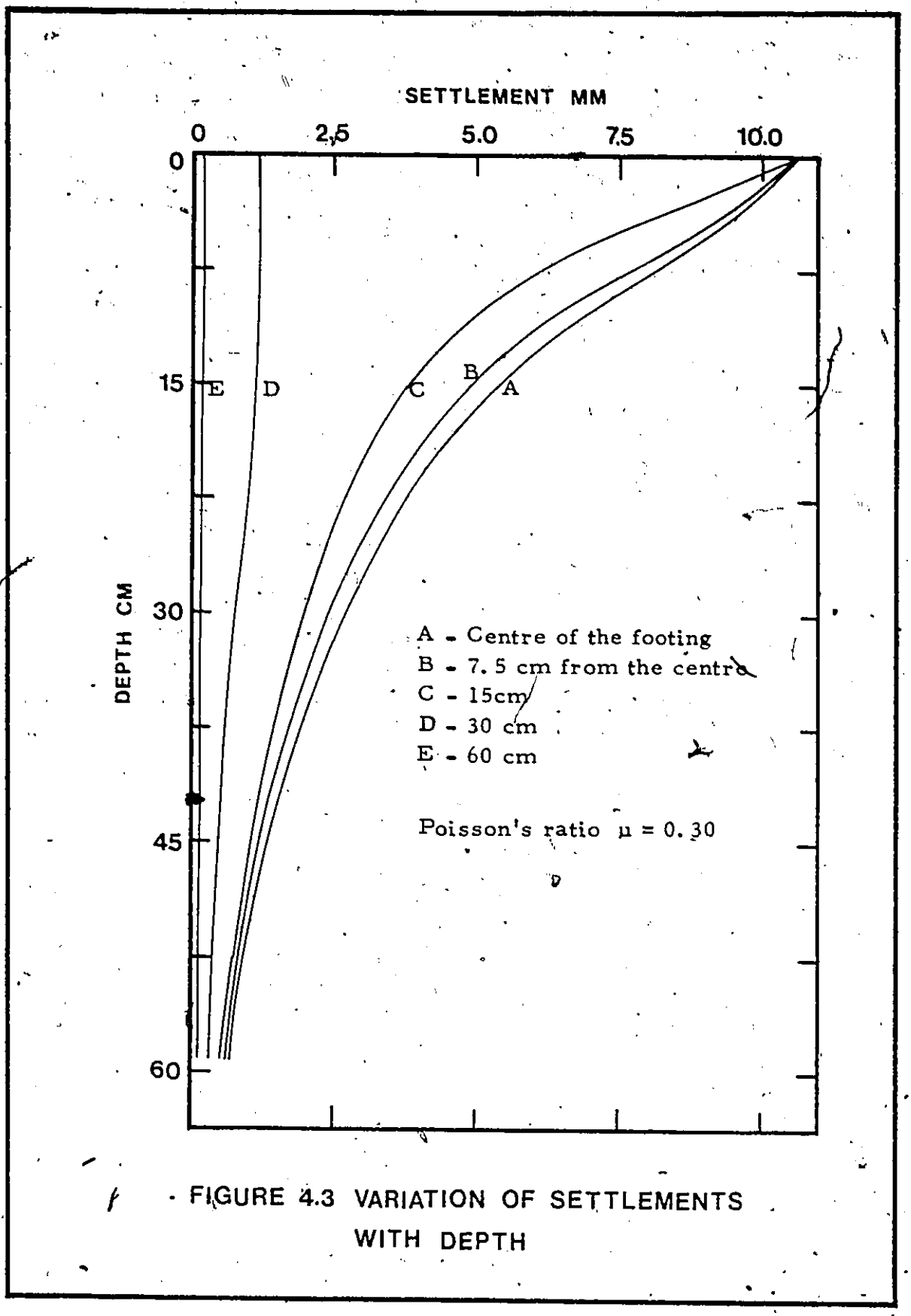

FIGURE 4.3 VARIATION OF SETTLEMENTS WITH DEPTH

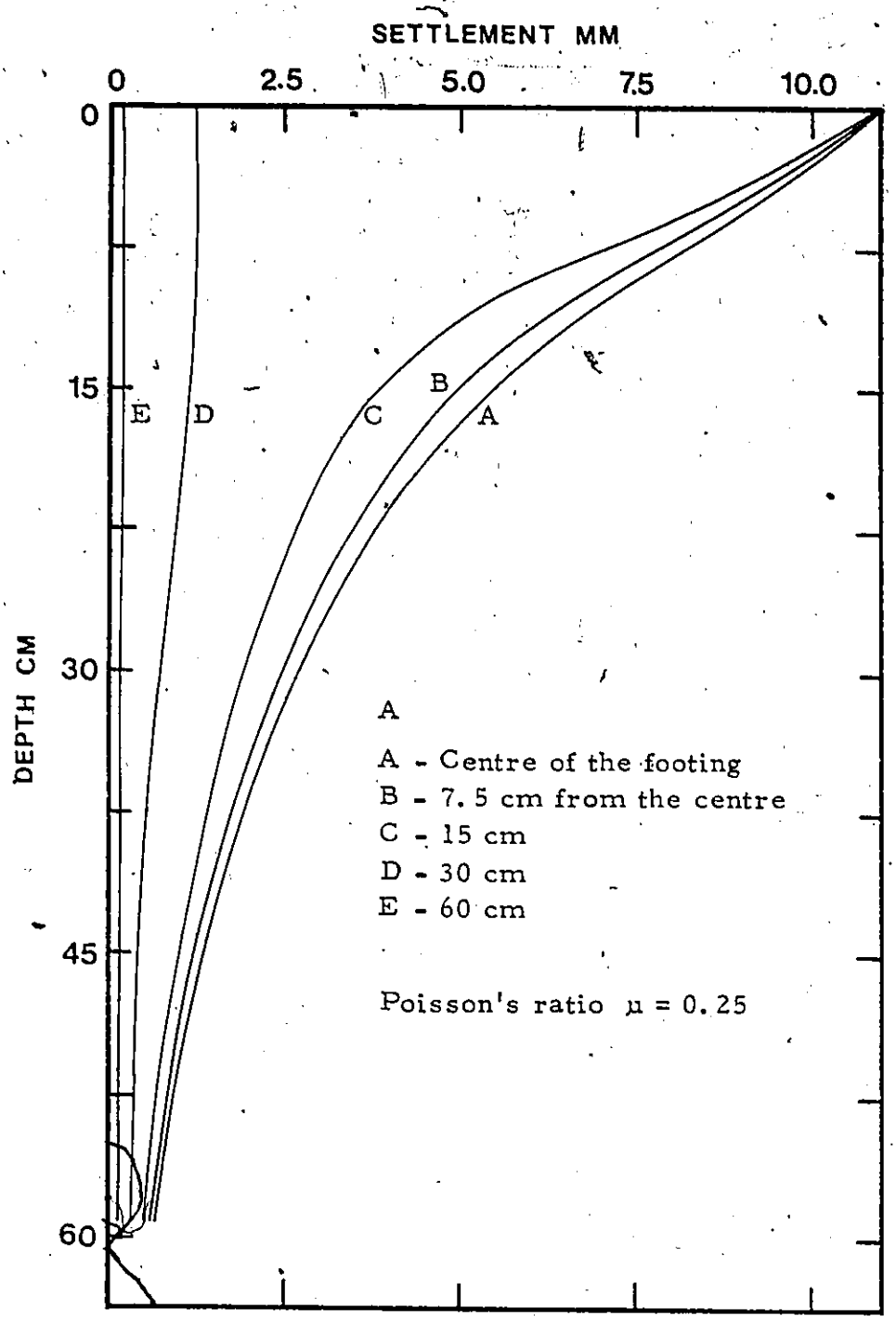

FIGURE 4.4 VARIATION OF SETTLEMENTS WITH DEPTH

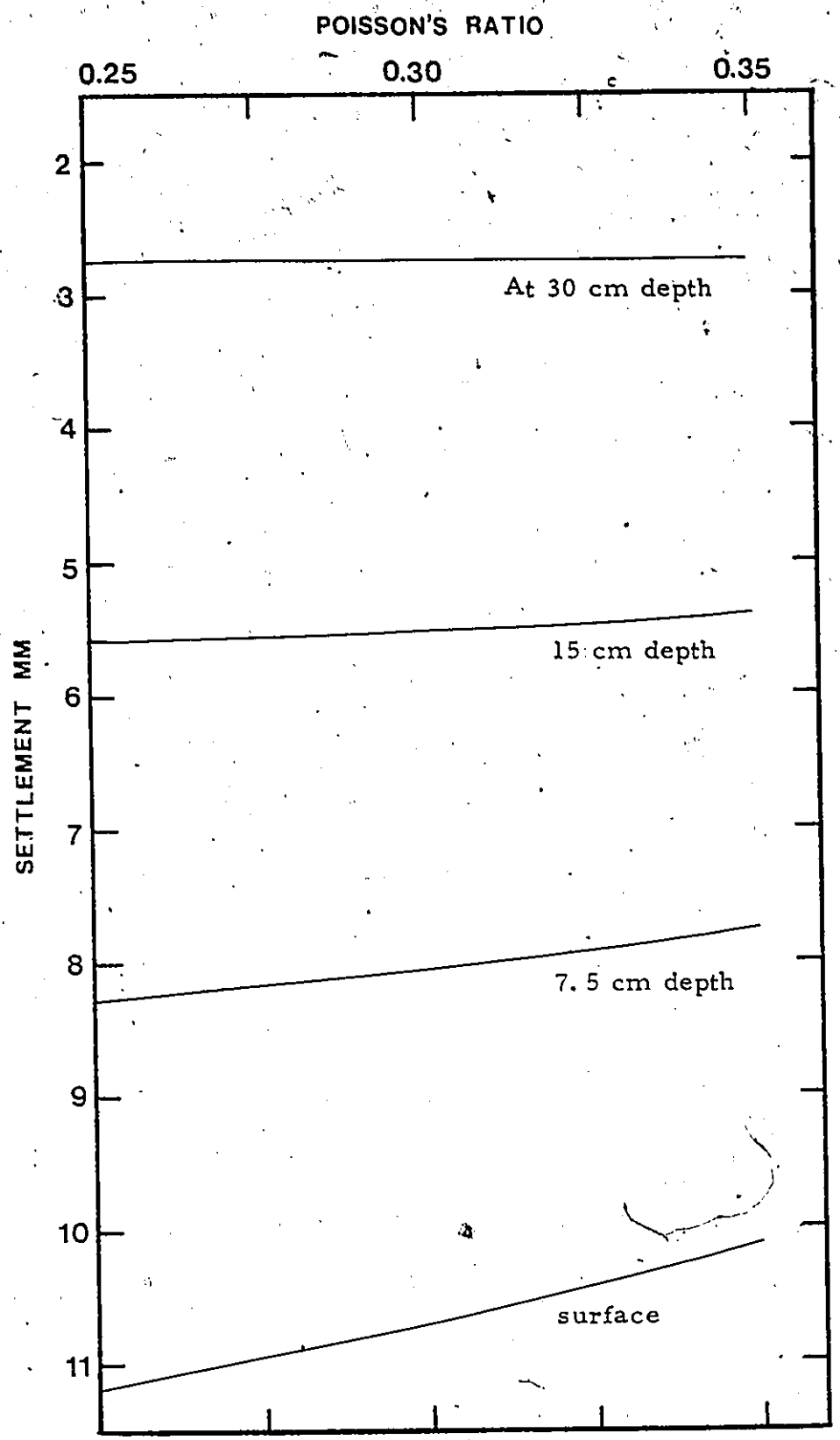

FIGURE 4.5 VARIATION OF SETTLEMENTS WITH POISSON'S RATIO (at centre)

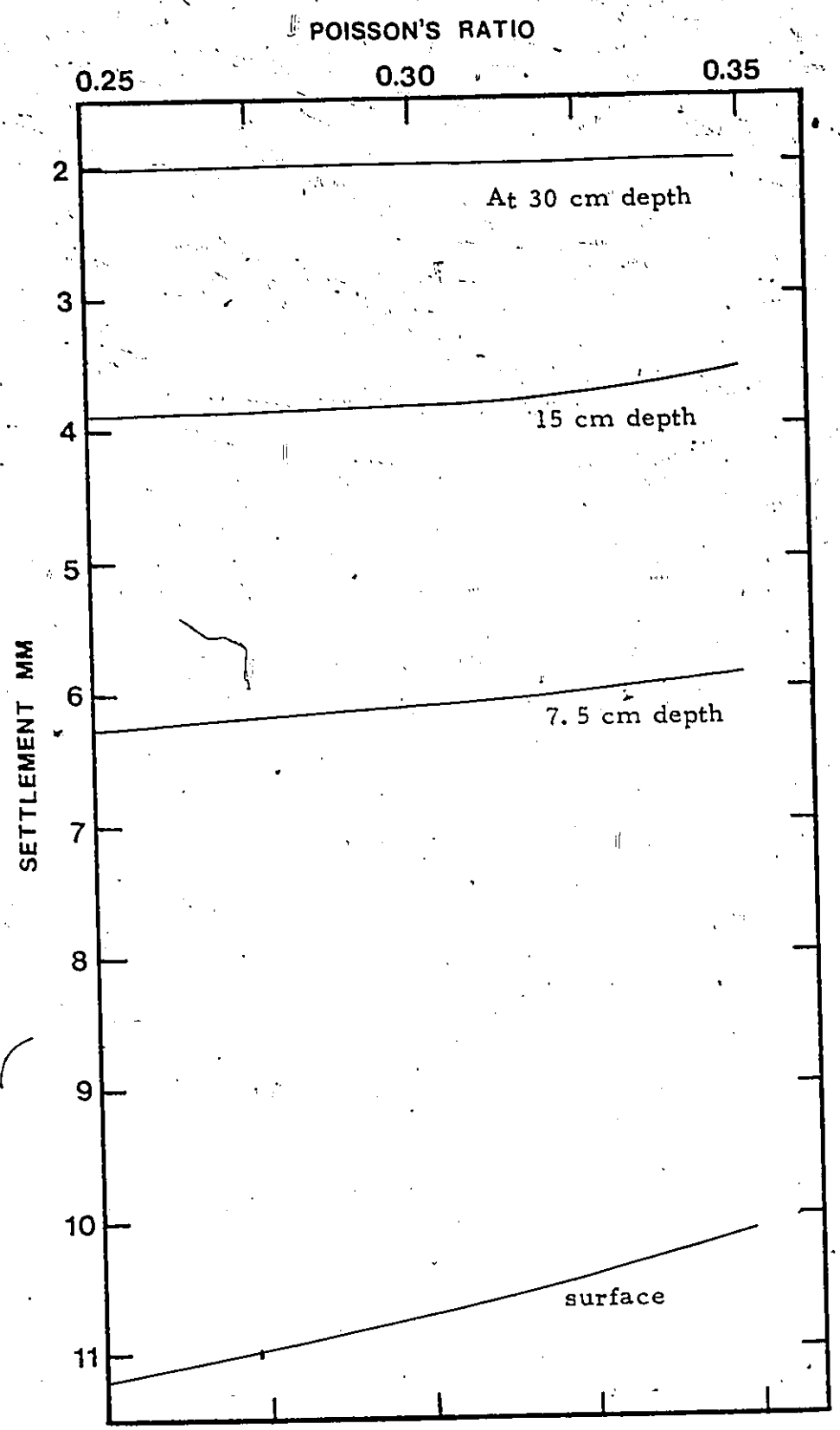

FIGURE 4.6 VARIATION OF SETTLEMENTS WITH POISSON'S RATIO (15 cm from centre)

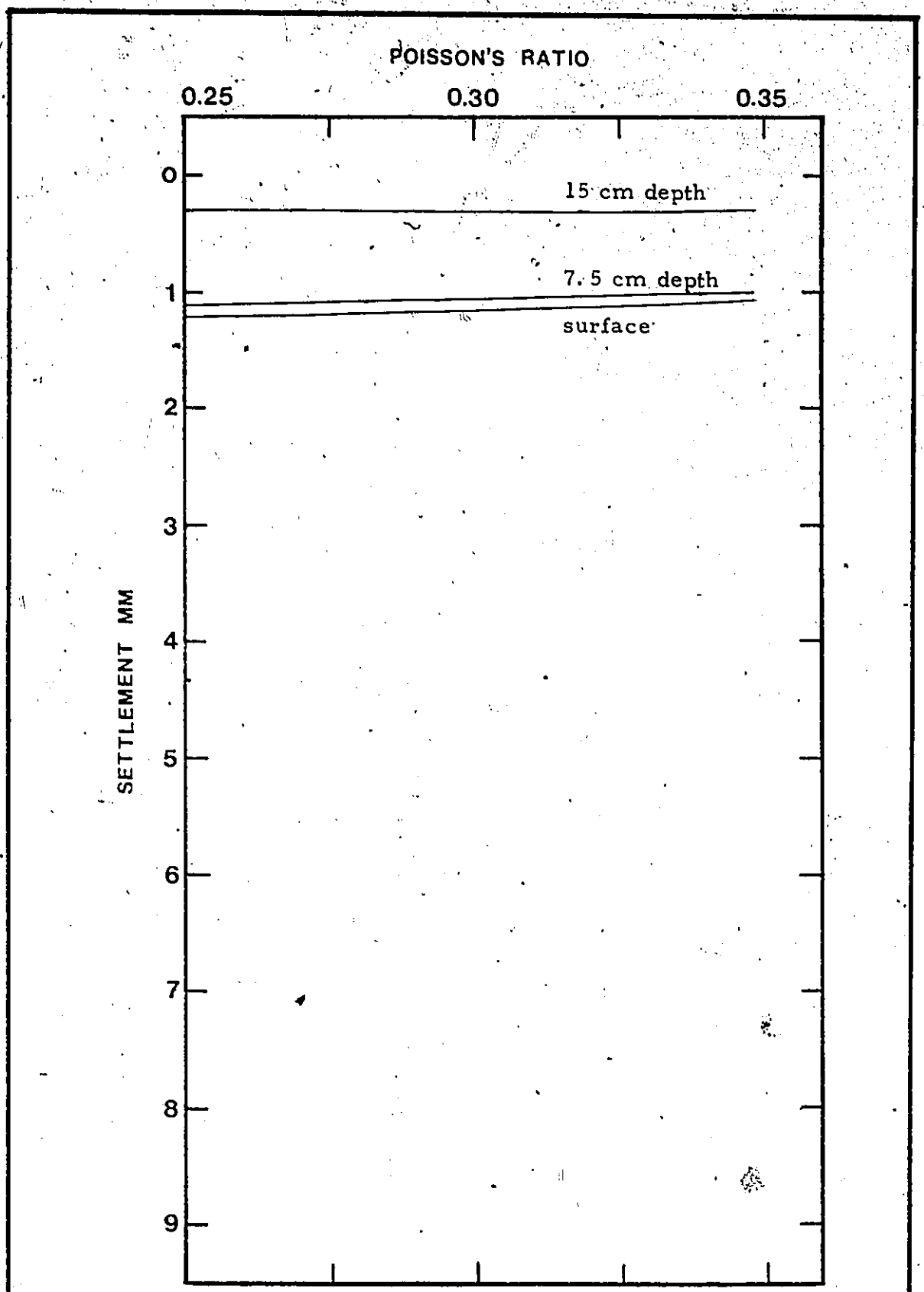

FIGURE 4.7 VARIATION OF SETTLEMENTS WITH POISSON'S RATIO (30 cm from centre)

of settlement with depth at the centre of the plate and at areas further away from the centre for various Poisson's ratio of sand. The settlement is maximum at the centre and decreases further away from the centre. The settlement becomes very negligible beyond the edge of the plate. Figure 4.5 through 4.7 shows the variation of settlement with the Poisson's ratio at various depths below the footing. The settlement decreases with the increase of Poisson's ratio. The surface settlement decreases by 8.7 percent by increasing the Poisson's ratio from 0.25 to 0.35. From the Figure 4.7 it is evident that the effect of Poisson's ratio on the settlement outside the plate area is very small.

Figures 4.8 through 4.10 represent settlement patterns around the plate at various depths of the footing. It is evident from the figures that the settlement at a depth twice the diameter of the plate is approximately 7 percent of the settlement occurring at the surface of the media.

Figure 4.11 shows how radial deformations take place at the centre and at increasing distances from the centre for various Poisson's ratio. The radial deformation is zero at the centre of the plate and increases to a maximum value at a distance of about 229 mm from the centre of the plate and then starts decreasing. The radial deformation increases with the increase of Poisson's ratio at all distances from the centre of the plate.

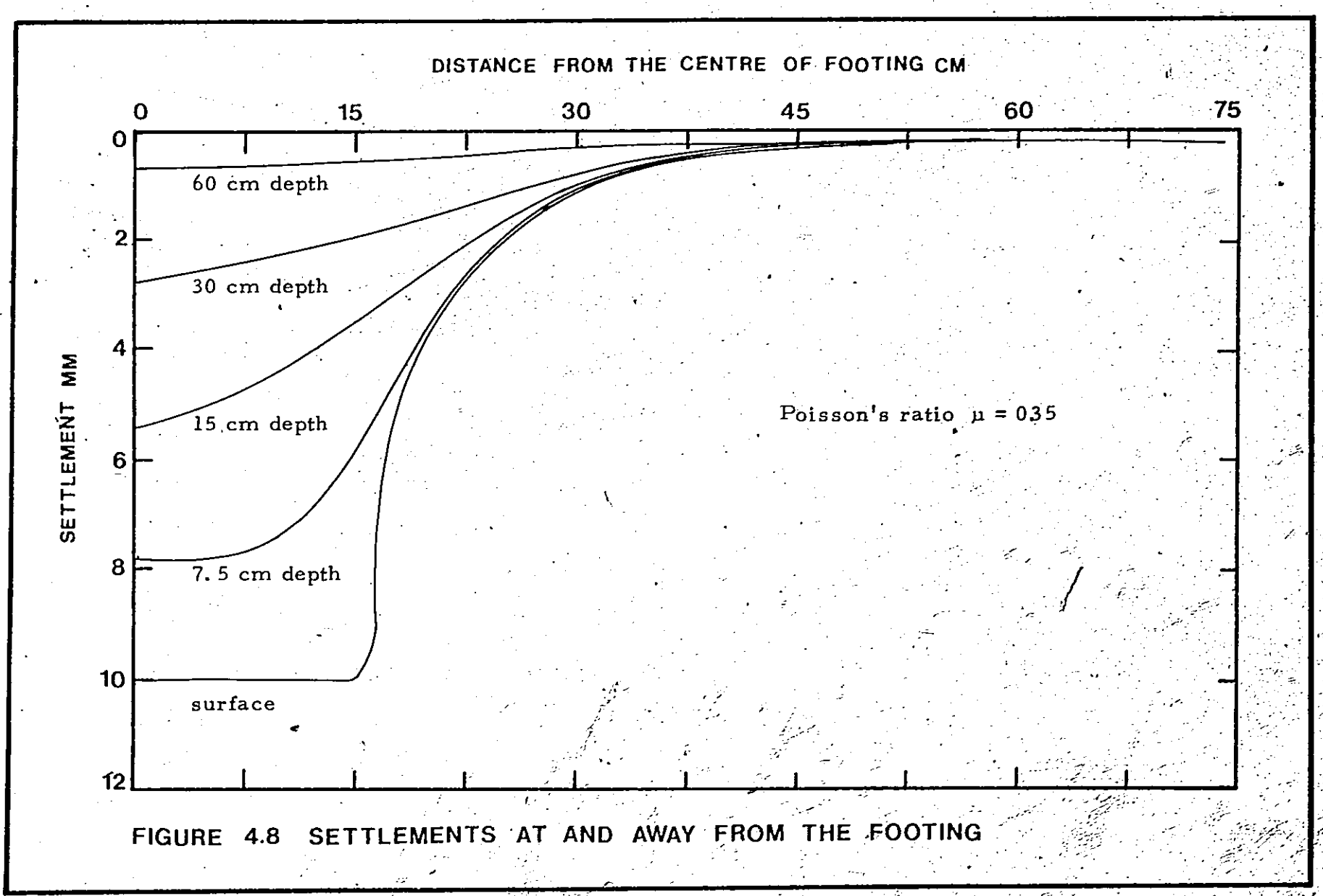

FIGURE 4.8 SETTLEMENTS AT AND AWAY FROM THE FOOTING

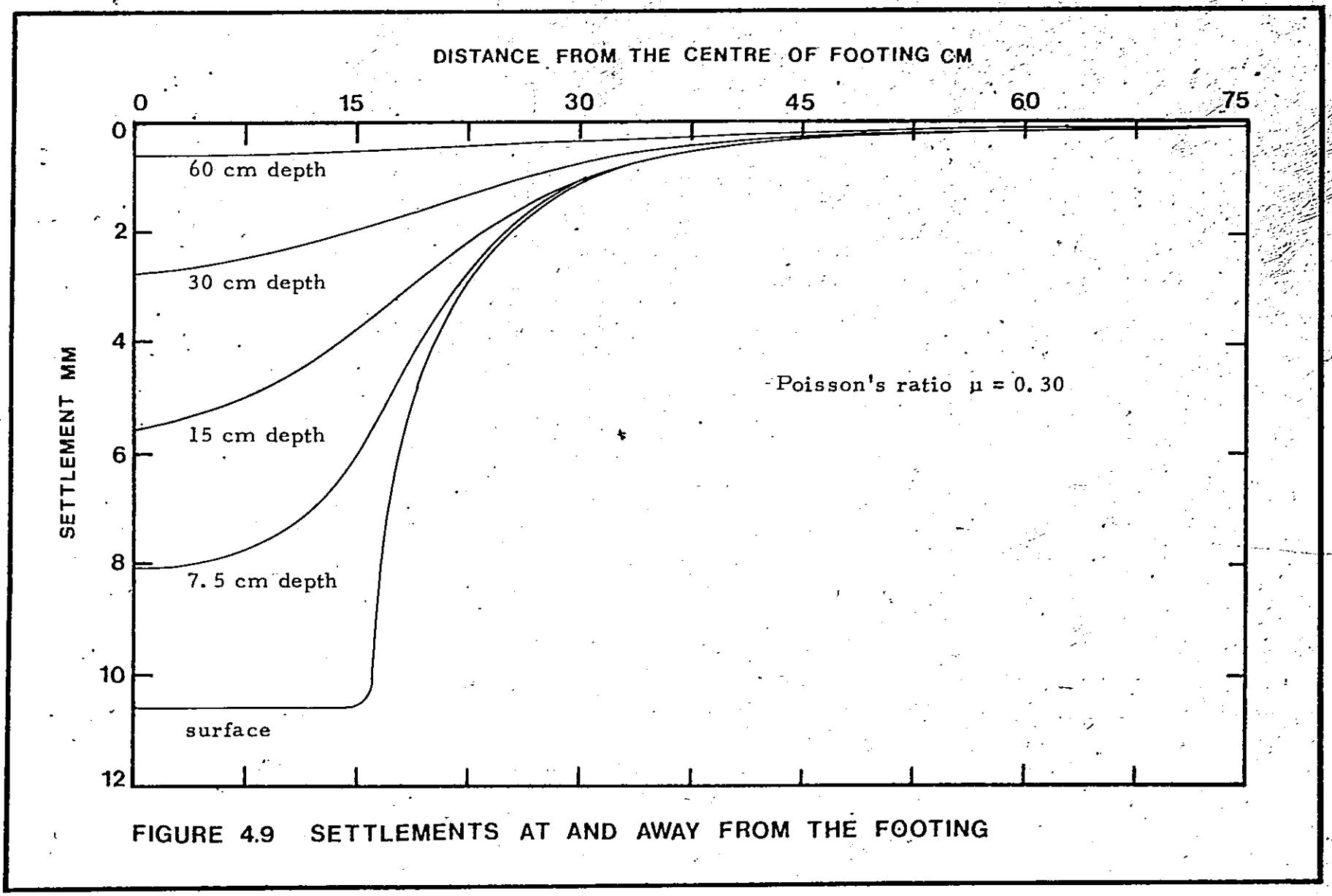

FIGURE 4.9 SETTLEMENTS AT AND AWAY FROM THE FOOTING

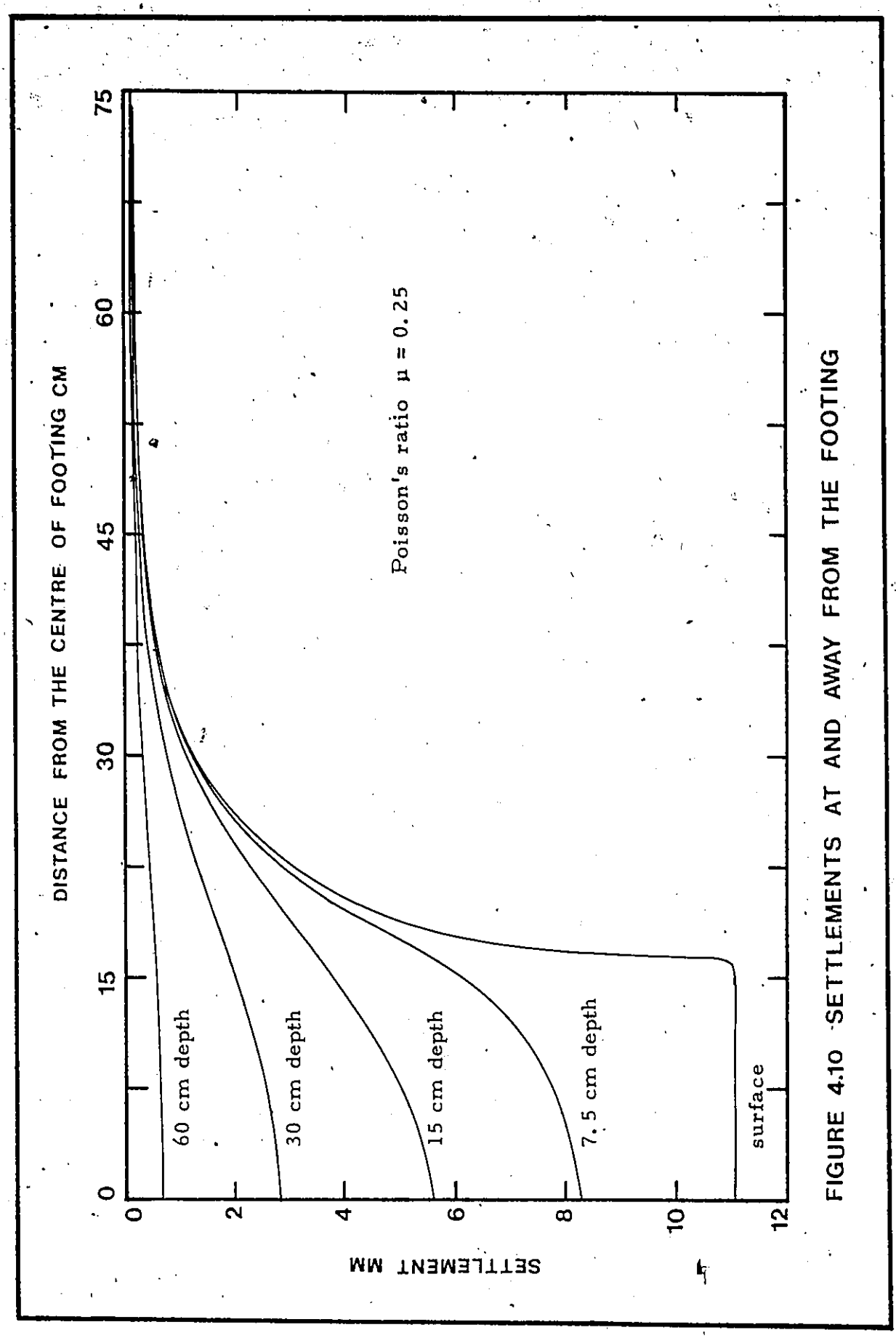

FIGURE 4.10 SETTLEMENTS AT AND AWAY FROM THE FOOTING

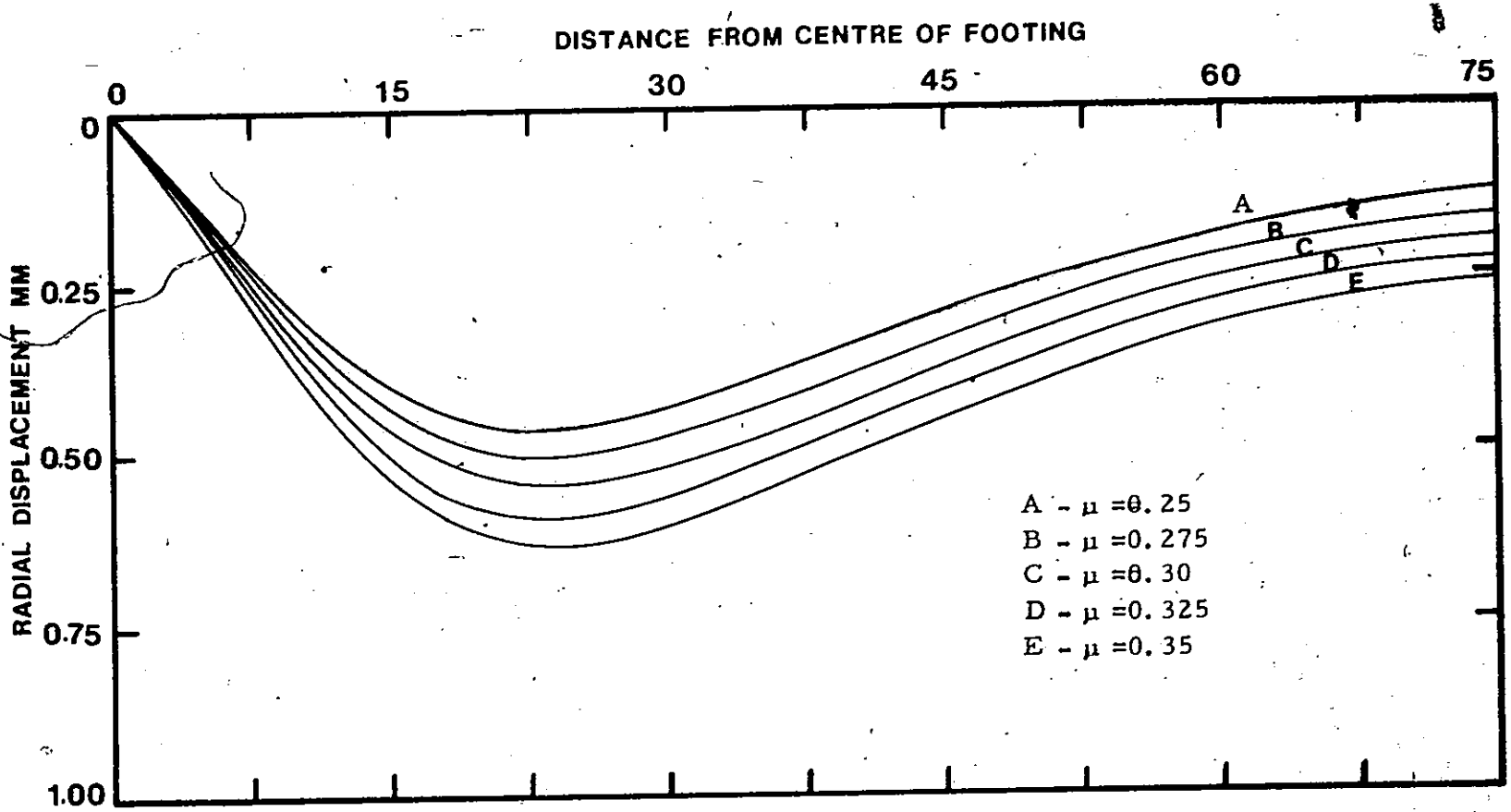

FIGURE 4.11 RADIAL DEEORMATION WITH DISTANCE FROM CENTRE (at 30 cm depth)

CHAPTER 5

ANALYSIS OF TEST RESULTS

5.1 Effect of Embedment

Although it has been established in the literature that the bearing capacity of a footing increases considerably due to the embedment into the ground, very little consideration has been given to the effect of penetration of the footing in the ground during the process of loading. Lambe (1967) recognized the fact that as the footing penetrates into the ground, the footing acquires some additional strength from its embedment achieved during the penetration. Larkin (1968) stated that in the case of a circular footing located on the surface, an increase in depth of about 0.09 to 0.13 of the footing diameter is sufficient to increase the bearing capacity by 100 percent. This could be one of reasons other than densification and increase of ϕ, why the theories consistently underestimate the actual bearing capacity of the footing.

In all the bearing capacity relations proposed in the literature, the embedment effect has been taken into consideration. In the present study only the bearing capacity equations proposed by Terzaghi (1943) and Brinch Hansen (1970) are considered to establish the effect of penetration on the bearing capacity.

In Figures 5.1, 5.2 and 5.3, the dotted curves are the original test curves which represent stress in kN/m^2 on the vertical axis, settlement in mm and relative settlement defined as the ratio of settlement to footing diameter on the horizontal axis. The straight lines show the effect of embedment according to Terzaghi's theory. The solid curves are obtained by substracting the effect of embedment from the original test curves. These curves represent the bearing capacity derived from the shear strength of the sand. The portion of the bearing capacity derived from the surcharge due to embedment is directly proportional to the depth of embedment. This portion is non-existent to the depth of embedment at the start of the test with the footing resting on the surface and its value starts increasing as the footing penetrates into the soil under the applied load. The original test curves do not show any failure of the footing. When the embedment effect is subtracted from the total, the peak becomes prominent and the load decreases with further penetration. At a relative settlement of 45 percent, most of the bearing capacity of the footing comes from the embedment.

The dotted curves in Figures 5.4, 5.5 and 5.6 are the original test curves. The solid curves (embedment) in all the above figures show the effect of embedment as the footing penetrates in the soil. This was calculated with the equation proposed by Brinch Hansen (1970). The other two solid curves in each of the above figures were obtained by subtracting the

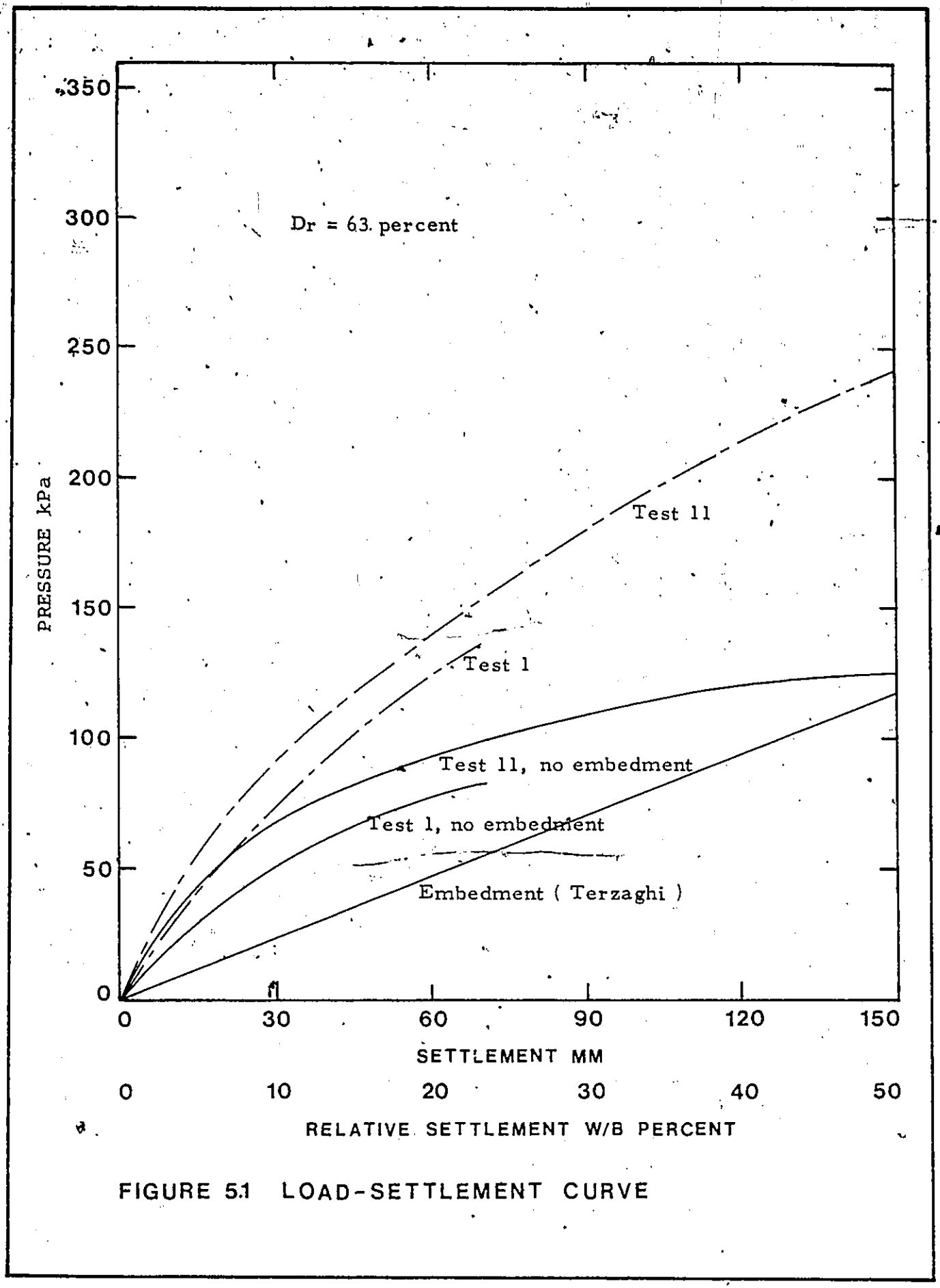

FIGURE 5.1 LOAD-SETTLEMENT CURVE

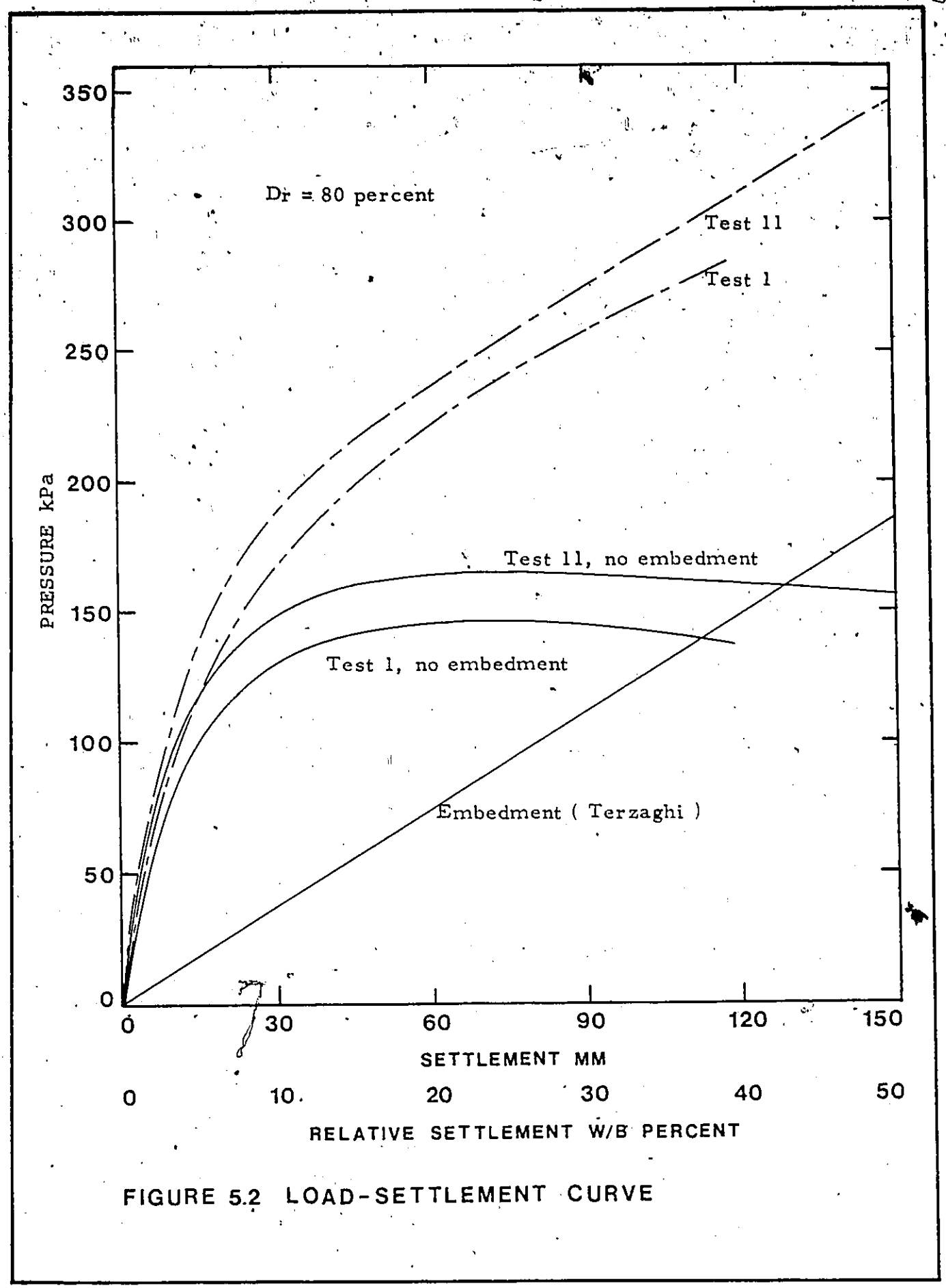

FIGURE 5.2 LOAD-SETTLEMENT CURVE

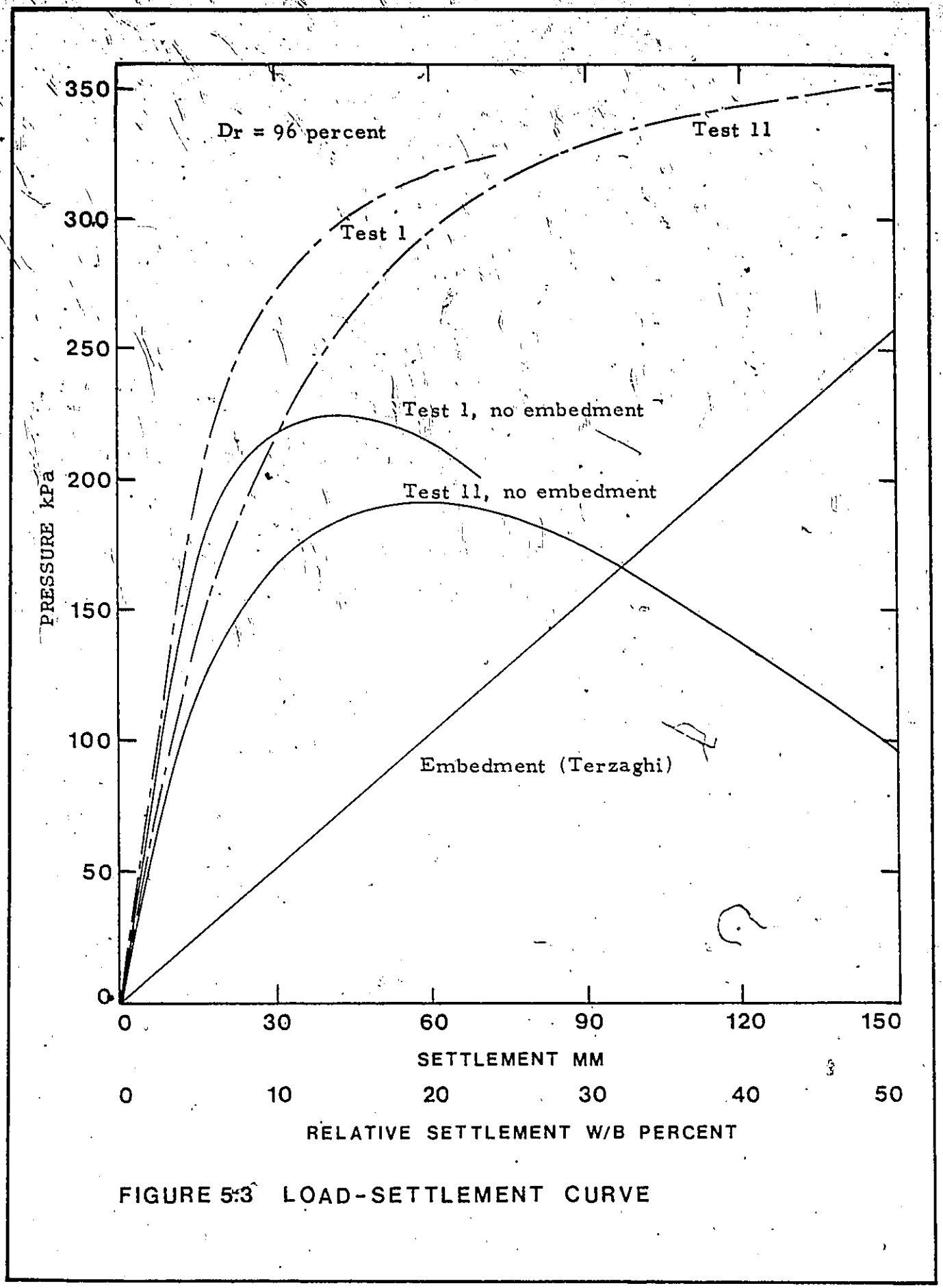

FIGURE 5.3 LOAD-SETTLEMENT CURVE

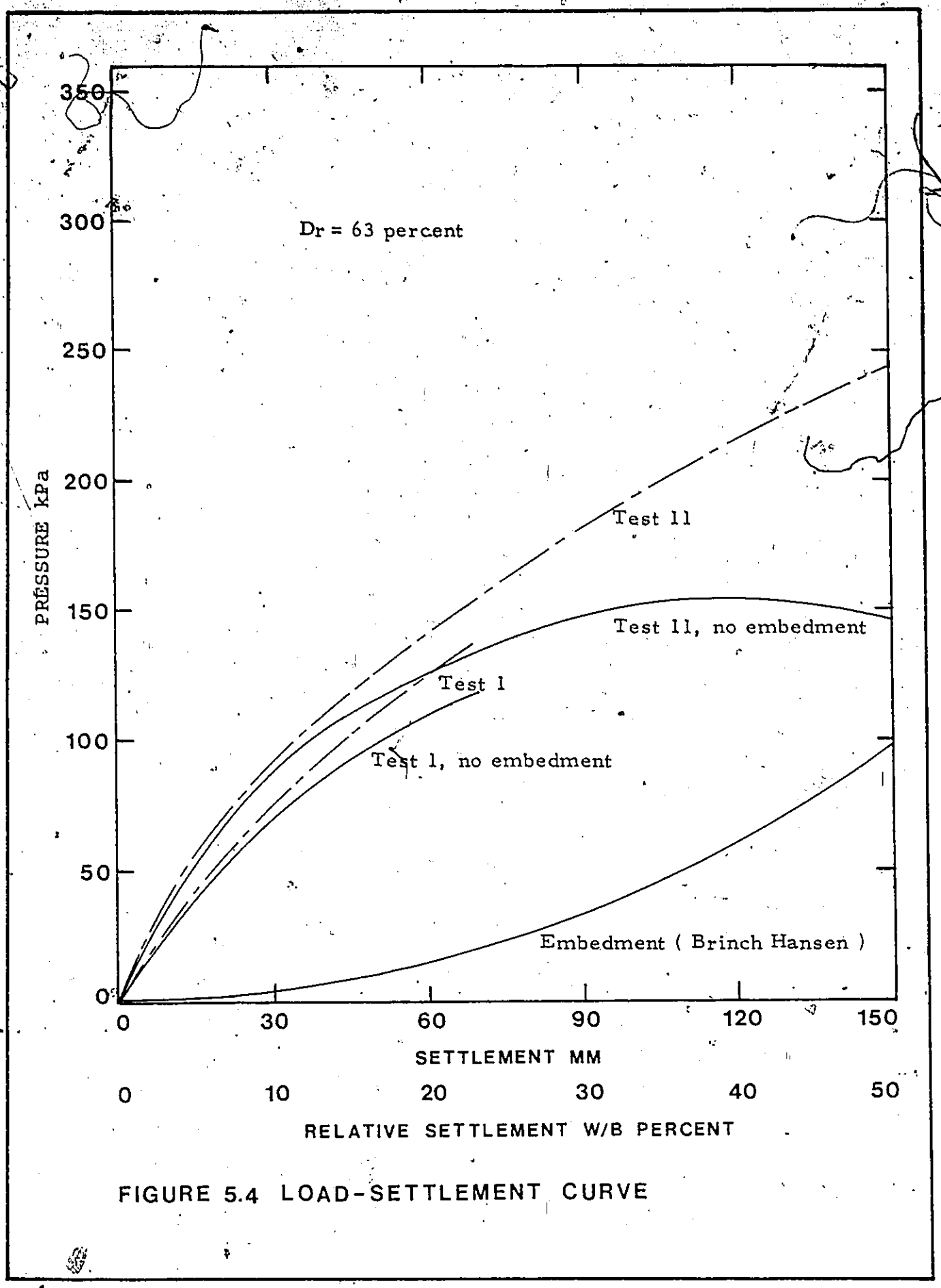

FIGURE 5.4 LOAD-SETTLEMENT CURVE

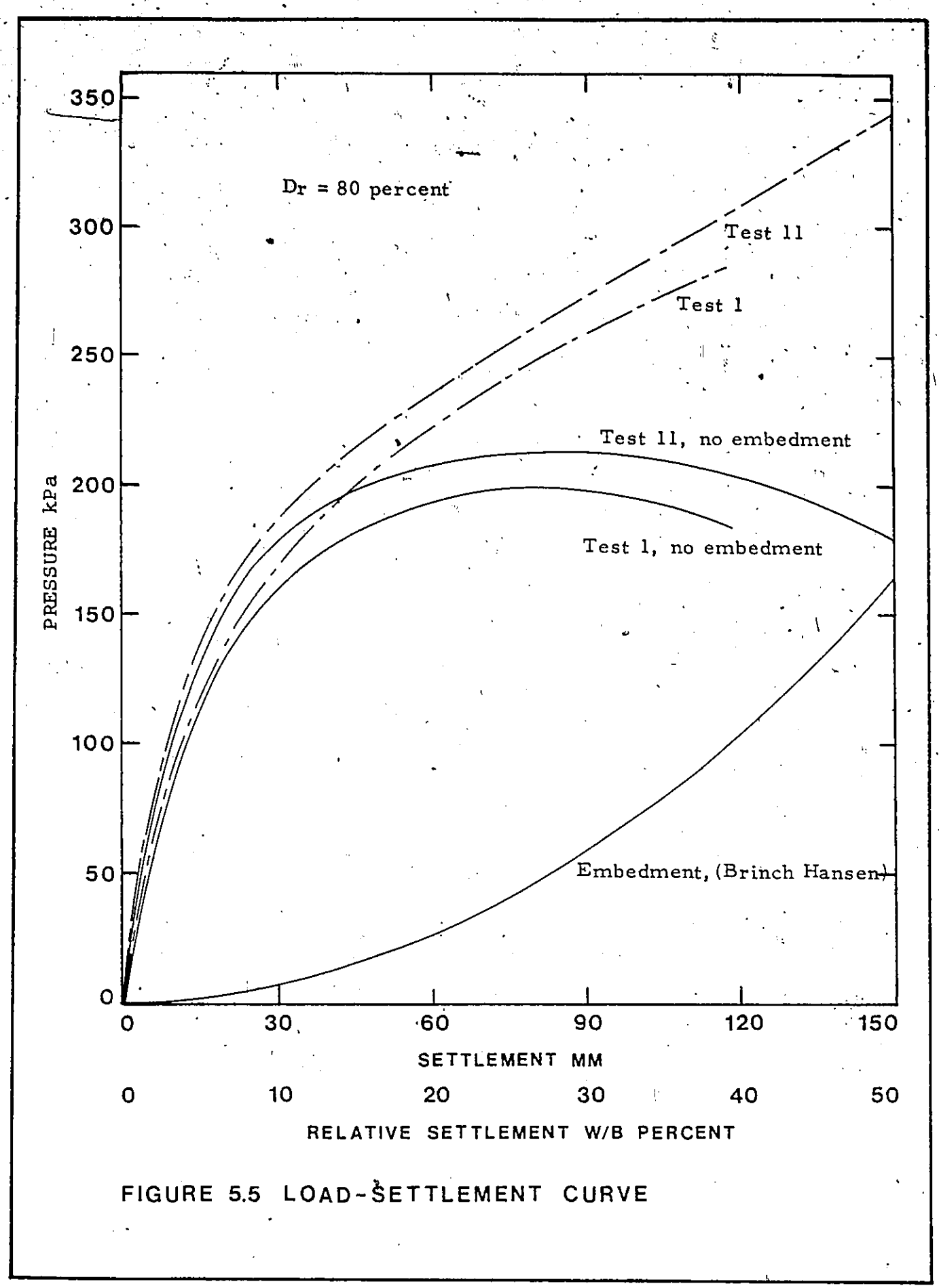

FIGURE 5.5 LOAD-SETTLEMENT CURVE

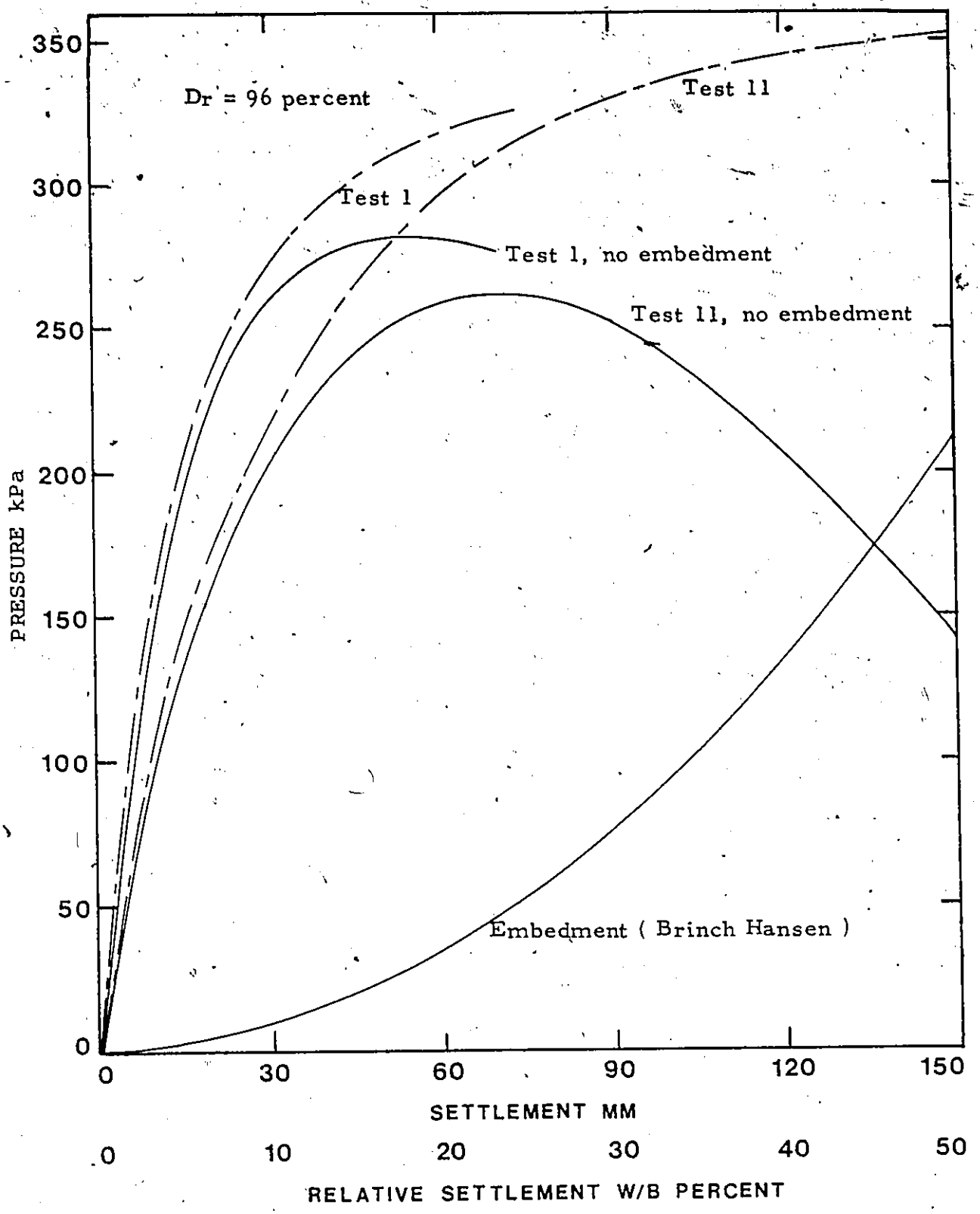

FIGURE 5.6 LOAD-SETTLEMENT CURVE

effect of embedment from the original test curves.

The difference between Brinch Hansen and Terzaghi's theory is that the bearing capacity due to embedment increases linearly in Terzaghi's equation but in Hansen's equation the embedment effect is very slight at the beginning of penetration but increases progressively with the increase in depth of penetration, that is, the slope of the curve increases with the embedment depth.

It can be established from this discussion that the load settlement curves drawn from the test results consist of two portions - one contributed by the shear strength of the soil directly below the base of the footing and the other by the embedment due to the penetration of the footing.

5.2 Ultimate Load

The failure load is obviously not clearly defined in any of the tests. This could be caused by embedment at higher densities, and at lower densities could be attributed to the combined effect of the densification of the sand directly below the footing and the embedment due to gradual penetration. There are quite a number of methods in the literature to estimate the failure load from the test curve. In this analysis the method suggested by Christiaens (See De Beer, 1970) was used to determine the ultimate load. According to this method, as described

in Figure 5.7, the values of W/B and $q/A\gamma B$ are plotted in a log-log plot where

W = Settlement of the footing

B = Diameter of the footing

q = Applied load

γ = Unit weight of the soil

A = A factor which is given by

$$A = \left(\frac{q_o}{\gamma B} + \frac{W}{B}\right) S_q \left(1 + 0.35 \frac{W}{B}\right) + \frac{S_r}{2}$$

where q_o = Initial lateral overburden pressure

$S_q = 1 + 0.2 \frac{B}{l}$

$S_r = 1 - 0.4 \frac{B}{l}$

l = Length of the footing

Christiaens (1966) stated that the intersection of the two curve portions would be the failure point. If there is no sharp well defined point, their upper and lower limits of the ultimate bearing capacity can be recommended.

It is observed from the curves in Figure 5.7 that failure occurs at a settlement/diameter ratio of 25 percent for a relative density of 63 percent, at ratio of 20 percent for 80 percent relative density and at ratios of 15 and 13 percent for a relative density of 96 percent. It is evident

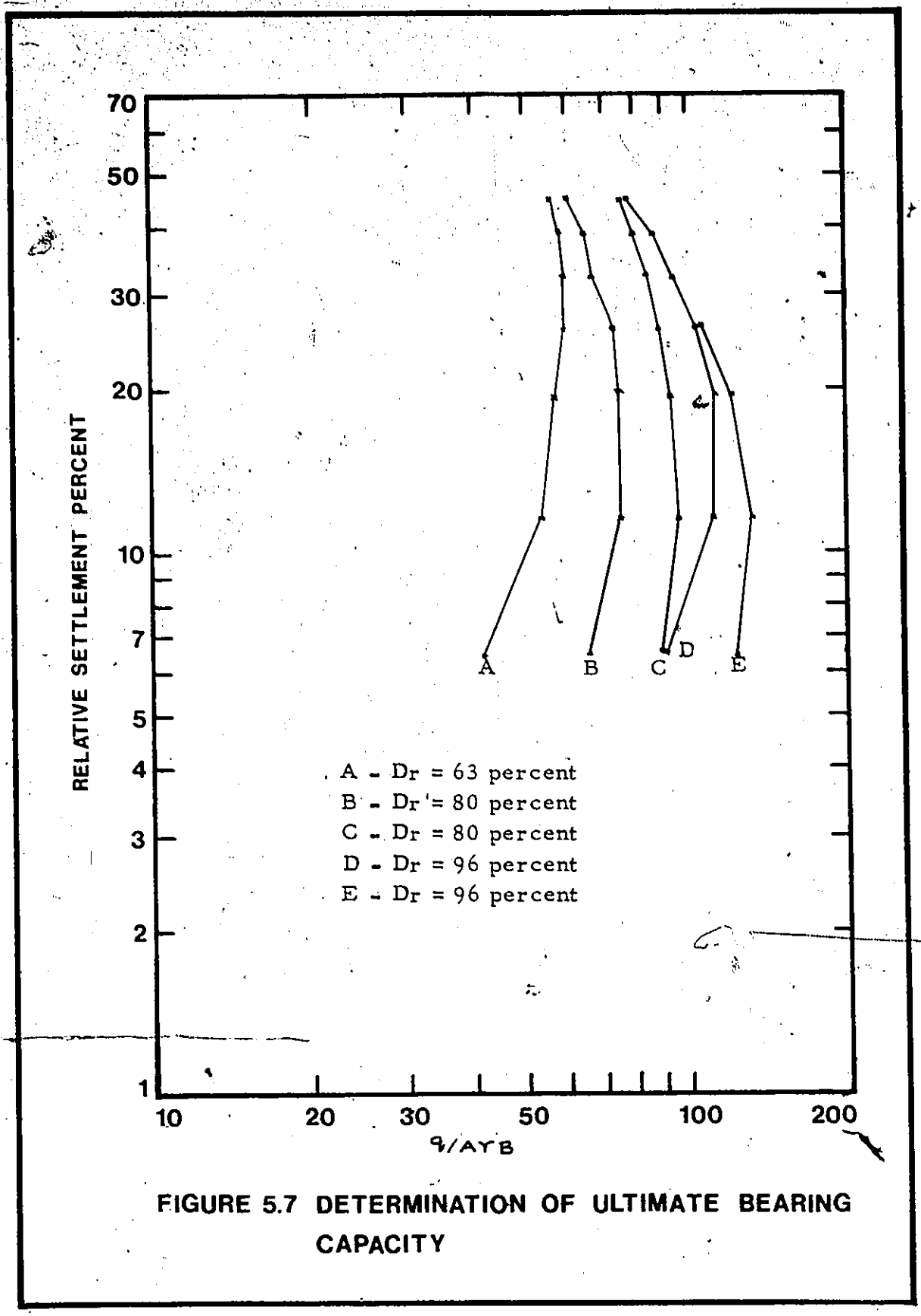

FIGURE 5.7 DETERMINATION OF ULTIMATE BEARING CAPACITY

that as the density of sand increases, the failure occurs at lower strain levels than in sand in a looser state.

The failure loads corresponding to these failure strains are determined from the load-settlement curves in Figure 5.1 through 5.3. Then average values are 162 kN/m^2 230 kN/m^2 and 280 kN/m^2 for relative densities 63, 80 and 96 percent respectively.

5.3 Ultimate Load and Theory

The test results are compared with Terzaghi (1943) and Brinch Hansen's (1970) theories. The rationale for selecting these two theories is that one is the earliest and the other quite recent and a development over the others.

The values of ultimate bearing capacity without surcharge by Terzaghi's theory are 80 kPa, 140 kPa and 231 kPa for the relative densities of sand 63, 80 and 96 percent respectively. The corresponding values are 82 kPa, 152 kPa and 207 kPa by Brinch Hansen's theory. If these values are plotted against the relative densities, in both cases, the bearing capacity increases with the relative density, but the rate of increment gets larger according to Terzaghi's equation, whereas it diminishes with Brinch Hansen's equation (Figure 5.8).

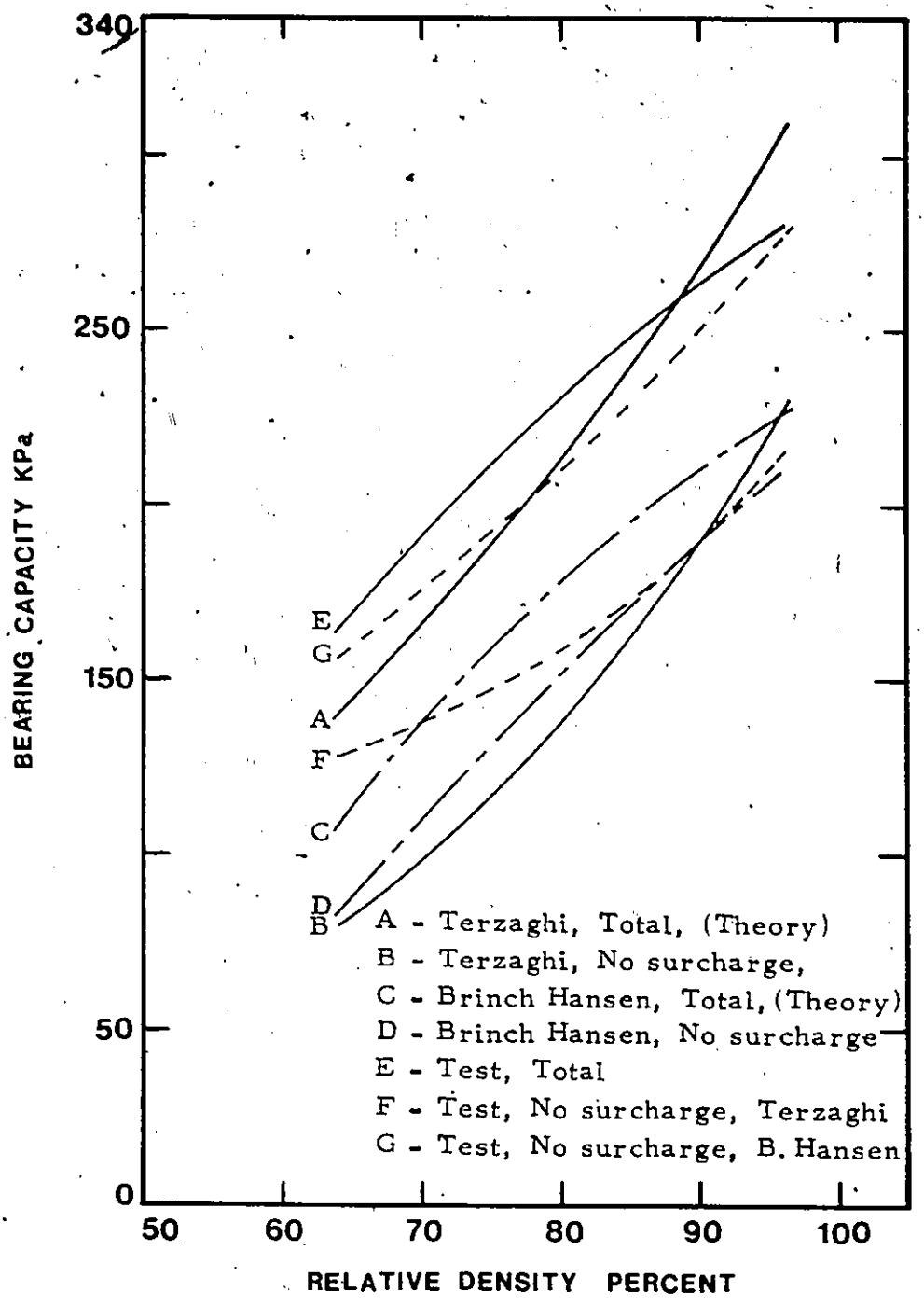

FIGURE 5.8 BEARING CAPACITY WITH RELATIVE DENSITY

The ultimate bearing capacity found during the tests for the three densities are 162 kPa, 230 kPa and 280 kPa and are definitely much higher than the values predicted by the theories considered. The test values are higher by factors of 2, 1.64 and 1.21 than those obtained by using Terzaghi's method for the three densities and 1.98, 1.5 and 1.35 times the values predicted by Brinch Hansen's equation.

The depth factor d_q in Brinch Hansen's equation is directly proportional to the ratio (D_f/B), of depth of embedment to the diameter of the footing. For a full size surface footing, when the penetration is limited by the requirement of the structure, the ratio D_f/B becomes very small, consequently the value of d_q also becomes negligibly small. So the portion of bearing capacity contributed by the embedment due to penetration may be neglected for all practical purposes.

The ultimate loads without the effect of surcharge using Brinch Hansen's criteria are 156, 211 and 278 kPa for the relative densities 63, 80 and 96 percent respectively. The corresponding values using Terzaghi's equation are 128, 158 and 217 kPa. These values are much lower than those obtained using Brinch Hansen's equation. This could be due to not taking into account the depth and shape factors which affect the bearing capacity.

All the bearing capacity values mentioned above are tabulated in Table 5.1 and plotted against relative density

in Figures 5.8

For easy comparison, the bearing capacities from the test are plotted (Figure 5.9) against the bearing capacities obtained from the theories. It is observed that the test values are always higher than the values predicted by the two methods considered. However, for very dense sand, the predicted values by Terzaghi's method are higher than the test value.

TABLE - 5.1

BEARING CAPACITY (THEORETICAL), kPa.

	D_r = 96%	D_r = 80%	D_r = 63%
Terzaghi	231	140	80
Brinch Hansen	207	152	82

BEARING CAPACITY (TEST), kPa.

	D_r = 96%	D_r = 80%	D_r = 63%
Test 1	290	222	
	280	230	
Test 2	270	238	162

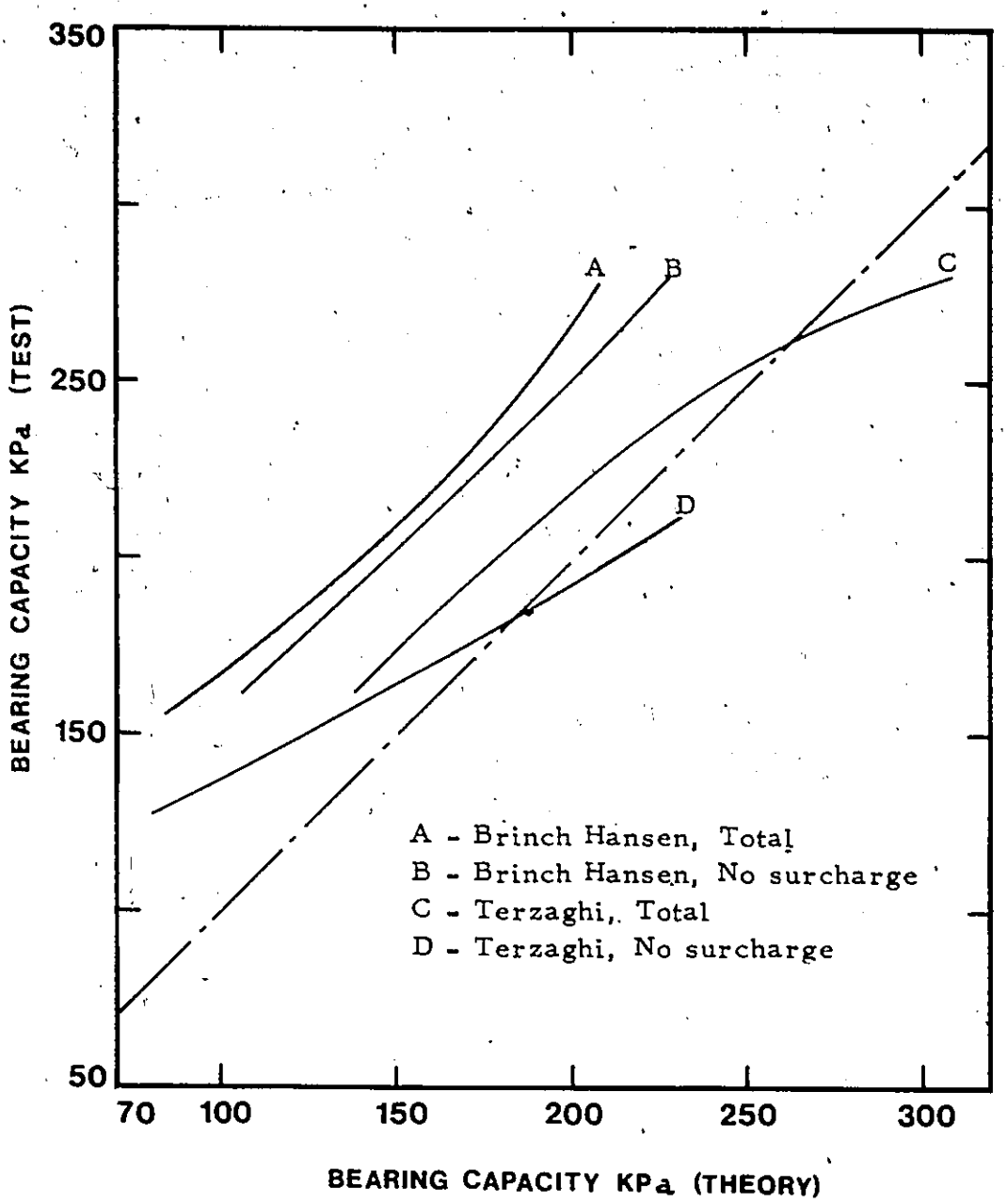

FIGURE 5.9 COMPARISON OF BEARING CAPACITIES

TABLE - 5.1 (Contd.)

BEARING CAPACITY (TEST, NO EMBEDMENT), kPa.

	D_r = 96%		D_r = 80%		D_r = 63%
Terzaghi Test	I 228		I 150		-
		211.5		158	
	II 195		II 160		II 128
Brinch Hansen	I 288		I 204		
		277.5		211	
	II 267		II 218		II 156

5.4 N_r-Values and Angle of Internal Friction

An intense effort has been made in the past to determine both theoretically and experimentally the correct ultimate bearing capacity of footings on sand; but this still remained unsolved because of discrepancies in obtaining the correct N_r-value which is the key factor in the bearing capacity equation. The N_r is an emperical bearing capacity factor which depends on the angle of internal friction ϕ and is very sensitive to the variation of ϕ. The correct N_r-value and in turn the correct ultimate bearing capacity depends on the selection

of the angle of internal friction.

The N_r-values suggested by various authors are summarized in the Figure 5.10 and the scatter of the values are plotted in Figure 5.11. The experimental curve A by De Beer gives very high values when ϕ is determined from triaxial test whereas by introducing the variation of ϕ with the mean pressure the experimental curve A_1 is obtained which is located well below the theoretical curves except for high densities. On the same figure are plotted the theoretical values of N_r given by the statically correct solution of Lundgren and Mortensen, those given by Meyerhof, the kinematically more acceptable hypothesis of Buisman and the value used by Terzaghi and Brinch Hansen.

The scatter of the values as plotted in Figure 5.11 shows that as the value of the angle of internal friction increases the scatter also increases. The scatter is low if De Beer's experimental values and Buisman's values are omitted.

The curve obtained by Muhs (see De Beer 1965) by testing a footing of 1 m^2 surface is different than the others. At low densities the value is very high and at high density the value is almost the average of the values given by others. Muhs explains this by the phenomenon of progressive rupture. During the gradual load increase on the soil, the shearing strength is not mobilized at all points of the slip surface,

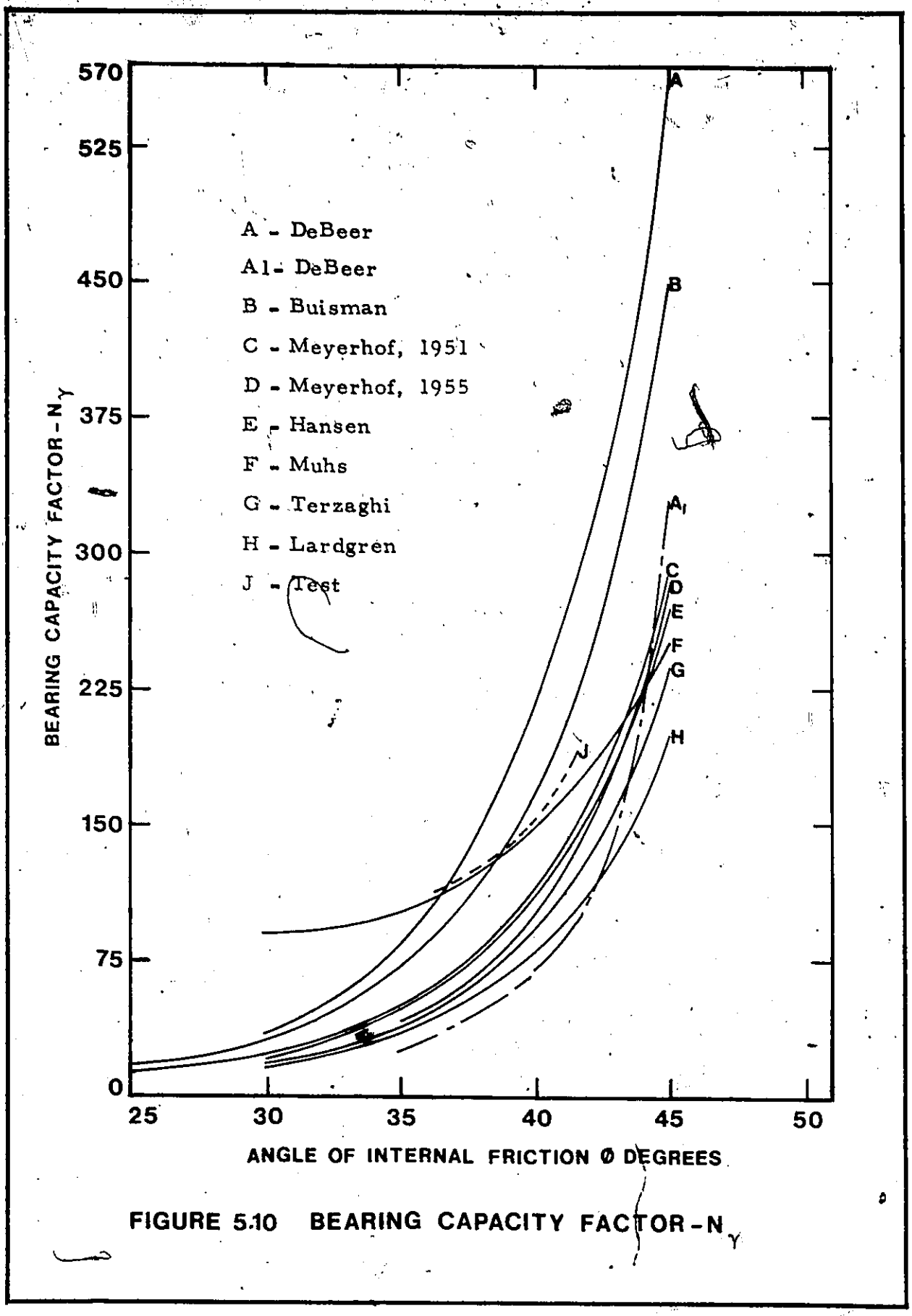

FIGURE 5.10 BEARING CAPACITY FACTOR - N_γ

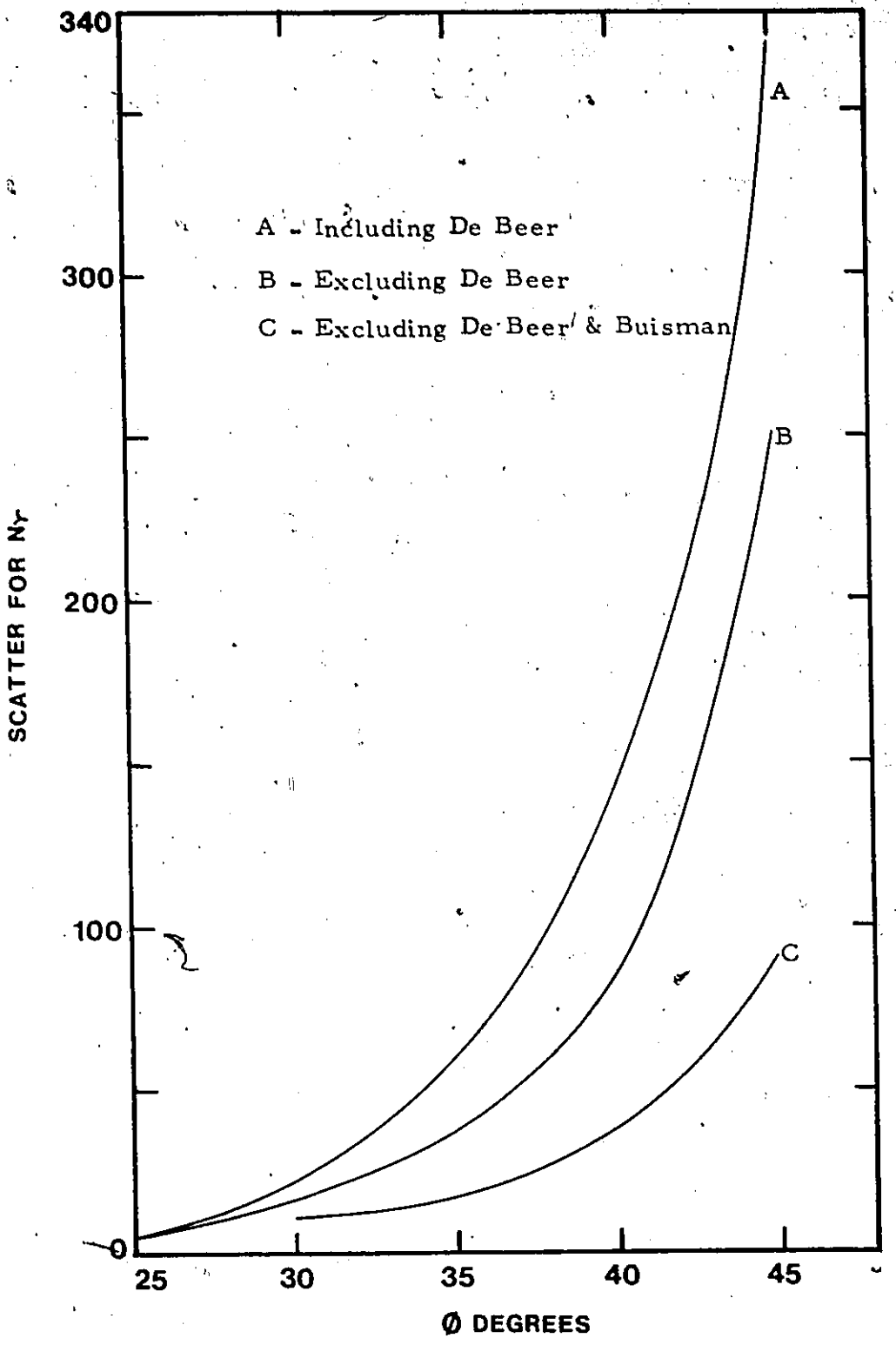

FIGURE 5.11 SCATTER OF N_γ WITH Ø

but only in the points, at first, where the shearing stresses are the largest and then from there gradually extends to other places. This phenomenon causes the modification of the soil properties along the slip surface. In loose soil, because of large deformation the density and consequently the shear strength increases before the moment of rupture.

In the soil with high density, in the zone of high concentrations the shearing strength is soon surpassed; there is a decrease in density and thus the shearing strength. Therefore the original shear strength is no longer available over the whole slip surface.

The results of this experiment are also plotted in the same Figure 5.10. The N_r-values, calculated using Brinch Hansen's equation which takes into account the various factors affecting the bearing capacity, fall very close to Muhs' curve. The size of the footing used during the test was in between Muhs' and De Beer's footing.

The N_r-values obtained are higher than those given by Brinch Hansen and by Vesic (1975). Now if we try to find the value of ϕ corresponding to the new N_r, it is found that the ϕ value increases. The rate of increment is not constant and depends on the initial value of ϕ. The increase is higher for lower initial ϕ values than those for higher initial ϕ (Figure 5.12).

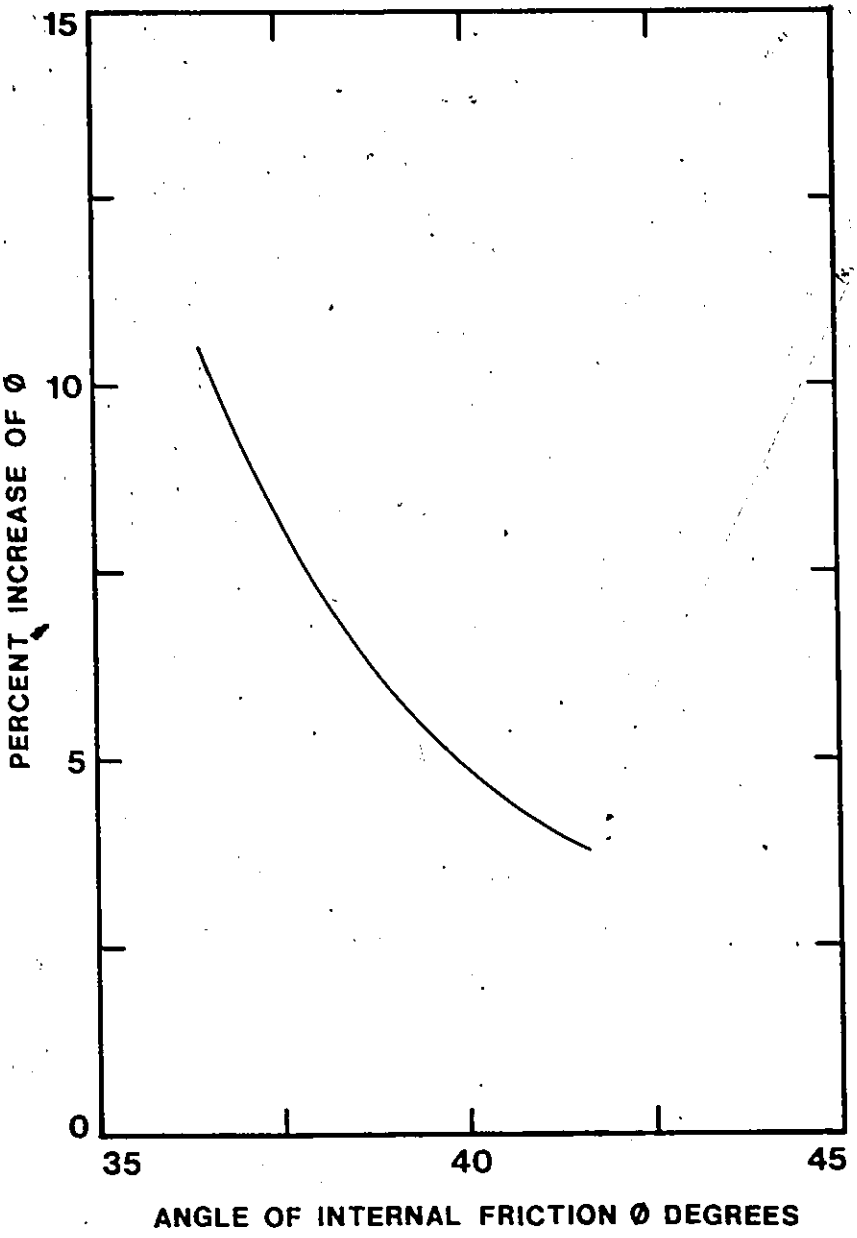

FIGURE 5.12 INCREASE OF Ø OBTAINED FROM TRIAXIAL TESTS

Brinch Hansen (1970) recommended the increase of the angle of internal friction ϕ obtained by triaxial test by 10 percent in case of plain strain condition which occurs under strip the footing but no mention is made of other types of footing. From the test of a circular footing, the results indicate that a 10.5 percent should be made for a ϕ of 36.5°, 4.6 percent for 40° and 3.6 percent for ϕ of 41.5°. With these increases of the angle of internal friction, the table given by Brinch Hansen for N_r-values can be used. Conversely if the ϕ-value is not modified, a new table is to be calculated for the N_r-values.

Another reason for the difference in the test results and the theoretical value of the bearing capacity is the selection of the value of the angle of internal friction. When the ϕ-value is determined by any method - the sample is loaded up to failure and the ϕ-value obtained is supposed to be the maximum value which can be obtained for a particular sample. In case of a footing test, certain amount of settlement needs to take place before the mobilization of the entire strength of the soil. It is not known what value of ϕ there is for a particular allowable settlement value.

Figure 5.13 shows the variation of the value of ϕ with strain in the triaxial test. The shaded area shows the ranges of value for a particular density of sand. For very dense sand, ϕ increases to a peak and then starts decreasing.

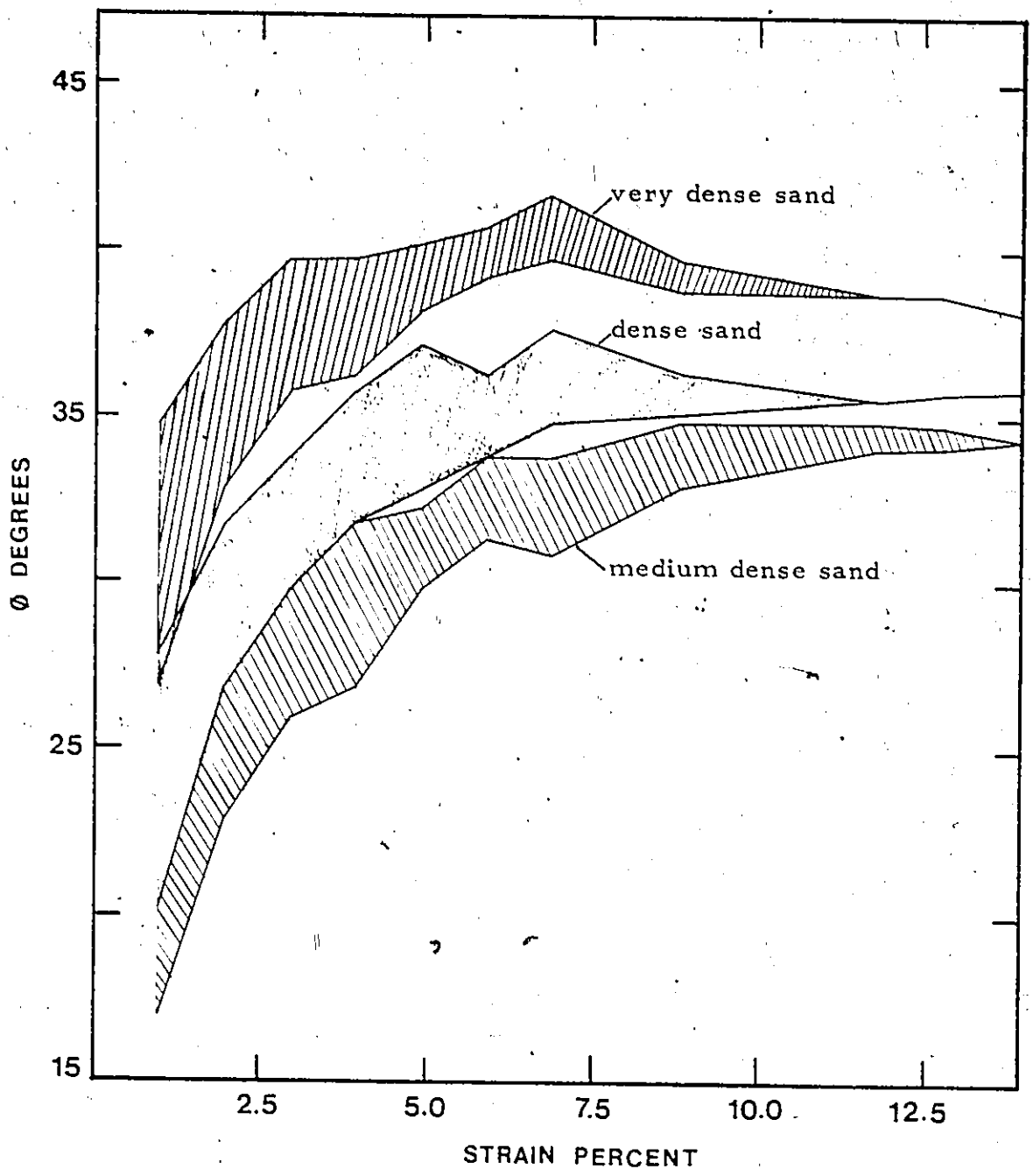

FIGURE 5.13 ANGLE OF INTERNAL FRICTION WITH STRAIN (Triaxial Test)

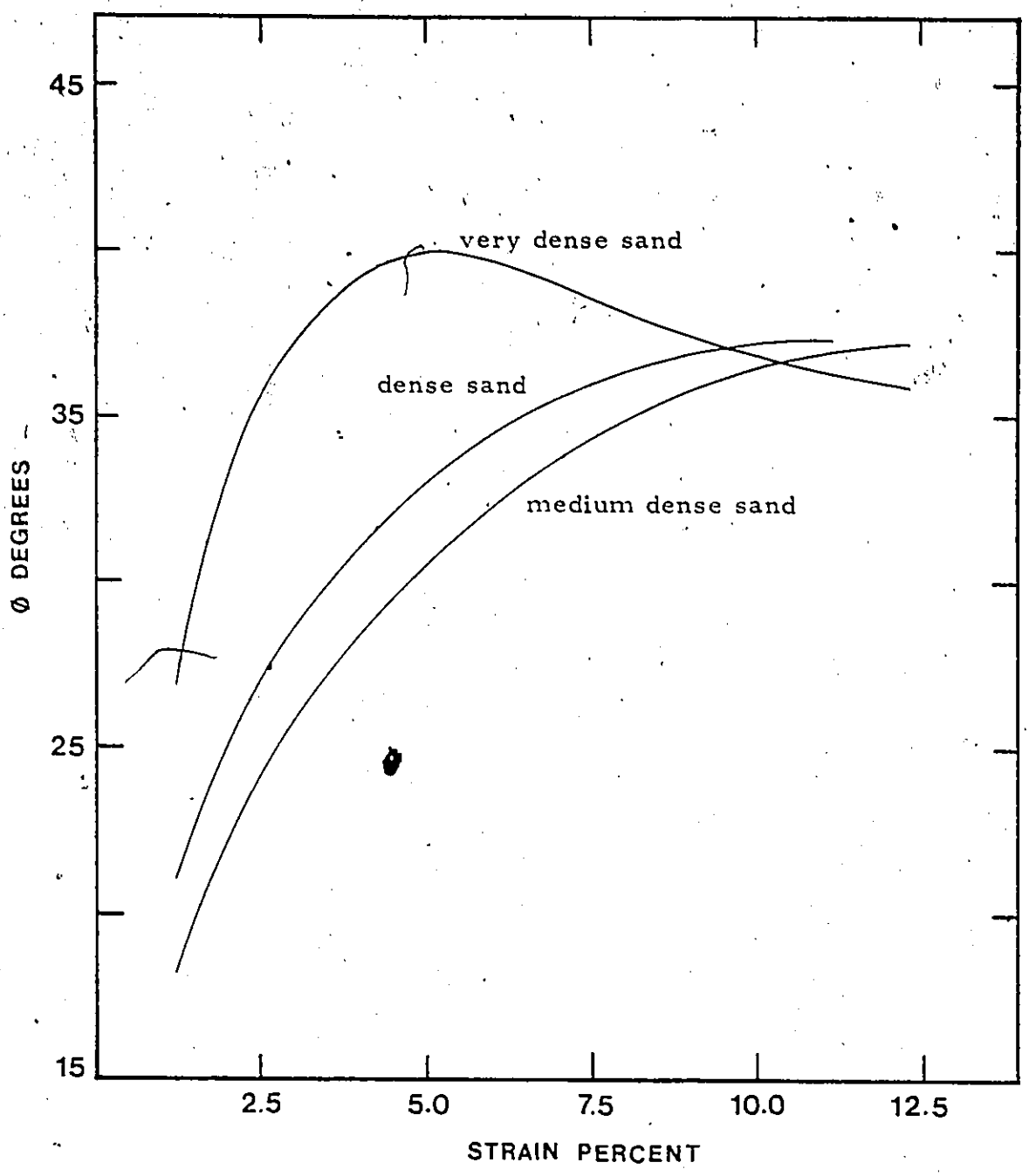

FIGURE 5.14 ANGLE OF INTERNAL FRICTION WITH STRAIN (Direct Shear Test)

The strain at which peak occurs will depend on the state of the sand. For medium dense sand there is no sharp peak but continuous increase and later becomes asymtotic to the strain value.

In direct shear tests the variations of the angle of internal friction with the strain are almost identical to the triaxial test (Figure 5.14).

5.5 Settlements

The settlements observed during the footing test in the sand box have already been plotted in relation to the depth in Figures 3.14a, 3.14b and 3.14c and the settlements obtained in the finite element analysis are plotted in Figures 4.2, 4.3 and 4.4. The ratio of the settlements at various depths to the surface settlement are plotted in Figures 5.15, 5.16, 5.17 against the relative depth which is defined as the ratio of the depth to the diameter of the footing. The same plots obtained in the finite element analysis are shown in Figure 5.19.

From the curves, 15 to 35 percent of the surface settlements occur at a relative depth of 2 depending on the relative density of the media and the applied stress level. This amount of settlement is quite appreciable and contrary to the general assumption that there is no influence of the load at depths greater than twice the diameter of the footing.

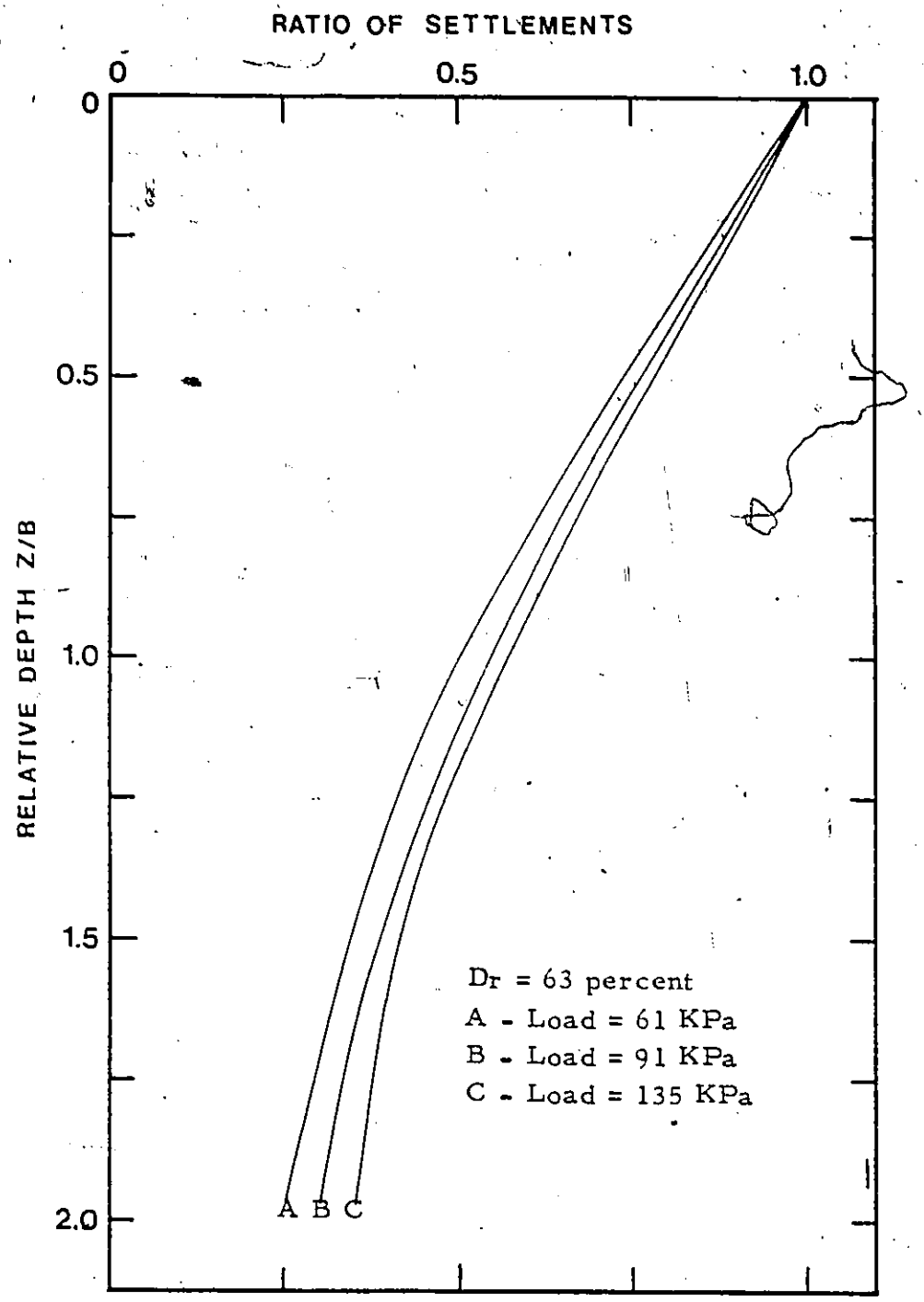

FIGURE 5.15 VARIATION OF RATIO OF SETTLEMENT WITH DEPTH

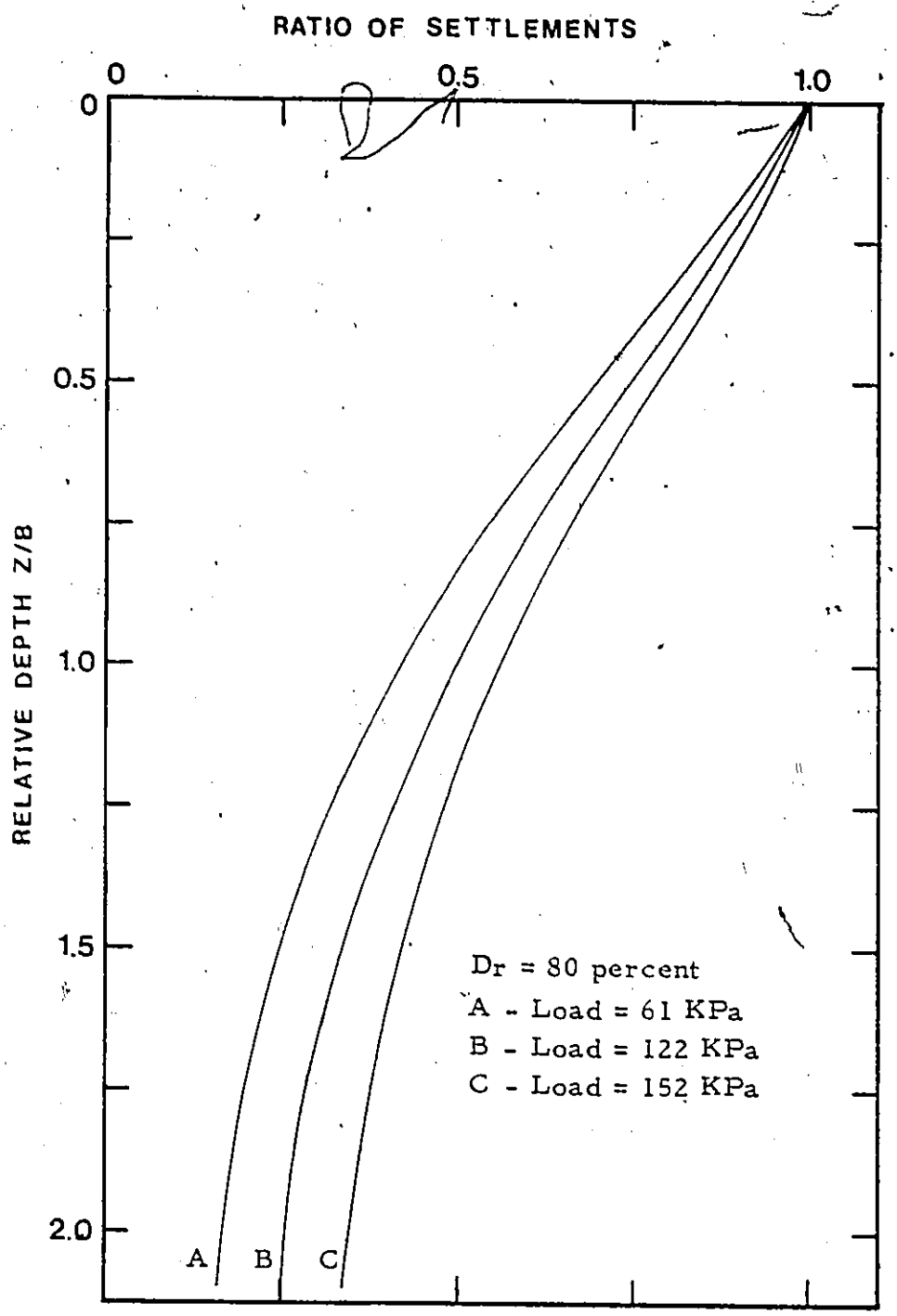

FIGURE 5.16 VARIATION OF RATIO OF SETTLEMENT WITH DEPTH

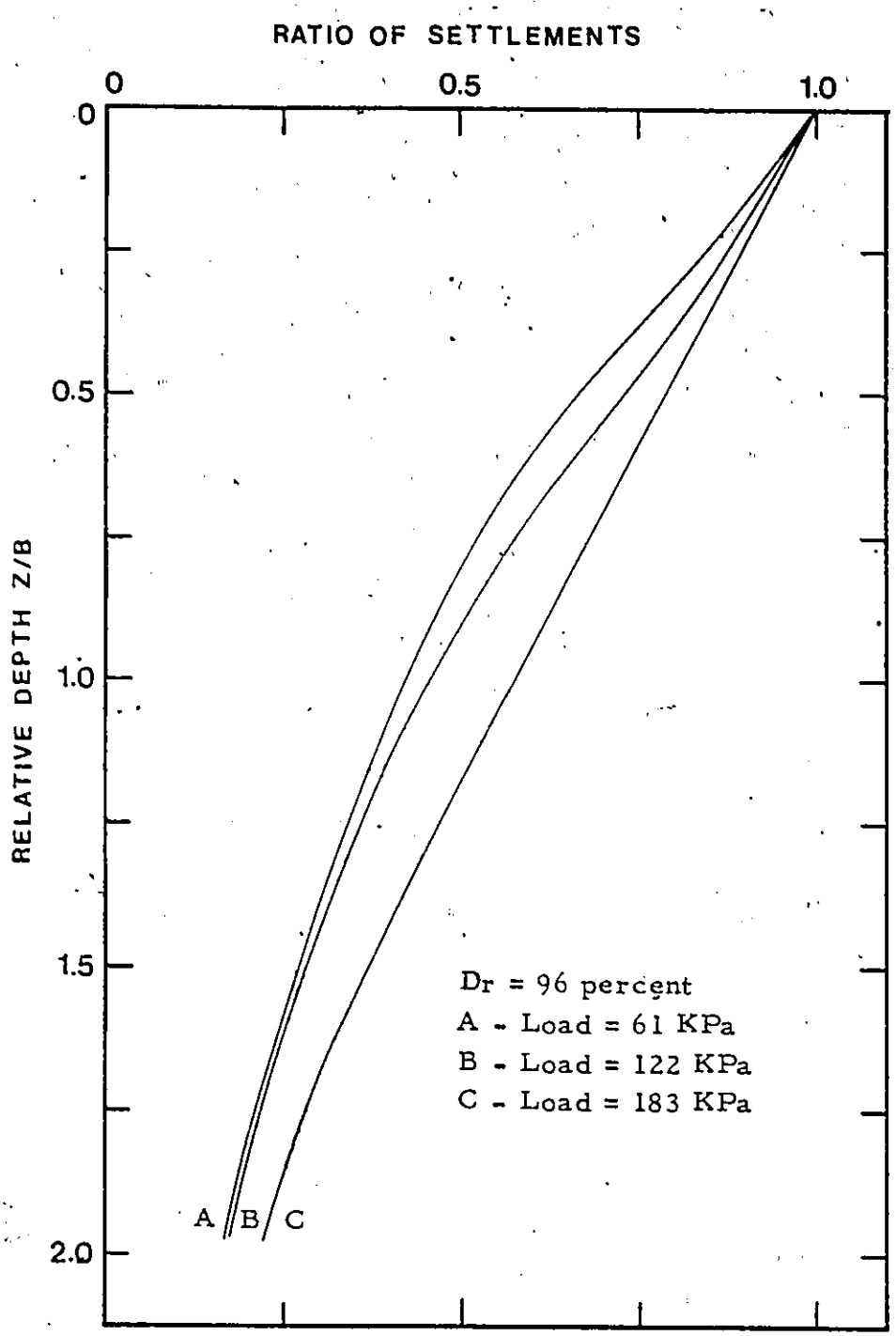

FIGURE 5.17 VARIATION OF RATIO OF SETTLEMENT WITH DEPTH

In the finite element analysis, at the same depth, about 7 percent of the surface settlement occurs. This low value may be due to the fact that the medium is isotropic and elastic.

In Figure 5.18 is a comparision between the ratio of test settlements and those obtained by various authors. The values, which depend on the soil properties and geological conditions, obtained from the literature are so erratic that it is difficult to compare and suggest any conclusion. If the values are compared with those obtained from the elastic theory, at low stress level and at high relative density over 90 percent, the values fall within the elastic range but at high stress level these fall outside the range. At lower densities, the sand behaves as inelastic at all stress level.

5.6 Strain in Soil Mass Beneath the Footing

The strain in the soil mass is defined as the deformation per unit depth below the foundation. The sand beneath the footing is divided into layers of 30 cm in depth and the deformation at the mid height of the layer is considered as the average for the whole layer.

In Figures 5.20 through 5.22, strains are plotted against relative depth for various densities and stress level. It is evident from the curves that for the same applied stress,

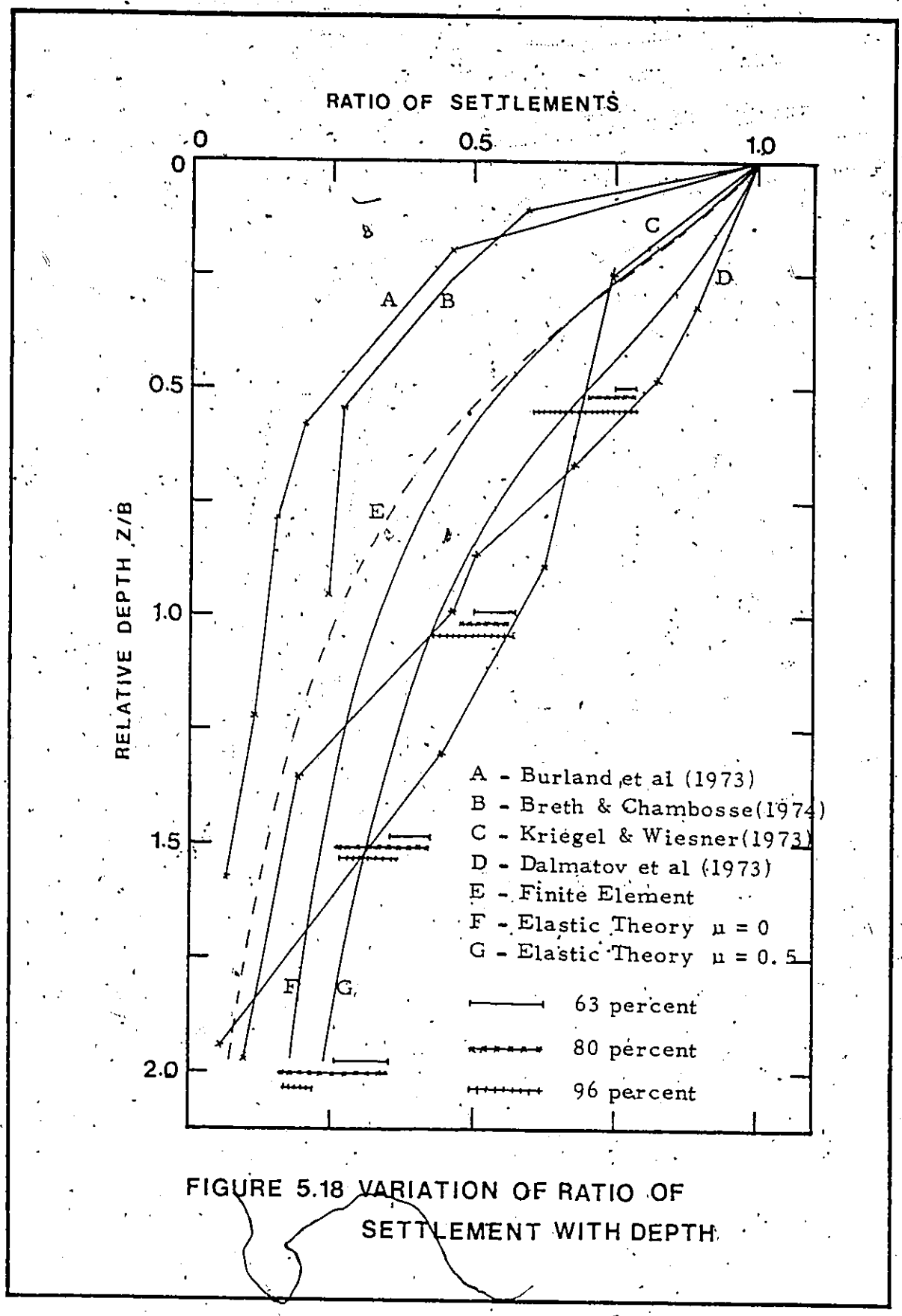

FIGURE 5.18 VARIATION OF RATIO OF SETTLEMENT WITH DEPTH

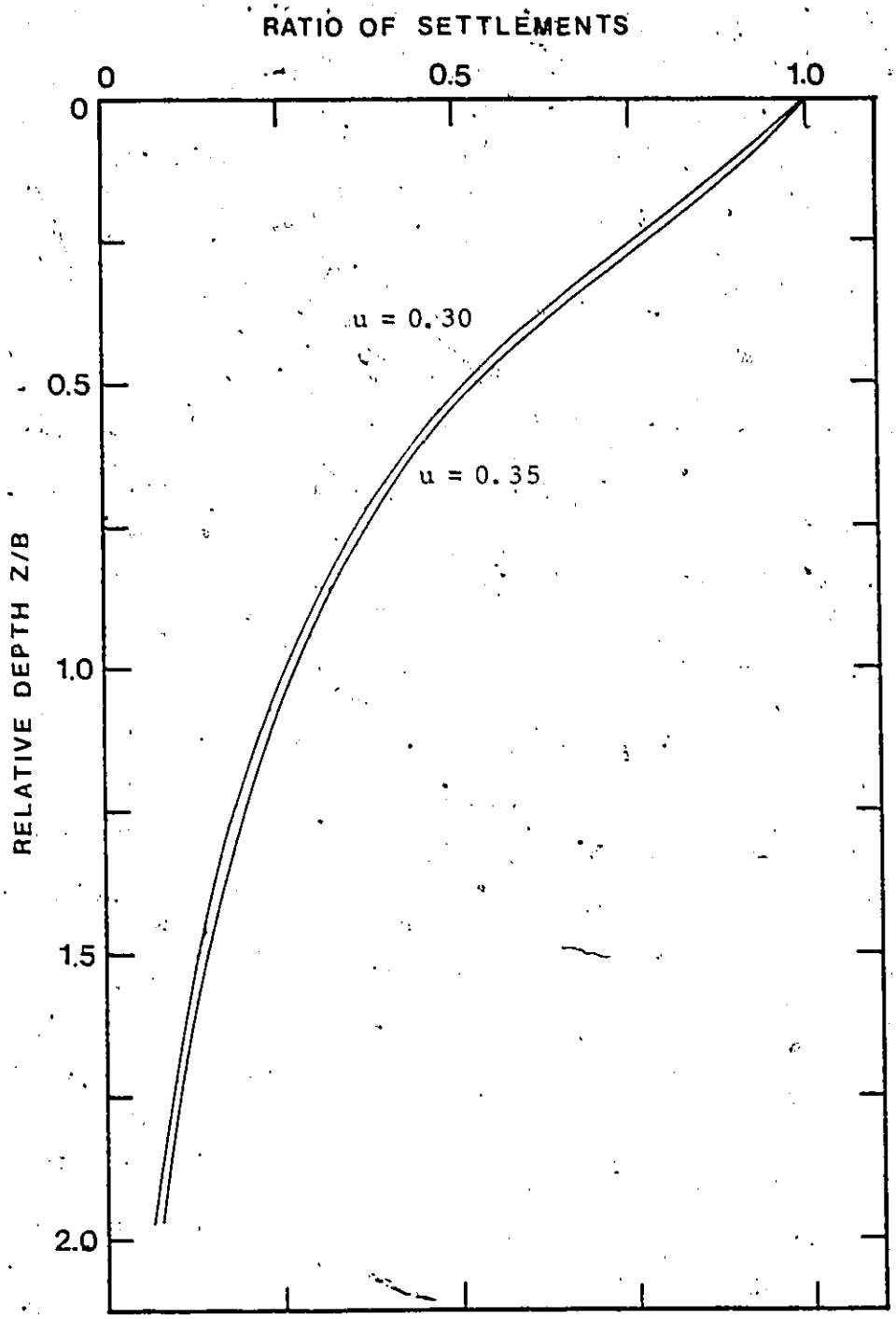

FIGURE 5.19 VARIATION OF RATIO OF SETTLEMENT WITH DEPTH
(from finite element analysis)

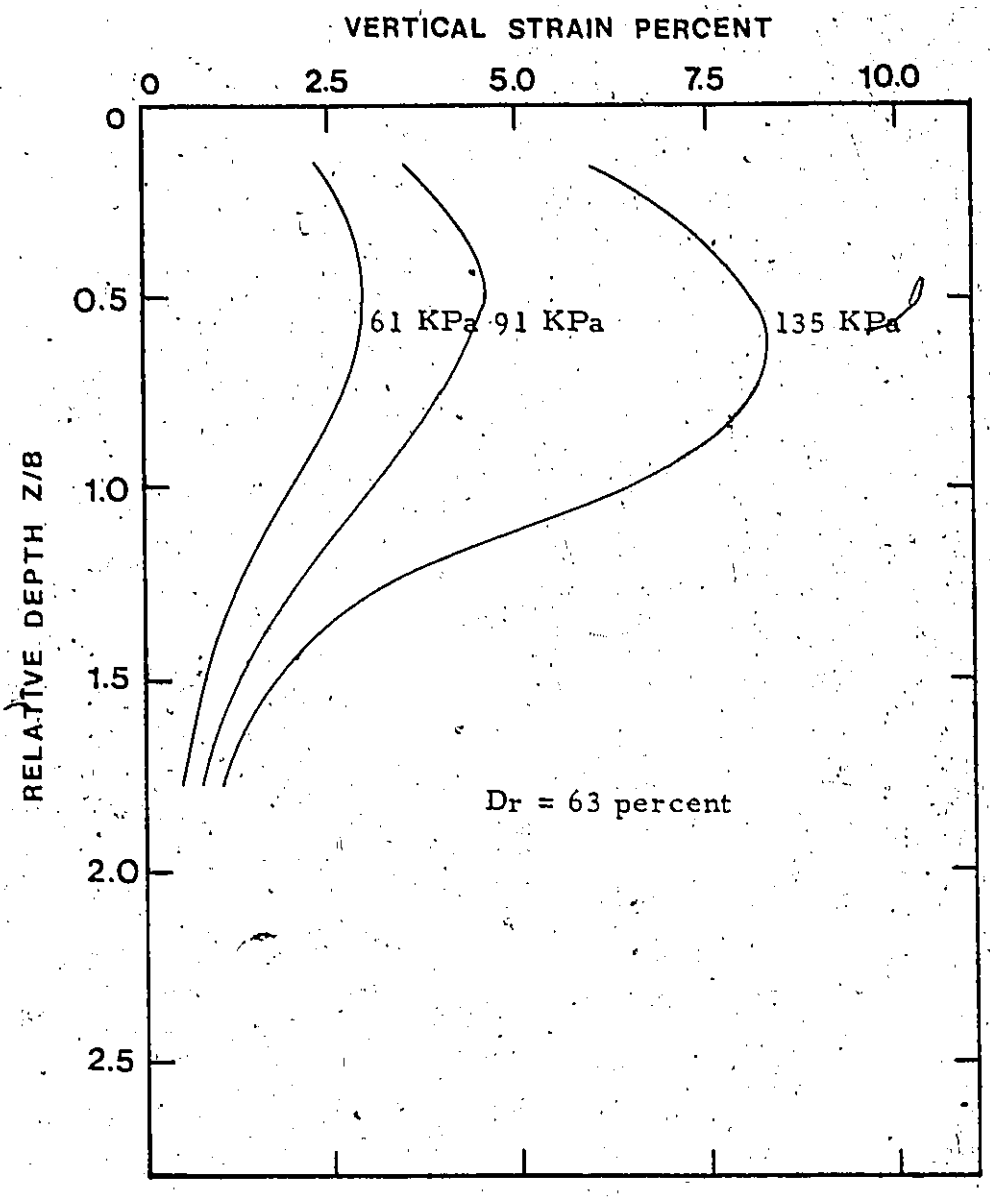

EIGURE 5.20 VARIATION OF STRAIN WITH DEPTH

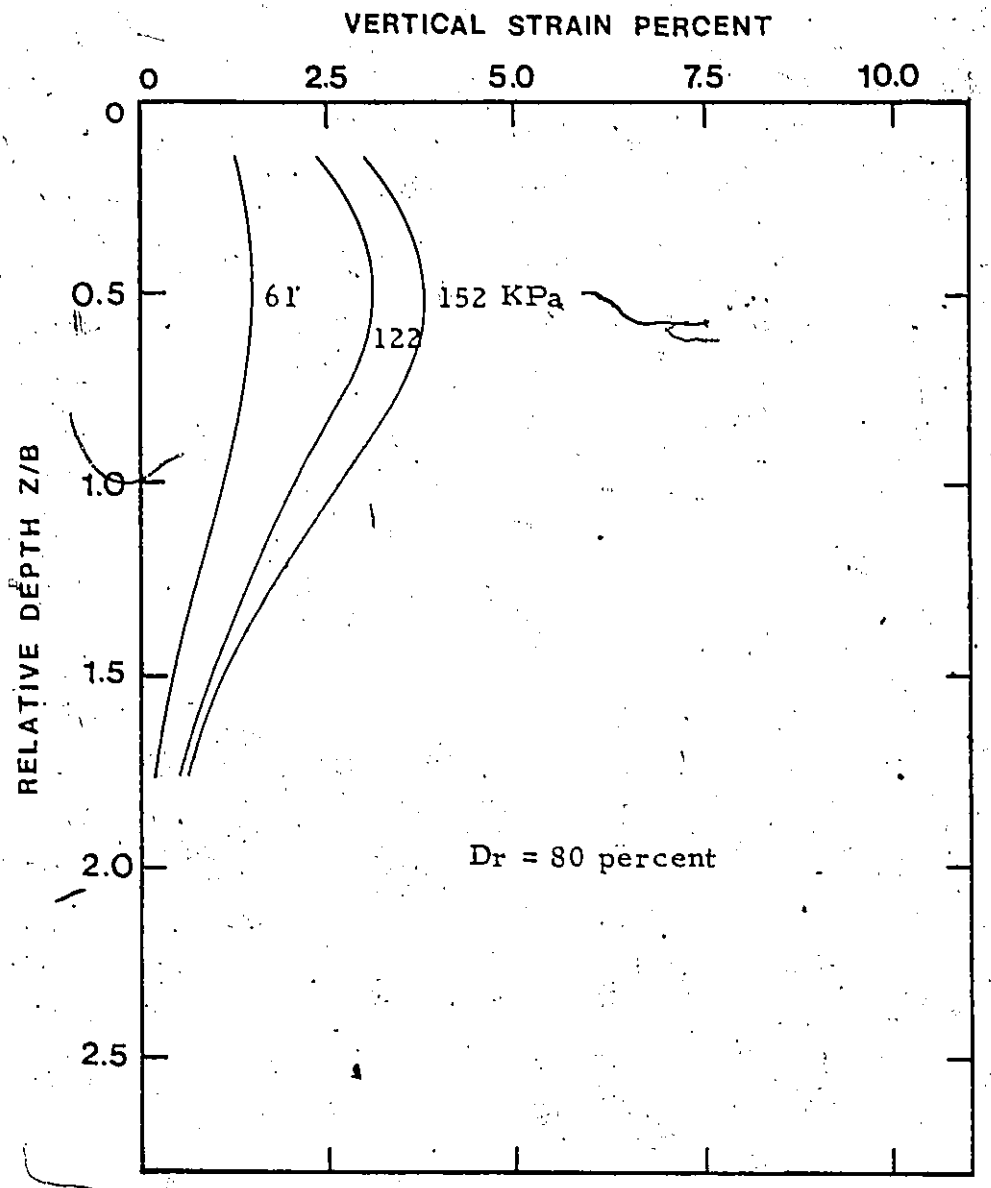

FIGURE 5.21 VARIATION OF STRAIN WITH DEPTH

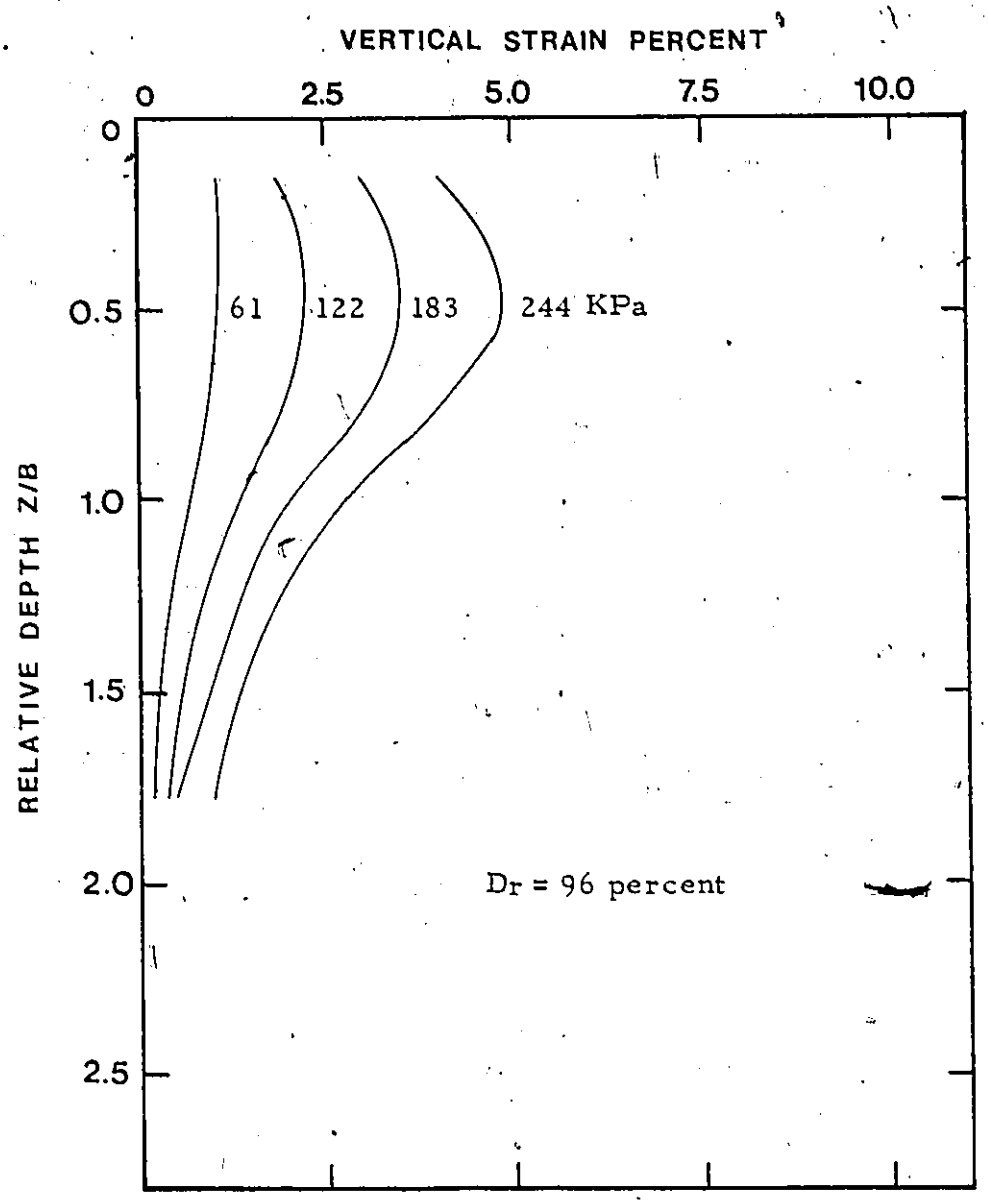

EIGURE 5.22 VARIATION OF STRAIN WITH DEPTH.

strains are higher for lower densities. Looking at the diagram from the tests, it is obvious that the maximum vertical strain does not occur immediately below the base of the footing, but at depths 0.5 to 0.7 times the diameter of the plate. As the density decreases, there is tendency in increasing this depth. These results agree with the test results obtained by Bond (1956) (see Eggested 1963) and Eggested (1963). However, Bond found this depth to be 0.4 to 0.7 times the diameter of the footing having the maximum vertical strain at smaller depth for dense sand than for loose sand. This depth is constant for all practical purposes, irrespective of the stress level.

The curves in Figure 5.23 are plotted from the results of finite element analysis. Although these curves do not show any pronounced peak at any depth, they show an increase in strain at a depth about 0.4 times the diameter of the footing and most of the strains take place within depth equal to the diameter of the footing.

5.7 Vertical Strain Influence Factor

The distribution of vertical strain within a linear elastic half-space subjected to a uniformly distributed load over an area at the surface can be described by

$$\epsilon_z' = \frac{q}{E} I_z$$

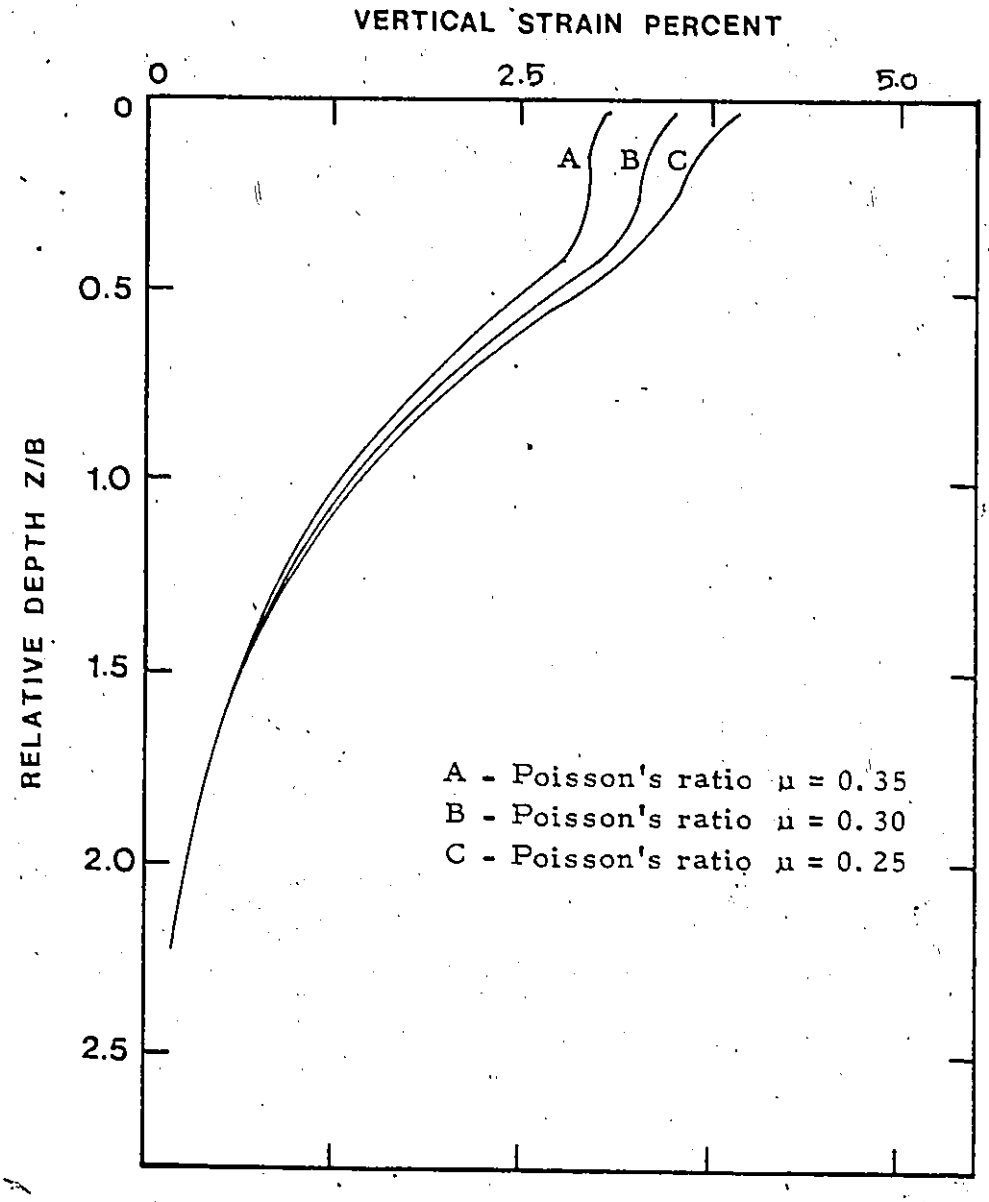

EIGURE 5.23 VARIATION OF STRAIN WITH DEPTHS (Finite Element)

in which q is the intensity of uniformly distributed load, E is Young's modulus of the elastic medium. I_z is the vertical strain influence factor which depends mainly on the Poisson's ratio and the location of the point. The distribution of the vertical strain influence factor for uniformly loaded circular area at the surface of the elastic half space is shown in Figure 5.24 for values of Poisson's ratio 0.5 and 0. The values obtained from the finite element analysis are also plotted in the same figure. The finite element analysis gives lower values up to a depth 0.8 times the diameter of the footing and after that the values almost coincides with the values obtained from the elastic theory. The reason for the low values may be attributed to the rigid boundaries of the box taken into consideration during the analysis.

The vertical strain influence factors for other Poisson's ratios and Young's modulus are presented in Figure 5.25. It is observed that the value of Poisson's ratio and Young's modulus both have some effect on the strain influence factor.

The values of strain influence factor from the test results are plotted in the Figures 5.26, 5.27 and 5.28. From this diagram it is observed that the stress level has some influence over the vertical strain influence factor. This effect is more pronounced at low densities than at high densities. This could be explained by the fact that at the initial

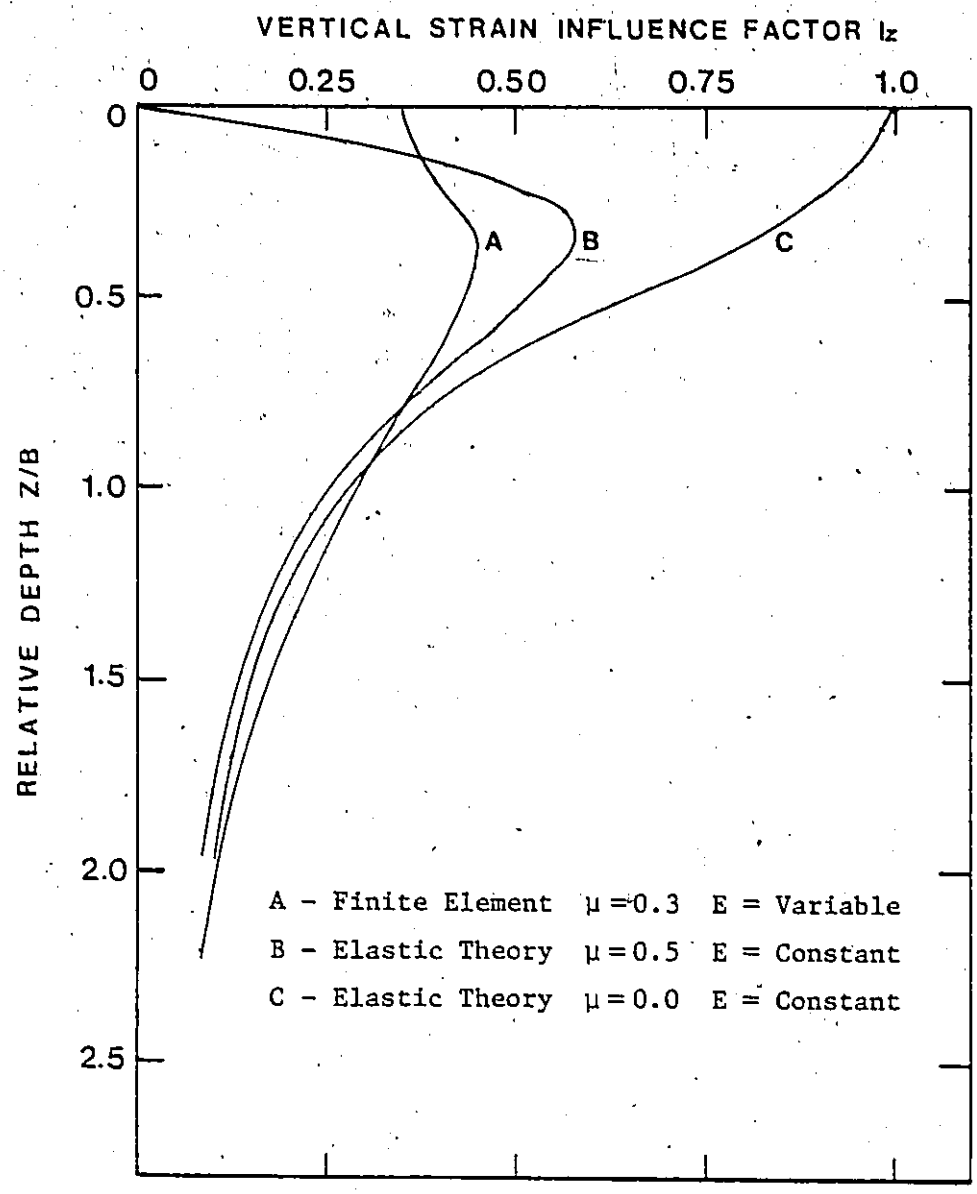

FIGURE 5.24 VERTICAL STRAIN INFLUENCE FACTORS WITH DEPTH

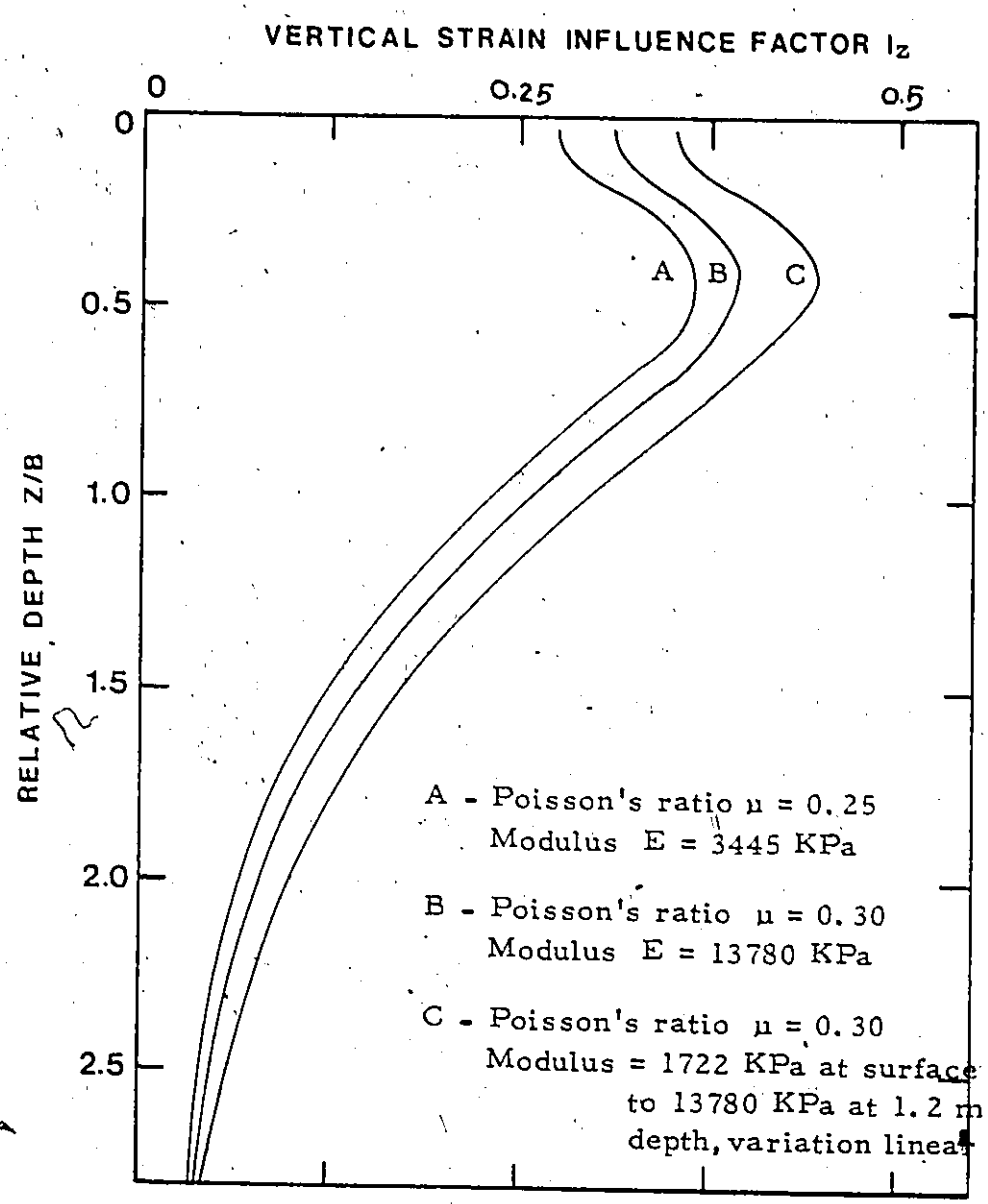

FIGURE 5.25 VERTICAL STRAIN INFLUENCE FACTORS WITH DEPTH

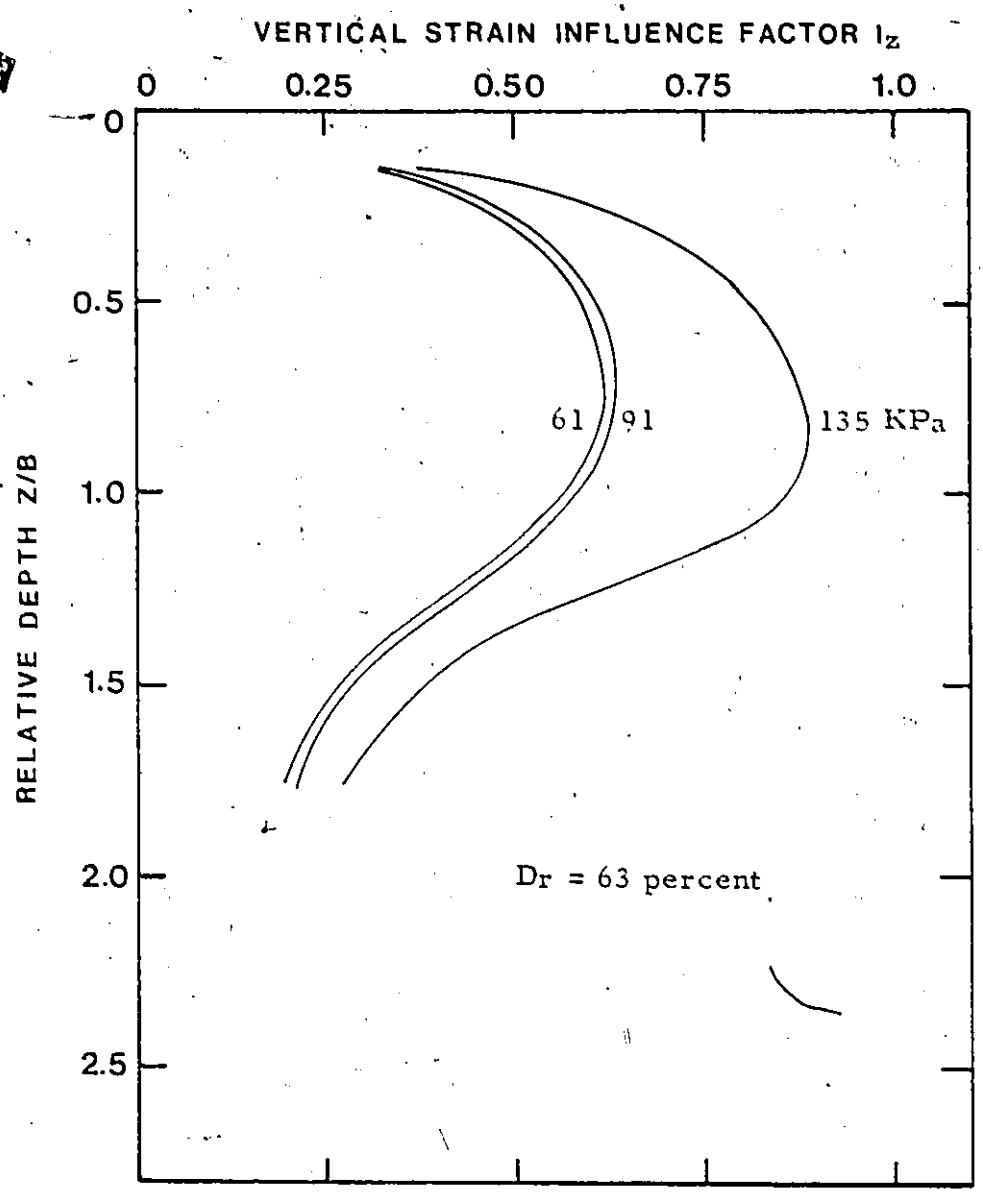

FIGURE 5.26 VERTICAL STRAIN INFLUENCE FACTORS WITH DEPTH

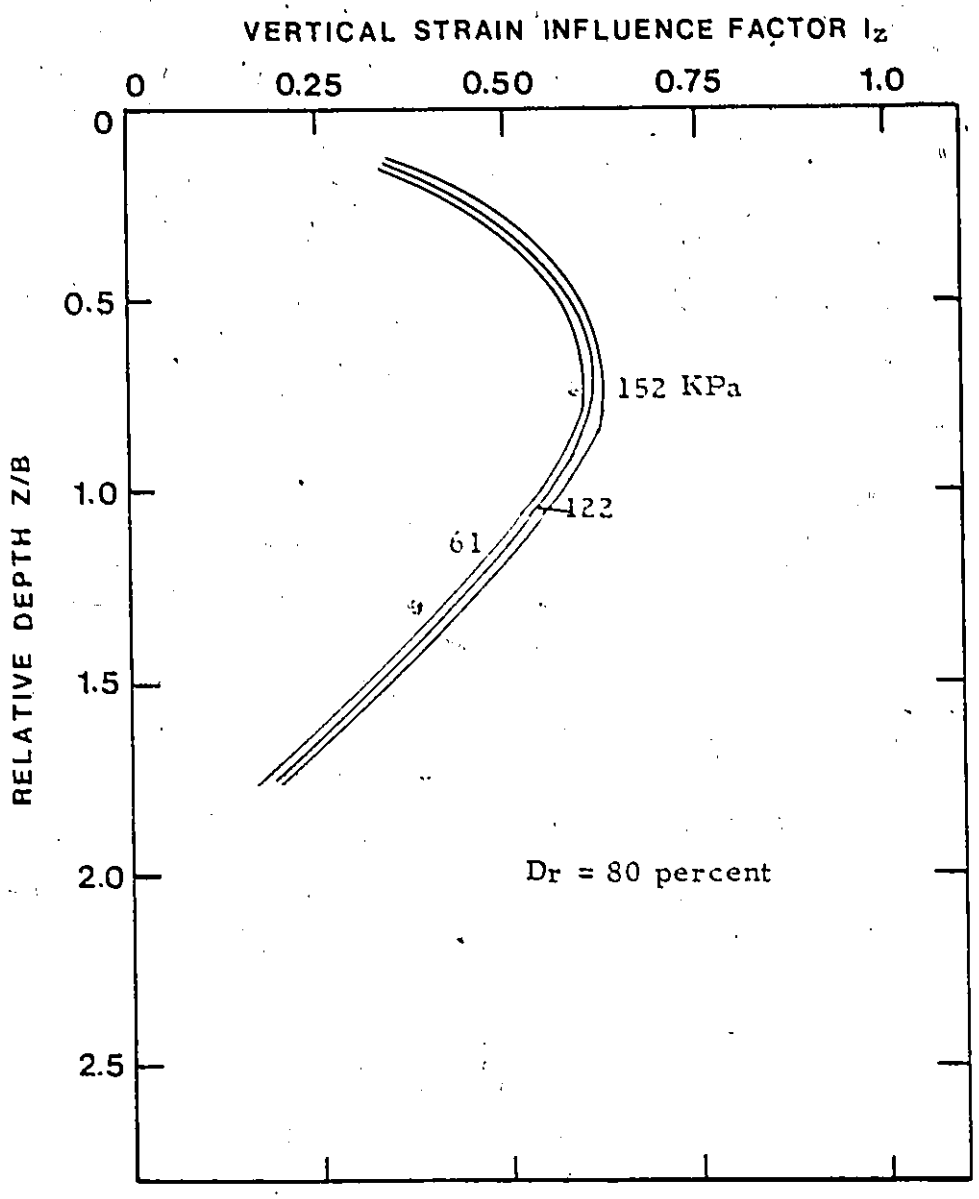

FIGURE 5.27 VERTICAL STRAIN INFLUENCE FACTORS WITH DEPTH

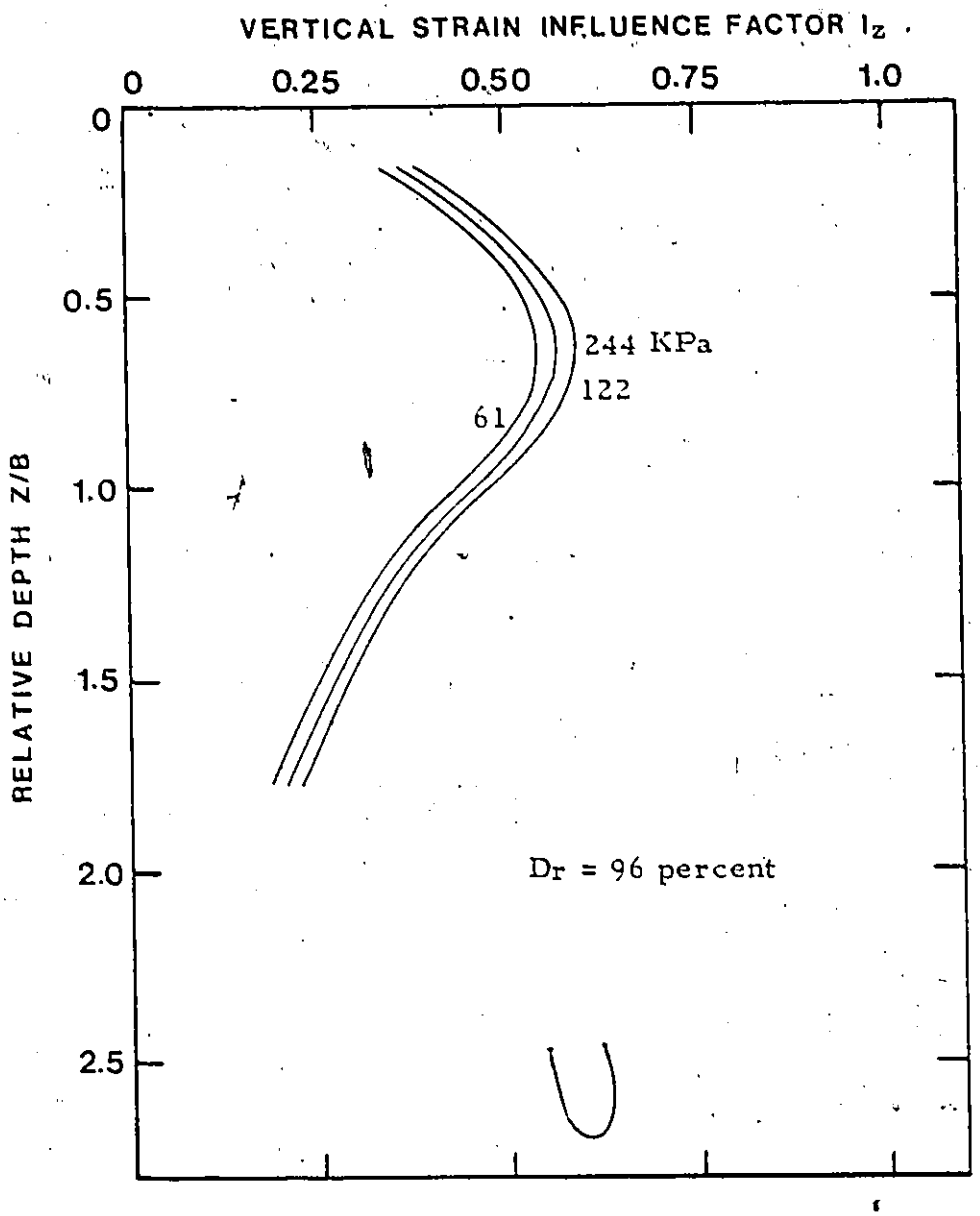

FIGURE 5.28 VERTICAL STRAIN INFLUENCE FACTORS WITH DEPTH

stages of loading the sand mass behaves as an elastic medium, but at the load increases the sand mass passes through various stages: elasto-plastic and finally plastic stages. The vertical strain influence factor increases more rapidly at high stresses specially at low densities. The strain influence factor reaches a maximum value of 0.80, 0.62 and 0.58 for relative densities of sand of 63, 80 and 96 percent respectively. These maximum values occur at depths between 0.7 and 0.8 times the diameter of the footing.

5.8 Evaluation of Settlement

Because no rational method for prediction of settlements due to distortion and compressibility of cohesionless masses is available, a number of empirical and semi-empirical methods have been developed. None of these methods are consistent in producing results either above or below average for varying soil conditions and foundation geometry.

The method proposed by Schmertmann, (1970), and subsequently modified (Schmertmann, 1978), which takes into account the successive strains in the soil mass produced by the loaded footing, provides the engineer with a more rational basis for evaluating the relative significance of various factors involved in the settlement problem. Schmertmann integrated the strains for the depth of influence which can be given by

$$S_d = \int_{z=0}^{2B} \varepsilon_z \, dz$$

$$= \Delta P \int_{0}^{2B} \frac{I_z}{E} \, dz$$

The above expression can be expressed as a summation of settlements of convenient approximately homogeneous layers and it becomes

$$S_d = C_1 \, C_2 \, \Delta P \sum_{i=1}^{n} \left(\frac{I_z}{E}\right)_i \Delta_{zi}$$

in which ΔP = Net load intensity at the foundation

I_z = Strain influence factor

E = Young's modulus at the middle of the ith layer

Δ_{zi} = Thickness of ith layer

C_1 & C_2 = Correction factors given by

$C_1 = 1 - 0.5 \left(\frac{\sigma'_o}{P}\right) > 0.5$

$C_2 = 1 + 0.2 \log_{10} \left(\frac{t}{.1}\right)$

where σ'_o = Effective in situ overburden pressure

t = Time in years after which the settlement is calculated

In this expression the value of I_z is taken from the "2B - 0.6 distribution" assumed by Schmertmann. From this analysis the Figures 5.24 through 5.28 show that the maximum value of I_z assumed by Schermartmann agrees well with the present analysis but the distribution is conservative as shown in the Figure 5.29. The author proposes to modify the distribution of I_z based on the test results, finite element results and the elastic analysis as shown in the Figure 5.29. In this modification the maximum value of I_z is considered to be 0.6 which occurs at a depth of 0.7 times the diameter of the footing and it extended to a depth 2.5 times the diameter.

Even with this distribution the settlement calculated by the formula proposed by Schmertmann is less than the settlement observed during the test due to factors depending on stress level specially at lower densities. From this some consideration should be given to the stress level and ultimate bearing capacity of the footing, therefore another correction factor should be introduced in the Schmertmann formula to take into account the ultimate bearing capacity of the footing. The settlement is given by the following:

$$S_d = C_1 C_2 C_3 \Delta P \sum_{i=1}^{n} \left(\frac{I_z}{E}\right)_i \Delta_{zi}$$

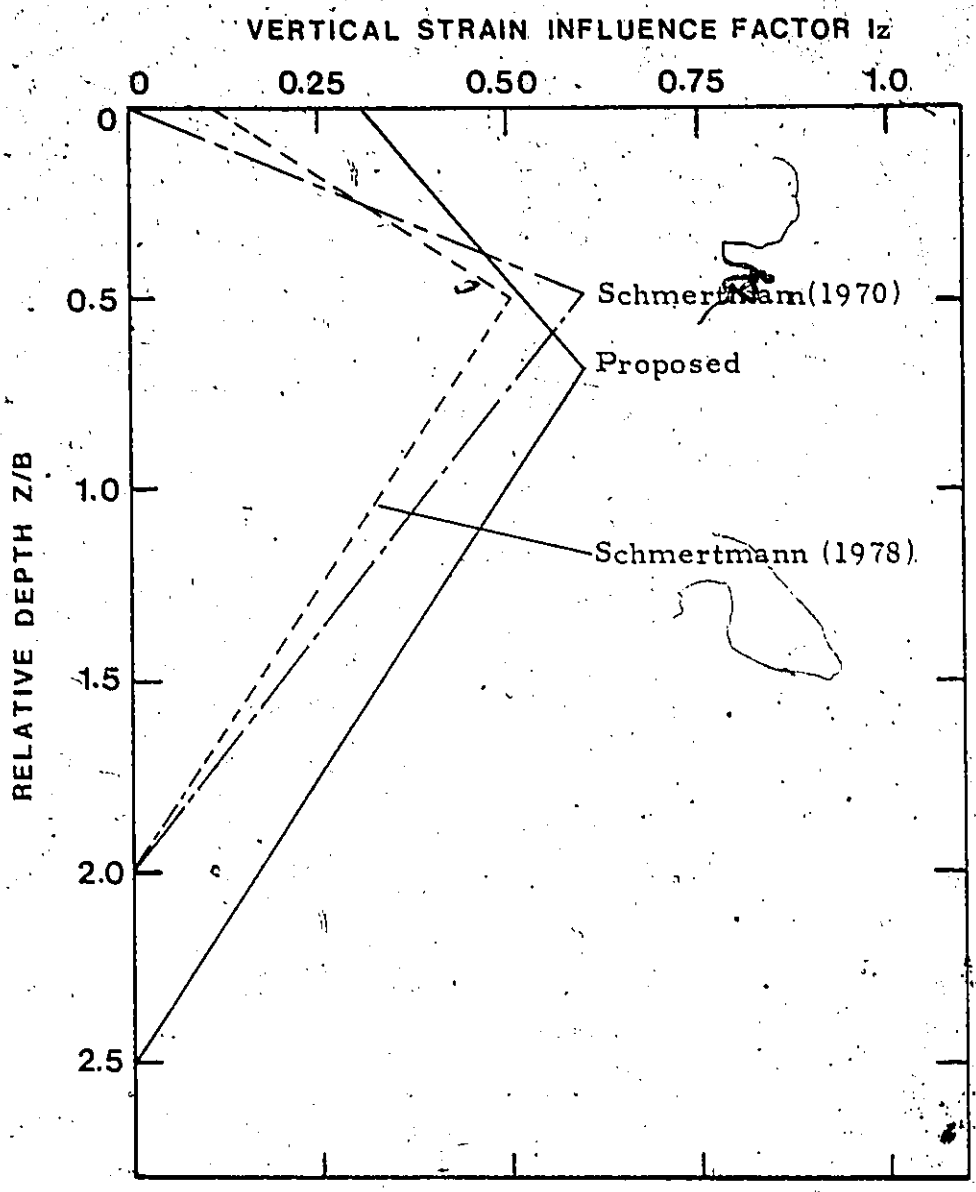

FIGURE 5.29 VERTICAL STRAIN INFLUENCE FACTORS WITH DEPTH

in which $C_3 = (1.2 + \frac{\Delta P}{q_u})$ - for medium dense sand

$C_3 = (1.0 + \frac{\Delta P}{q_u})$ - for dense sand

$C_3 = 1.2$ - for very dense sand

5.9 Heaving Around the Footing

When a footing on sand is loaded, heaving around the footing does not start occurring until the load reaches a certain value depending on the relative density of the sand. Figure 5.30 represents the variation of R defined as the volumetric ratio of heave to depression with ratio of the applied load to the ultimate load and the Figure 5.31 shows at what load the heaving starts occurring depending on the relative density of sand. It is observed that at the relative densities of 63, 80 and 96 percent the heaving starts at loads that are 39, 27 and 22 percent of the ultimate load respectively. From this, it can be concluded that there will always be some compression within the sand mass irrespective of the density before any heaving occurs.

At the ultimate load the volume of heave around the footing is about 2.3 and 1.4 times the volume of depression directly beneath and around the footing at the relative densities of 96 and 80 percent respectively. But at the relative density of 63 percent the volume of heave is only

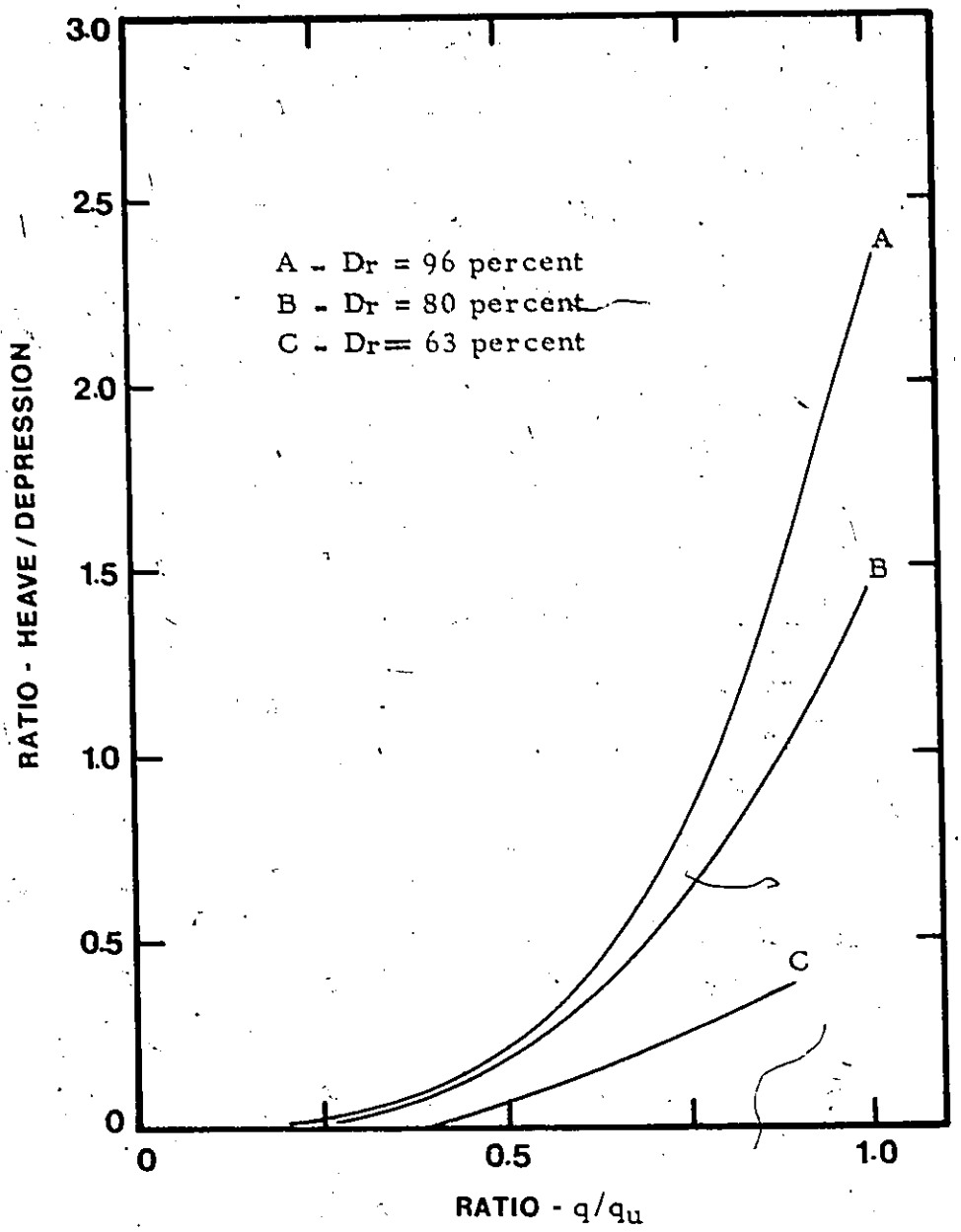

FIGURE 5.30 OCCURANCE OF HEAVE WITH LOAD

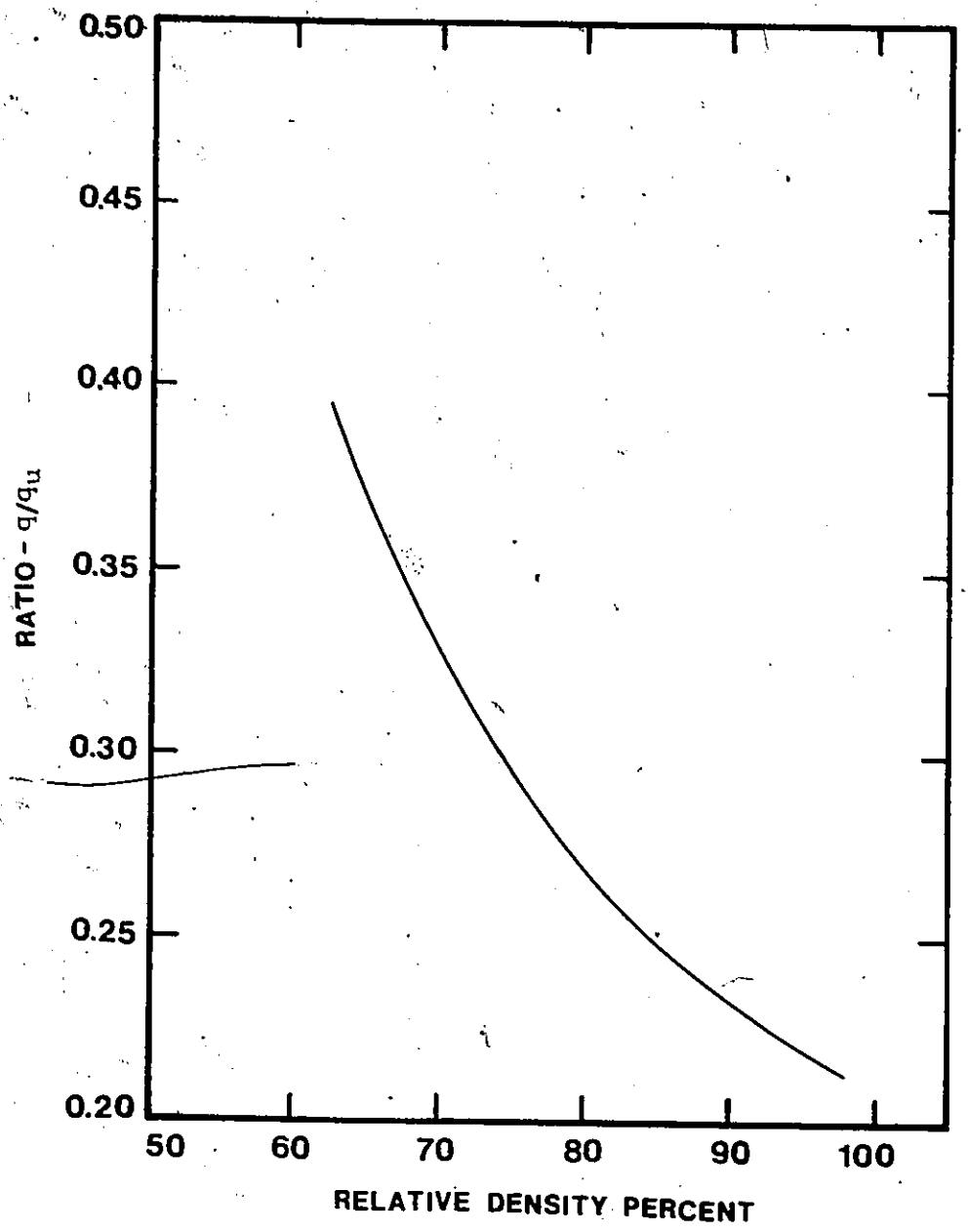

FIGURE 5.31 RATIO q/q_u AT WHICH HEAVING OCCURS WITH RELATIVE DENSITY

50 percent of the volume of depression at the ultimate load. The amount of heave does not depend only on the density of the media but also on the grain shape, grain size distribution, mineralogy, overburden pressure and so on.

CHAPTER 6

CONCLUSIONS AND RECOMMENDATIONS

6.1 Summary

This research was undertaken to review the problem of bearing capacity and settlement in sand and suggest some improvements for the method of evaluation. As most of the current theories are based on the results of small scale tests performed in the laboratory, an attempt was made to carry out some tests in what is closer to field conditions. To simulate field conditions, the test bed was prepared by freely dropping sand particles from predetermined heights resulting in a particular density of the soil media. As the sand is freshly deposited, the effects of time on various factors could not be taken into account.

Altogether, seven tests were performed. The first test was carried out to test the instrumentation and to commission the whole system of the test. No results are presented from this test. Subsequently, two tests at each of the three densities were performed.

In the analysis, the test results were compared with widely used theories. In the case of bearing capacity analysis, some variations in the bearing capacity factor N_r were noticed, but it agrees with a value obtained from a large scale test.

Another important factor in using the bearing capacity equation is the angle of internal friction. As the value of N_r is very sensitive to the variation of angle of internal friction, ϕ, a correct evaluation procedure for ϕ is needed.

Another aspect of this research was to study the problem of settlement in grannular soil. No method available to date, is consistent in predicting settlement values which agree reasonably well with the field measurements. The method proposed by Schmertmann (1970, 1978) which takes into account the soil modulus and deformation characteristics, was compared with the observed values and some modification has been suggested.

6.2 Observations

1. Total resistance is offered partly by the shearing strength of the soil directly beneath the footing and partly by the surcharge around the footing gained during the process of testing due to gradual embedment. The load settlement curves plotted from the loading test always show some effect of embedment.

2. The resistance due to surcharge, according to Terzaghi's theory, increases linearly with the depth of embedment, whereas according to Brinch Hansen's theory, the increment is nonlinear and the effect is very small at the beginning of penetration.

6.3 Conclusions

1. Both Terzaghi and Hansen's theories yield values consistently lower than the test results for the bearing capacity at alll states of the sand. With the decrease in density, the gap between the observed and predicted values increases, and can go as high as 50 percent of the observed value for medium dense sand.

2. The value of the bearing capacity factor N_r calculated from the test are higher for low density and identical on the average to the values given by others, at high density, which is consistent with the values obtained by Muhs.

3. The angle of internal friction obtained from the triaxial test should be increased in the case of a circular footing, by a certain percentage (Figure 5.12) which depends on the initial density of the sand whereas Brinch Hansen suggested an increase of 10 percent in the case of strip footing.

4. The angle of internal friction is not a constant, but rather increases with the increase in strain and then becomes either constant or decreases at about 10 percent of strain.

5. The very dense sand used in the test behaves elastically at low stress levels and non-elastically at high stress but others behave as non-elastic at all stress levels.

6. About 15 to 35 percent of the total settlement was observed at a depth twice the diameter of the footing whereas only 7 percent was indicated by the finite element analysis in which the sand was considered as isotropic, elastic and non-homogeneous.

7. The maximum vertical strain occurs at depth 0.5 to 0.6 times the diameter of the footing. This depth increases with the decrease in density of sand.

8. The maximum value of vertical strain influence factor depending on the stress level, especially at low densities occurs at depth between 0.7 and 0.80 times the diameter of the footing.

9. A modification to Schmertmann's '2B - 0.6' distribution is suggested in Figure 5.29 in which the depth is increased to 2.5B instead of 2B and the value at the surface increased to 0.3 instead of 0.

10. A factor C_3 (elaborated in Art. 5.8) depending on applied load and the ultimate bearing of the media is introduced in Schmertmann's equation to take into account the effect of stress level on settlement.

11. The deformation of the sand surface around the footing depends on the stress level and relative density of sand. The heaving starts occurring at a load of 0.39 q_u, 0.27 q_u

and 0.22 q_u for the relative densities 63, 80 and 63 percent respectively.

12. At the ultimate load, the volume of heave around the footing is about 2.3, 1.4 and 0.5 times the volume of depression directly beneath and around the footing at the relative densities of 96, 80 and 63 percent respectively.

13. The radial deformation decreases with the increase in distance from the centre of the footing. From the finite element analysis, the radial deformation increases from the centre of the footing to a maximum value at a distance of 0.75 times the diameter and then starts decreasing.

6.4 Recommendations

1. During the loading and penetration of the footing, properties such as angle of internal friction, unit weight and modulus change continuously. An experimental program could be elaborated to determine these properties which are important in predicting the bearing capacity and settlement.

2. The suggested settlement equation should be checked and verified using known soil properties with the observed settlement values in the field.

REFERENCES

Balla, A., (1962), "Bearing Capacity of Foundations", Proc. ASCE, Vol. 88, SM 5, pp. 13-34.

Bent Hansen, (1961), "The Bearing Capacity of Sand, Tested by Loading Circular Plates", Proc. Fifth Int. Conf. on Soil Mech. & Found. Engg., Paris, pp. 659-664.

Bond, D., (1961), "The Influence of Foundation Size on Settlement", Geotechnique, Vol. 11, pp. 121-143.

Briand, J.L., (1979), "The Pressuremeter: Application to Pavement Design", Ph.D. Thesis, University of Ottawa.

Brinch Hansen, J., (1961), "A General Formula for Bearing Capacity", Bulletin No. 11, Danish Geotechnical Institute, Copenhagen, pp. 38-46.

Brinch Hansen, J., (1965), "The Philosophy of Foundation Design: Design Criteria, Safety Factors and Settlement Limits", Proc. Symp. Bearing Capacity and Settlement of Foundation, Duke University, pp. 9-13.

Brinch Hansen, J., (1966), "Improved Settlement Calculation for Sand", Bulletin No. 20, Danish Geotechnical Institute, Copenhagen, pp. 15-17.

Brinch Hansen, J., (1970), "A Revised and Extended Formula for Bearing Capacity", Bulletin No. 28, Danish Geotechnical Institute, Copenhagen, pp. 5-11.

Chen, W.F. and Davidson, H.L. (1973), "Bearing Capacity Determination by Limit Analysis". Proc. ASCE, Vol. 99, SM 6, pp. 433-449.

D'Appolonia, D.J., D'Appolonia, E., and Brissette, R.F., (1968), "Settlement of Spread Footing on Sand", Proc. ASCE, Vol. 94, SM3, pp. 735-760.

D'Appolonia, D.J., D'Appolonia, E., and Brissette, R.F., (1970), "Discussion on Settlement of Spread Footing on Sand", Proc. ASCE, Vol. 96, SM2, pp. 754-761.

D'Appolonia, D.J., Lambe, T.W., (1970), "Method of Predicting Initial Settlement", Proc. ASCE, Vol. 96, SM2, pp. 523-545.

D'Appolonia, D.J., Poulos, H.G.., Ladd, C.C., (1971), "Initial Settlement of Structure on Clay", Proc. ASCE, Vol. 97, SM10, pp. 1359-1377.

De Beer, E.E., (1965), "Bearing Capacity and Settlement of Shallow Foundation on Sand", Proc. Symp., Bearing Capacity and Settlement of Foundations, Duke University (Publ. 1967), pp. 15-33.

De Beer, E.E., (1970), "Experimental Determination of the Shape Factors and the Bearing Capacity Factors of Sand", Geotechnique, Vol. 20, No. 4, pp. 387-411.

De Beer, E.E. and Ladanyi, B., (1961), "Etude Expémentale de la Capacité Portante du Sable Sous de Foundation Circulaires Etablies en Surface," Proc. Fifth Int. Conf. on Soil Mech. Found. Engg., Paris, Vol. 1, pp. 527-581.

Desai, C.S. and Christian, J.T., (1977), "Numerical Methods in Geotechnical Engineering", McGraw Hill.

Deschenes, J.H., (1978), "Bearing Capacity of Footings close to slopes of Cohesionless Soil", Ph.D. Thesis, University of Ottawa.

Eggested, Aa., (1963), "Deformation Measurements Below a Model Footing on the Surface of Dry Sand", Proc. European Conf. on Soil Mech. and Found. Engg., Vol. 1, Wiesbaden, pp. 233-239.

Feda, Jaroslav, (1963), "Validity of Some Settlement Computations Theories as tested in Laboratory Conditions on Grannular Soils", Proc. European Conf. on Soil Mech. and Found. Engg., Vol. 1, Wiesbaden, pp. 61-77.

Feda, Jaroslav, (1978), "Stresses in Subsoil and Methods of Final Settlement Calculation", Elsevier Scientific Publishing Company, New York, 1st Edition.

Fellenius, W., (1929), Jordstatiska berakningar for Vertical belastning pa horisontal mark under antagande av cirkularcylindriska glidytor, Teknisk tidskrift, Vol. 59, No. 21, p. 57, Stockholm.

Hasnain, Mohammed, (1974), "Shear Strength Characteristics of a Crushed Quartz Sand", M.A.Sc. Thesis, University of Ottawa.

Jorden, E.E., (1977), "Settlement in Sand - Methods of Calculating and Factors Affecting", Ground Engineering, Vol. 10, No. 1, pp. 30-37.

Jumikis, A.R. (1961), "Shape of Rupture Surface in Dry Sand", Proc. Fifth Int. Conf. on Soil Mech. and Found. Engg., Paris, Vol. 2, pp. 693-698.

Karafiath, Leslie L., (1970), "Shape Factors in Bearing Capacity Equation", Proc. ASCE, Vol. 96, SM4, pp. 1493-1497.

Lambe, T.W., (1964), "Methods of Estimating Settlement", Proc. ASCE, Vol. 90, SM5, pp. 43-68.

Lambe, T.W. and Whitman, R.V., (1969), "Soil Mechanics" John Wiley & Sons Inc.

Larkin, Lawrence A., (1968), "Theoretical Bearing Capacity of very Shallow Footings", Proc. ASCE, Vol. 94, SM6, pp. 1347-1357.

Louw, J.M., (1977), "Estimating Settlements on Cohesionless Soils from S.P.T. Data", Civil Engineer, South Africa, Vol. 19, No. 12, pp. 275-282.

Matsumoto, Takashi, (1976),"Finite Element Analysis of Immediate and Consolidation Deformations Based on Effective Stress Principle", Soils and Foundation, Japan Society of Soil Mechanics and Foundation Engineering Vol. 16, No. 4, pp. 23-34.

Meyerhof, G.G., (1970), "Ultimate Bearing Capacity of Sand Layer Overlying Clay", Canadian Geotechnical Journal, Vol. 11, No. 2, pp. 223-229.

Meyerhof, G.G., (1970), "Safety Factors in Soil Mechanics" Canadian Geotechnical Journal, Vol. 7, No. 4, pp. 349-355.

Meyerhof, G.G., (1965), "Shallow Foundations" Proc. ASCE, Vol. 91, SM2, pp. 21-31.

Meyerhof, G.G., (1963)), "Some Recent Research on the Bearing Capacity of Foundations", Canadian Geotechnical Journal, Vol. 1, pp. 16-26.

Meyerhof, G.G., (1956), "Penetration Tests and Bearing Capacity of Cohesionless Soils", Proc. ASCE, Vol. 82, SM1, pp. 1-19.

Meyerhof, G.G., (1951), "Ultimate Bearing Capacity of Foundation", Geotechnique, Vol. 2, pp. 301-332.

Mizuno, T., (1953), "On the Bearing Power of Soil under a uniformly Distributed Circular Load", Proc. Third Int. Conf. on Soil Mech. and Found. Engg., Vol. 1, pp. 446-449.

Morgan, J.R. and Gerrard, C.M., (1971), "Behaviour of Sands under Surface Loads", Proc. ASCE, Vol. 97, SM 12, pp. 1675-1699.

Musharrafuzzamam, Md., (1979), "Finite Element Analysis of Interaction Between an Elastic Circular Plate and an Isotropic Elastic Medium", M. Engg. Thesis, Carleton University.

Oda, Masanobu, (1975), "On the Relation $\tau/\sigma_n = K \tan\phi$ in the simple Shear Test" Soils and Foundation, Japan Society of Soil Mechanics and Foundation Engineering, Vol. 15, No. 4, pp. 35-41.

Parry, R.H.G., (1978), "Estimating Foundation Settlement in Sand from Plate Bearing Tests", Geotechnique, Vol. 28, No. 1, pp. 107-118.

Peck, R.B., (1965), "Bearing Capacity and Settlement: Certainties and Uncertainties", Proc. Symp. Duke University, pp. 3-8.

Peck, R.B. and Bazaraa, A.R.S., (1969), Discussion of: "Settlement of Spread Footing on Sand" by D'Appolonia et al (May 1968, ASCE), Proc. ASCE, Vol. 95, SM3, pp. 905-909.

Peck, R.B., Hanson, W.E. and Thornburn, T.H., (1974), "Foundation Engineering", 2nd Edition, John Wiley and Sons, Inc. New York.

Pfeifle, Tom W. and Das, Braja M., (1979), "Model Tests for Bearing Capacity in Sand", Proc. ASCE, Vol. 105, GT9, pp. 1112-1116.

Pfeifle, Thomas, W. and Das, Braja M. (1979), "Bearing Capacity of Surface Footings on Sand Layer Resting on a Rigid Rough Base", Soil Mechanics and Foundation, Japan Society of Soil Mechanics and Foundation Engineering, Vol. 19, No. 1, pp. 1-11.

Perloff, William H. (1975), "Pressure Distribution and Settlement", Foundation Engineering Handbook Edited by H.F. Winterkorn and H.Y. Fang, Van Nostrand Reinhold Company, New York, pp. 148-196.

Poulos, H.G. and Davis, E.H., (1968), "Elastic Solutions for Soil and Rock Mechanics", John Wiley and Sons, Inc., New York.

Schmertmann, J.H., (1970), "Static Cone to Compute Static Settlement over Sand", Proc. ASCE, Vol 96, SM3, pp. 1011-1043.

Schmertmann, J.H., Hartman, J.P. and Brown, P.R., (1978), "Improved Strain Influence Factor Diagrams", Proc. ASCE, Vol. 104, GT8, pp. 1131-1135.

Schwab, E.F., (1976), "Bearing Capacity, Strength and Deformation Behaviour of Soft Organic Sulphide Soils", Royal Institute of Technology, Stockholm.

Selvadurai, A.P.S. (1979), "Elastic Analysis of Soil-Foundation Interaction", Elsevier Scientific Publishing Company, New York.

Shields, D.H., Scott, J.D., Bauer, G.E., Deschenes, J.H., Barsvary, A.K., (1977), "Bearing Capacity of Foundations Near Slopes", Proc. Ninth Int. Conf. on Soil Mech. and Found. Engg., Tokyo, Vol. 1, pp. 715-719.

Skempton, A.W., (1951), "The Bearing Capacity of Clays", Build. Res. Cong., London, Division 1, part 3, pp. 180-189.

Sutherland, H.B., (1972), "General Report: Granular Materials", Settlement of Structures Conf., British Geotechnical Society, pp. 473-499.

Terzaghi, K., (1943), "Theoretical Soil Mechanics", John Wiley and Sons, Inc., New York.

Terzaghi, K. and Peck, R.B., (1967), "Soil Mechanics in Engineering Practice", 2nd Edition, John Wiley and Sons, Inc., New York.

Tolia, D.S., (1977), "Interpretation of Dynamic Cone Penetration Tests - with Particular Reference to Terzaghi and Peck's chart", Ground Engineering, Vol. 10, No. 10, pp. 37-41.

Tschebofarioff, G.P., (1951), "Soil Mechanics, Foundation and Earth Structures", McGraw-Hill, New York.

Vesic, A.S., (1975), "Bearing Capacity of Shallow Foundations" Foundation Engineering Handbook Edited by H.F. Winterkorn and H.Y. Fang. Van Nostrand Reinhold Company, pp. 121-147.

Vesic. A.S., (1965a), "Ultimate Loads and Settlement of Deep Foundations in Sand", Proc. Symp. Bearing Capacity and Settlement, Duke university, pp. 53-68.

Vesic, A.S., (1973), "Analysis of Ultimate Loads of Shallow Foundations", Proc. ASCE, Vol. 99, SM1, pp. 45-73.

Vesic, A.S., (1969), "Effects of Scale and Compressibility on Bearing Capacity of Surface Foundation", Proc. seventh Int. Conf. on Soil Mech. and Found. Engg., Vol. III, p. 270.

APPENDIX - 1

FACTORS FOR BEARING CAPACITY EQUATION

$$q_u = CN_c S_c d_c i_c g_c b_c + qN_q S_q d_q i_q g_q b_q + \frac{1}{2} rBN_r S_r d_r i_r g_r b_r$$

Shape factors:

$$S_c = 1 + N_q B/N_c L$$

$$S_q = 1 + (B/L)\tan\phi$$

$$S_r = 1 - 0.4B/L$$

when $\phi = 0$, $S_c = 0.2B/L$

Depth factors:

$$d_c = 1 + 0.4 \frac{D}{B} \qquad D \leq B$$

$$d_c = 1 + 0.4 \tan^{-1} \frac{D}{B} \qquad D > B$$

$$d_q = 1 + 2 \tan\phi (1 - \sin\phi)^2 \frac{D}{B} \qquad D \leq B$$

$$d_q = 1 + 2 \tan\phi (1 - \sin\phi)^2 \tan^{-1} \frac{D}{B} \qquad D > B$$

$d_r = 1.00$ for all value of

when $\phi = 0$ $\qquad d_c = 0.4\ D/B \qquad D \leq B$

$$d_c = 0.4 \tan^{-1} \frac{D}{B} \qquad D > B$$

Inclination factors:

$$i_c = 0.5 - 0.5\sqrt{1 - H/A_f C} \qquad \text{for } \phi = 0$$

$$i_c = i_q - (1 - i_q)/(N_q - 1)$$

$$i_q = \left(1 - \frac{0.5\ H}{V + A_f\ C\ Cot\phi}\right)^5$$

$$i_r = \left(1 - \frac{0.7\ H}{V + A_f\ C\ Cot\phi}\right)^5 \qquad \text{horizontal ground}$$

$$i_r = \left(1 - \frac{(0.7 - \eta^\circ/450^\circ)H}{V + A_f\ C\ Cot\phi}\right)^5 \qquad \text{sloping ground}$$

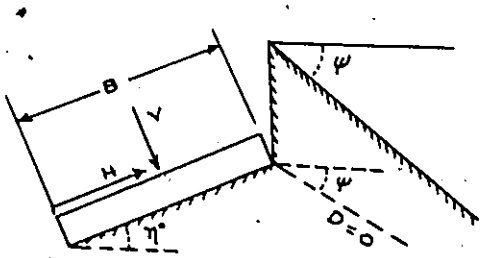

Ground factors:

$g_c = 0.0$ for $\phi = 0$ horizontal ground

$g_c = \frac{\psi^\circ}{147^\circ}$ for $\phi = 0$

$g_c = 1 - \frac{\psi^\circ}{147^\circ}$

$g_q = g_r = (1 - 0.5\ \tan\psi^\circ)^5$

$g_q = g_r = 1.00$ for horizontal ground

Base factors

$b_c = 0.0$ for $\phi = 0$ horizontal ground

$b_c = \frac{\eta^o}{147^o}$ for $\phi = 0$

$b_c = 1 - \frac{\eta^o}{147^o}$

$b_q = \exp(-2\,\eta \tan\phi)$

$b_r = \exp(-2.7\,\eta \tan\phi)$

$b_q = b_r = 1.00$ for horizontal ground

where A_f = Effective footing contact area $B'L'$

L' = Effective footing length = $(L - 2e_L)$

B' = Effective footing width = $(B - 2e_B)$

D = Depth of footing.

e_L, e_B = Eccentricity of load

H, V = Load component parallel and perpendicular to footing respectively

η, ψ = As shown in the fig.

To use the above expressions for various factors following limitations should be observed

$H \leq V \tan\delta + CA_f$

$i_q\, i_r > 0.0$

$$\psi \leq \phi$$

$$\eta + \psi \leq 90$$

where tan δ is the coefficient of friction between footing and the soil.

APPENDIX - 2

TEST RECORDS

TABLE - 1

LOAD AND SETTLEMENT RECORDS

Load kPa	DEFORMATION IN MM					
	D_r = 96%		D_r = 80%		D_r = 63%	
	Test-I	Test-II	Test-I	Test-II	Test-I	Test-II
30.50	-	-	3	2.5	8	7
61.0	6	7	6	5	23	17
91.50	-	-	10	8	38	27
122.0	11	13	16	13	58	47
130.	-	-	-	-	-	62
135	-	-	-	-	68	-
153	-	-	23	18		68
183	16	22	36	28		90
213	-	-	-	-		116
239	-	-	-	-	-	142
244	24	38	74	64		
272	-	-	-	86		
290	-	-	120	-		
305	42	60	-	113		
340		100	-	142		
350		120	-	-		
355		140	-	-		

TABLE - 2

LOAD AND SETTLEMENTS AT VARIOUS DEPTHS

RELATIVE DENSITY - 63 PERCENT

TEST	Load kPa	Settlement at Depths mm				
		0	150	300	450	600
I	61	16	11.5	8	5	4
	91	26	21	14.5	11	8.5
	135	54	-	28	21	16.5
II	61	17	12.5	7.5	6	3.5
	91	28	21.5	15	11.5	9.5
	135	56.5	42.	29		17
Av. of I&II	61	16.5	12	7.75	5.5	3.75
	91	27	21.25	14.75	11.25	9
	135	55.25	41.75	27	21.5	16.75

TABLE - 3

LOADS AND SETTLEMENTS AT VARIOUS DEPTHS

RELATIVE DENSITY - 80 PERCENT

TEST	Load kPa	Settlements at Depths mm				
		0	150	300	450	600
I	61	6.5	5	3	1.5	1
	122	17	12.5	8.5	5	4.5
	152	23	17.5	-	10.5	7.5
II	61	7.5	5.5	2.5	1.5	1
	122	16	12	7.5	6	4
	152	-	18.5	13.0	10	-
Av. of I&II	61	7	5.25	2.75	1.5	1
	122	16.5	12.25	8	5.5	4.25
	135	23	18	13	10.25	7.5

TABLE - 4

LOAD AND SETTLEMENTS AT VARIOUS DEPTHS

RELATIVE DENSITY - 96 PERCENT

TEST	Load kPa	Settlements at Depths mm				
		0	150	300	450	600
I	61	5.5	5	4	3	1.5
	122	11	7.5	5.5	3.5	2
	183	16.5	11	7	4.5	2.5
	244	24.5	16.5	-	6	4
II	61	6.5	4	3	2	1
	122	10.5	8	5	3	1.5
	183	17	11.5	6.5	4.5	2
	244	24	16	10	5.5	-
Av. of I&II	61	6	4.5	3.5	2.5	1.25
	122	10.75	7.75	5.25	3.25	1.75
	183	16.75	11.25	6.75	4.5	2.25
	244	24.25	16.25	10.0	5.75	4

TABLE - 5

SURFACE MOVEMENT AROUND THE FOOTING

RELATIVE DENSITY - 63 PERCENT

TEST - 1

Measurements At	Load kPa	Location of Gauges from the Edge of Footing mm					
		75	150	225	387	562	887
1	61	-1.80	-0.23	+0.14	+0.1	0	0
	91	-2.50	-0.08	+0.20	+0.15	0	0
	135	-3.3	-1.01	+0.25	+0.15	+0.08	0
2	61	-1.76	-0.20	+0.2	+0.10	+0.05	0
	91	-2.43	-0.10	+0.25	+0.30	+0.20	0
	135	-3.15	-1.2	+0.30	+0.70	+0.40	0
3	61	-2.0	-0.18	+0.15	+0.10	+0.13	+0.04
	91	-2.71	-0.27	+0.50	+0.57	+0.17	+0.09
	135	-3.47	-1.15	+0.70	+1.2	+0.72	+0.2

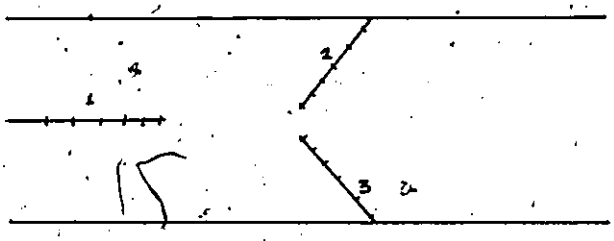

TABLE - 6

SURFACE MOVEMENT AROUND THE FOOTING

RELATIVE DENSITY - 63 PERCENT

TEST - II

Measurements At	Load kPa	Location of Gauges from the Edge of Footing mm					
		75	150	225	387	562	887
1	61	-2.20	-1.10	+0.21	+0.13	0	0
	91	-3.10	-1.52	+0.35	+0.22	+0.10	0
	135	-4.20	-2.53	+0.57	+0.38	+0.22	+0.17
2	61	-2.70	-1.70	+0.15	+0.15	0	0
	91	-3.30	-1.53	+0.20	+0.22	+0.05	0
	135	-4.53	-2.70	+0.45	+0.48	+0.15	+0.07
3	61	-2.50	-1.35	+0.12	+0.14	0	0
	91	-3.20	-1.40	+0.27	+0.18	+0.05	0
	135	-4.15	-2.10	+0.47	+0.26	+0.12	0

TABLE - 7

SURFACE MOVEMENT AROUND THE FOOTING

RELATIVE DENSITY - 80 PERCENT

TEST - 1

Measurements At	Load kPa	Location of Gauges from the Edge of Footing mm					
		75	150	225	387	562	887
1	61	0.22	0.29	0.15	0.05	0	0
	122	0.38	0.60	0.42	0.18	0.09	0
	152	0.42	0.98	0.90	0.52	0.25	0.11
	183	0.50	1.65	1.42	0.78	0.30	0.17
2	61	0.43	0.23	0.16	0.09	0	0
	122	0.50	0.55	0.48	0.19	0.08	0
	152	0.38	1.10	0.87	0.56	0.21	0.12
	183	0.35	1.45	1.35	0.75	0.35	0.18
3	61	0.35	0.30	0.18	0.12	0	0
	122	0.45	0.58	0.43	0.20	0.12	0
	152	0.40	0.95	0.81	0.51	0.27	0.15
	183	0.28	1.55	1.45	0.79	0.32	0.20

TABLE - 8

SURFACE MOVEMENT AROUND THE FOOTING

RELATIVE DENSITY - 80 PERCENT

TEST - II

Measurements At	Load kPa	Location of Gauges from the Edge of Footing mm					
		75	150	225	387	562	887
1	61	0.26	0.28	0.11	0.05	0	0
	122	0.34	0.55	0.37	0.14	0.07	0
	152	0.37	1.05	0.92	0.47	0.27	0.12
	183	0.43	1.55	1.43	0.77	0.30	0.15
2	61	0.56	0.21	0.17	0.02	0.01	0
	122	0.48	0.58	0.66	0.14	0.08	0
	152	0.35	0.94	1.22	0.62	0.22	0
	183	0.40	1.39	1.80	0.99	0.37	0.01
3	61	0.26	0.21	0.15	0.07	0.03	0
	122	0.23	0.67	0.52	0.19	0.09	0
	152	0.22	1.13	0.93	0.55	0.19	0.03
	183	0.42	1.67	1.52	0.96	0.32	0.08

TABLE - 9

SURFACE MOVEMENT AROUND THE FOOTING

RELATIVE DENSITY - 96 PERCENT

TEST - 1

Measurements At	Load kPa	Location of Gauges from the Edge of Footing mm					
		75	150	225	387	562	887
1	61	-0.22	0.15	0.41	0.22	0.09	0
	122	-0.50	0.49	0.94	0.58	0.15	0
	183	0.70	1.52	2.13	1.31	0.26	0.15
	244	1.50	4.24	5.15	3.29	0.56	0.23
2	61	-0.12	0.18	1.10	0.35	0.19	0
	122	-0.36	0.42	1.60	0.61	0.32	0.18
	183	0.52	1.60	2.60	1.28	0.58	0.22
	244	2.14	3.59	4.26	3.05	1.24	0.28
3	61	-0.20	0.21	0.37	0.29	0.12	0.09
	122	-0.42	0.57	0.85	0.70	0.31	0.20
	183	0.72	1.56	1.95	1.55	0.61	0.35
	244	2.05	4.94	5.14	3.84	1.41	0.50

TABLE - 10

SURFACE MOVEMENT AROUND THE FOOTING

RELATIVE DENSITY - 96 PERCENT

TEST - II

Measurements At	Load kPa	Location of the Gauges from the Edge of Footing mm					
		75	150	225	387	562	887
1	61	-0.30	0.22	0.58	0.22	0.12	0
	122	-0.52	0.51	1.15	0.62	0.25	0.05
	183	0.80	1.70	2.45	1.52	0.72	0.30
	244	1.62	3.85	5.10	3.41	0.85	0.40
Failure Plane		228	232	234	216	160	90
2	61	-0.28	0.17	0.49	0.19	0.09	0
	122	-0.44	0.45	0.97	0.55	0.27	0.13
	183	0.73	1.50	2.35	1.43	0.55	0.22
	244	1.51	3.72	4.75	3.21	0.72	0.29
Failure Plane		244	260	254	240	180	100
3	61	-0.17	0.20	0.52	0.21	0.11	0.05
	122	-0.38	0.49	1.10	0.55	0.22	0.12
	183	0.75	1.62	2.50	1.41	0.53	0.19
	244	1.82	3.45	4.97	3.15	0.69	0.30
Failure Plane		250	260	257	245	190	120

APPENDIX - 3

PROPERTIES OF SAND

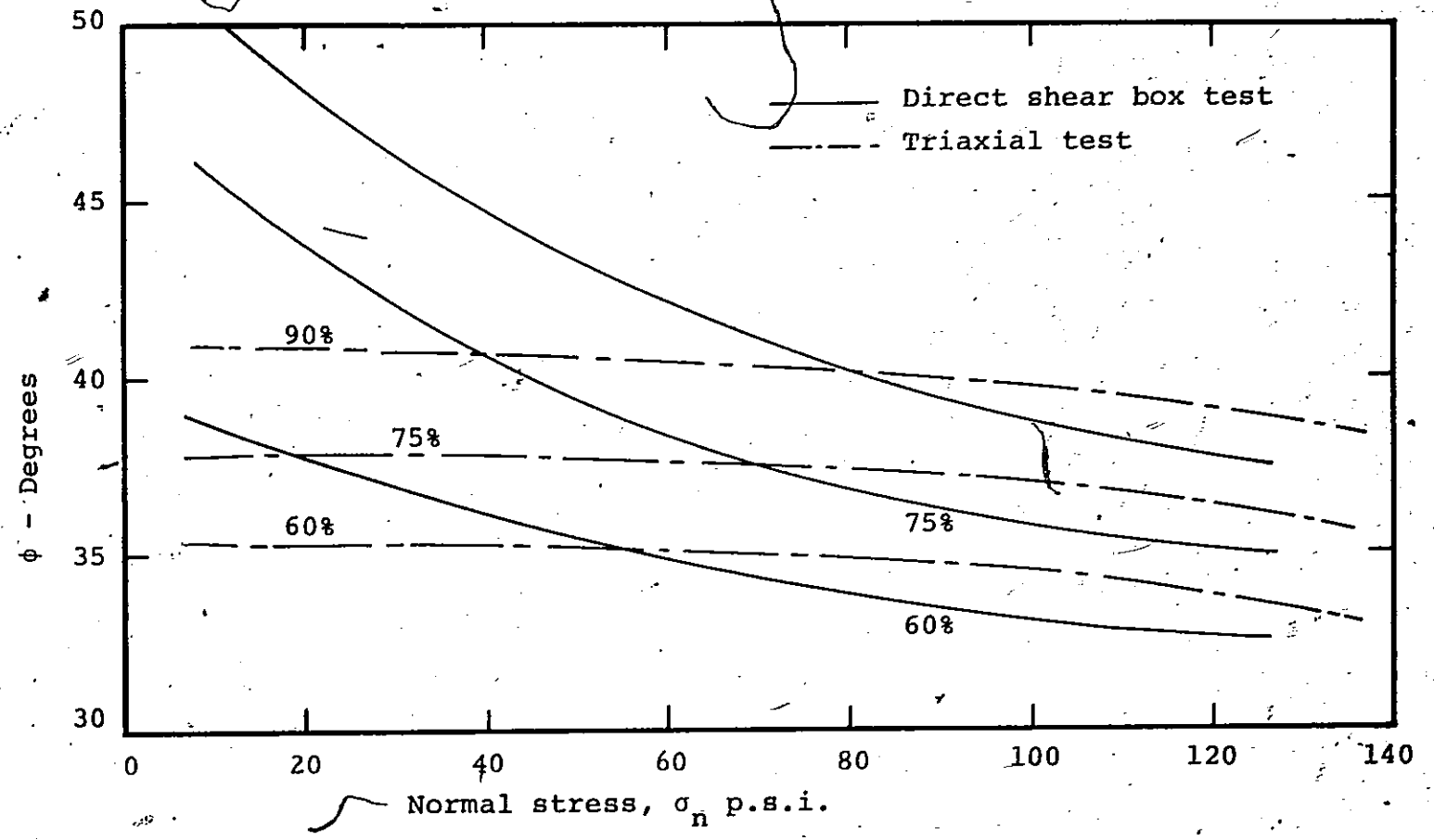

FIGURE 1 RELATIONSHIP BETWEEN NORMAL STRESS AND ANGLE OF INTERNAL FRICTION FOR DIRECT SHEAR AND TRIAXIAL COMPRESSION.

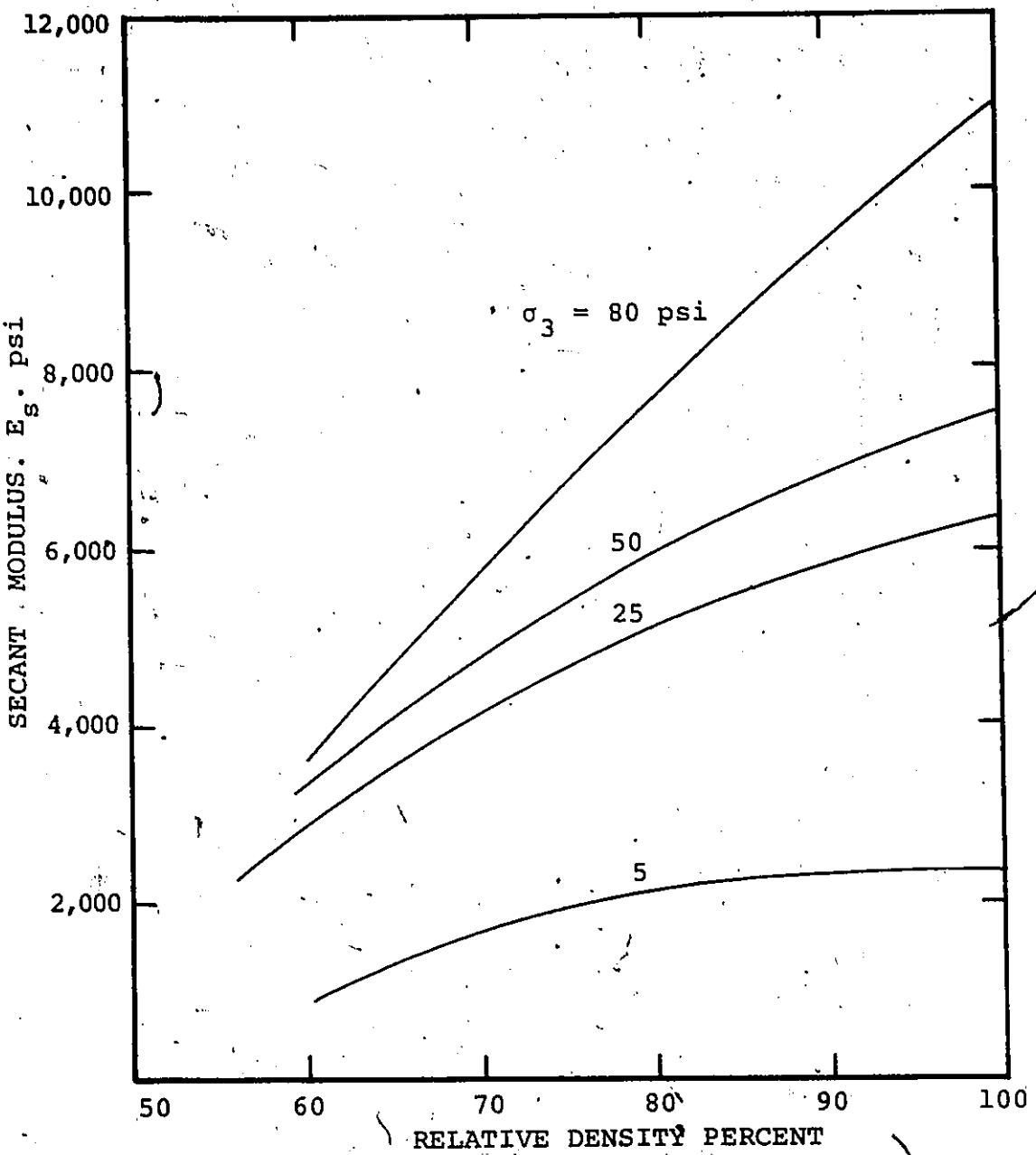

FIGURE 2 VARIATION OF SECANT MODULUS AT 1/2 PEAK WITH RELATIVE DENSITY AND CONFINING PRESSURE

* 1 psi = 6.89 kPa

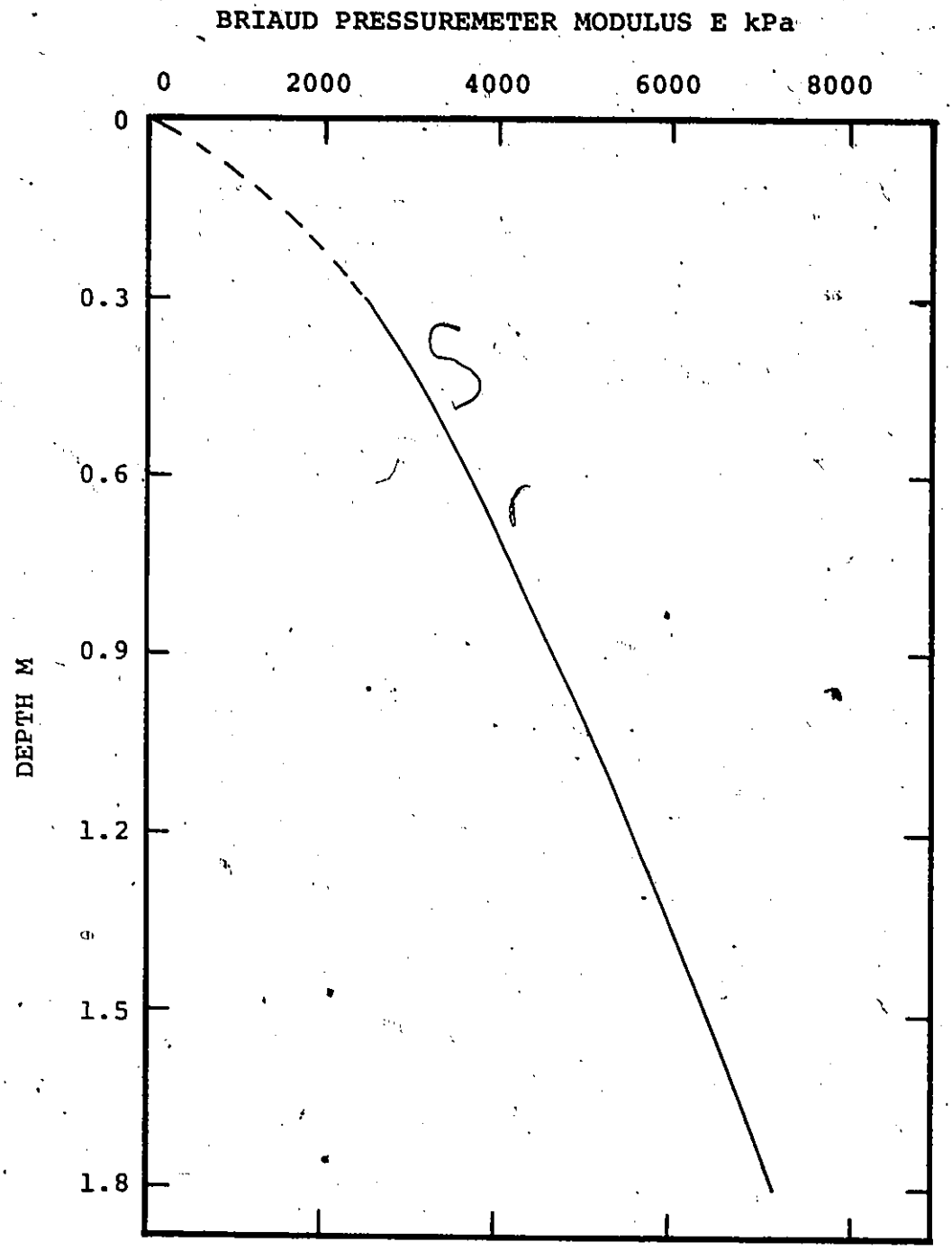

FIGURE 3 SAND BOX. COMPACT SAND
MODULUS Vs DEPTH

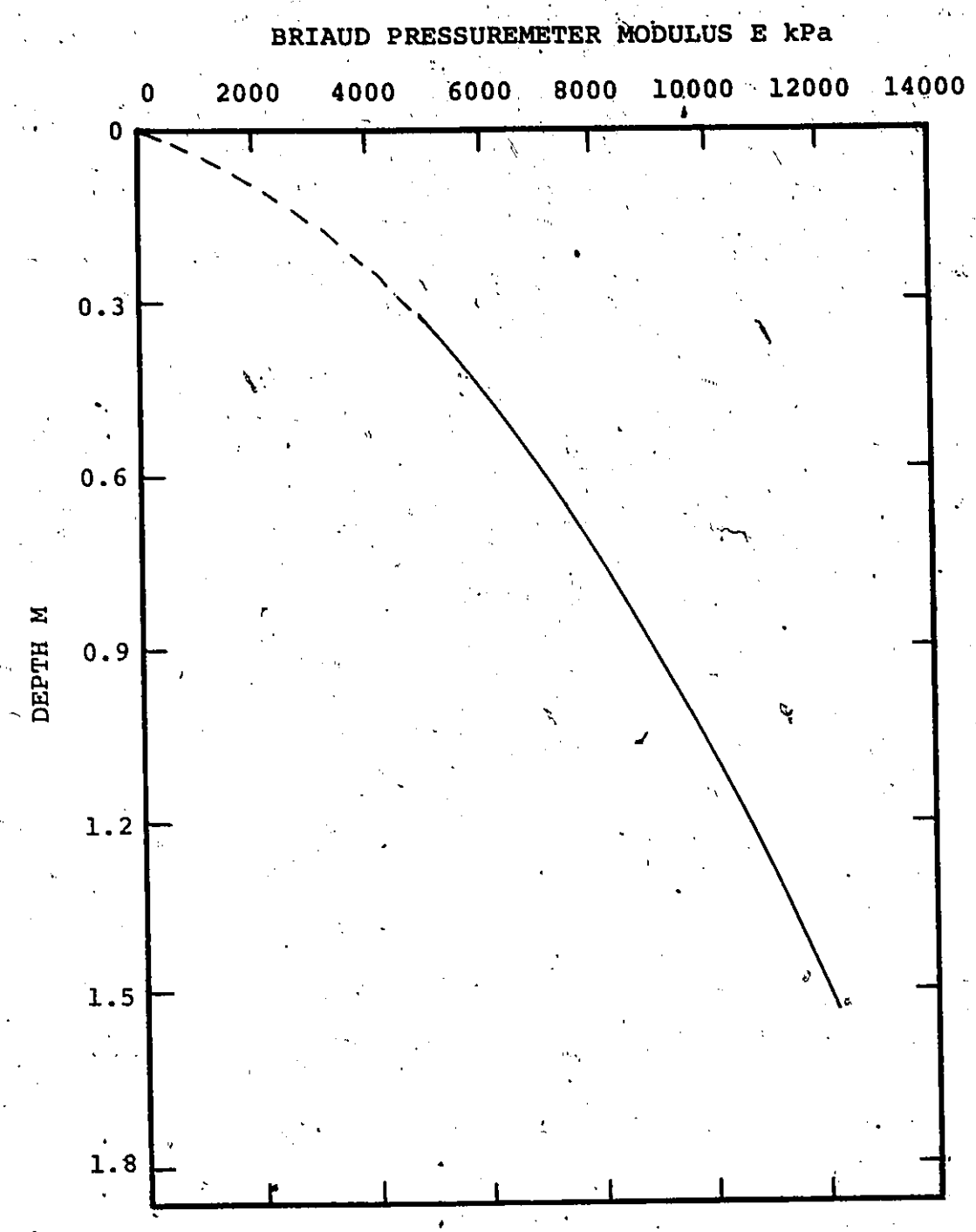

FIGURE 4 SAND BOX. DENSE SAND
MODULUS Vs DEPTH

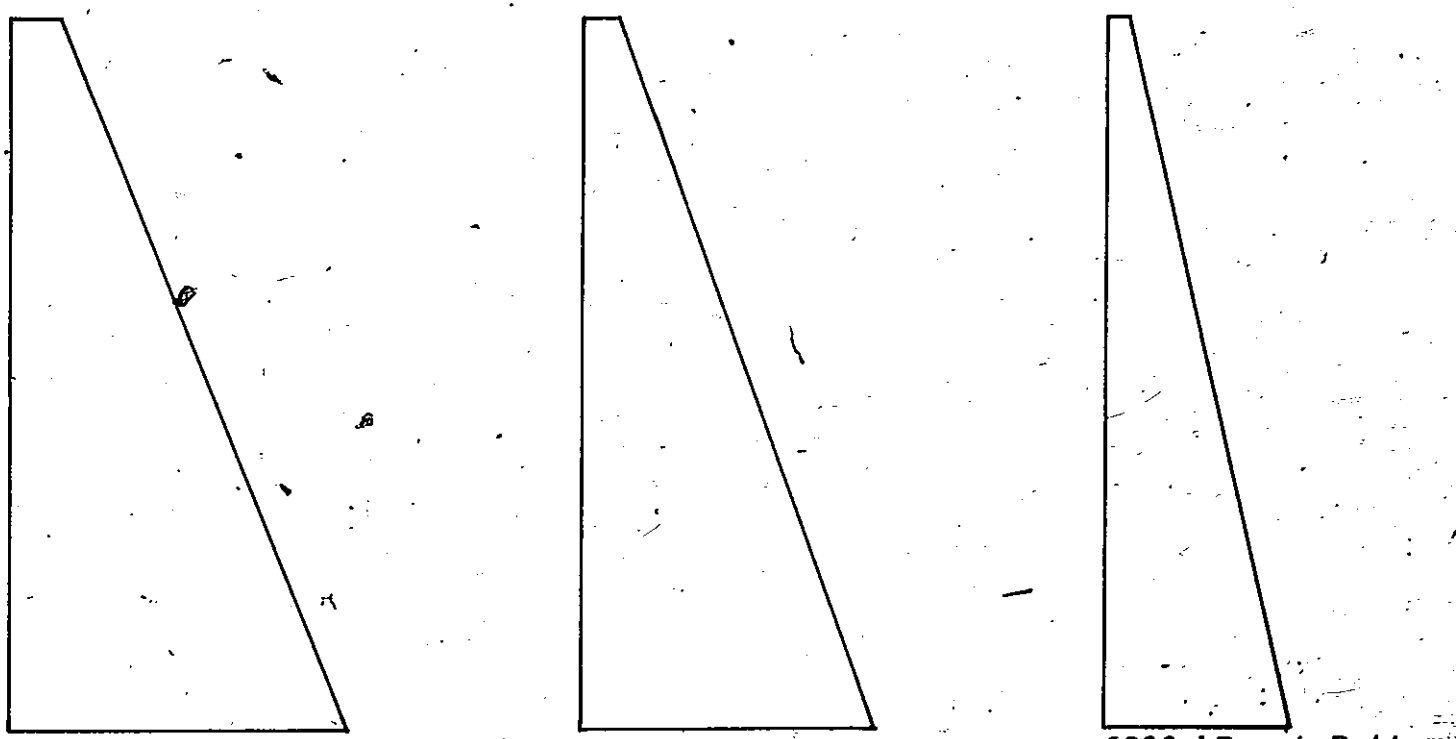

FIGURE 5 SOIL MODULUS USED IN ALL CALCULATIONS